

AD-A062 205

NAVAL POSTGRADUATE SCHOOL MONTEREY CALIF F/G
HOT FLOW TESTING OF MULTIPLE NOZZLE EXHAUST EDUCTOR SYSTEMS. (U)
SEP 78 D R WELCH

F/G 20/4

UNCLASSIFIED

1 OF 2
AD A062205

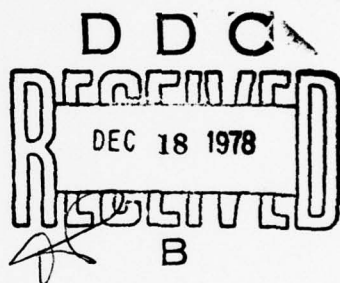
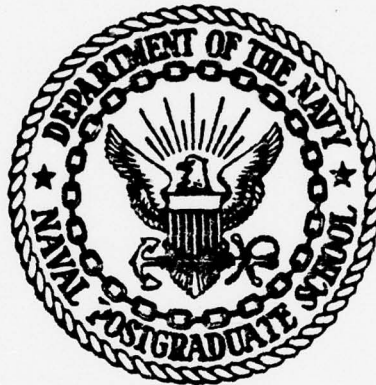


AD A0 622205

DDC FILE, COPY

2 LEVEL II

NAVAL POSTGRADUATE SCHOOL
Monterey, California



THESIS

HOT FLOW TESTING OF MULTIPLE
NOZZLE EXHAUST EDUCTOR SYSTEMS

by

Daniel Roy Welch

September 1978

Thesis Advisor:

P. F. Pucci

Approved for public release; distribution unlimited.

60 26 11 1978

UNCLASSIFIED

SECURITY CLASSIFICATION OF THIS PAGE (When Data Entered)

REPORT DOCUMENTATION PAGE		READ INSTRUCTIONS BEFORE COMPLETING FORM
1. REPORT NUMBER	2. GOVT ACCESSION NO.	3. RECIPIENT'S CATALOG NUMBER
4. TITLE (and subtitle) ⑥ Hot Flow Testing of Multiple Nozzle Exhaust Eductor Systems,		5. TYPE OF REPORT & PERIOD COVERED Engineer's Thesis September 1978
7. AUTHOR(s) ⑩ Daniel Roy Welch		6. PERFORMING ORG. REPORT NUMBER
9. PERFORMING ORGANIZATION NAME AND ADDRESS Naval Postgraduate School Monterey, California 93940		10. PROGRAM ELEMENT, PROJECT, TASK AREA & WORK UNIT NUMBERS
11. CONTROLLING OFFICE NAME AND ADDRESS Naval Postgraduate School Monterey, California 93940		12. REPORT DATE ⑪ September 1978
14. MONITORING AGENCY NAME & ADDRESS (if different from Controlling Office) ⑨ Master's Thesis		13. NUMBER OF PAGES 131
16. DISTRIBUTION STATEMENT (of this Report) Approved for public release; distribution unlimited. ⑫ 132 p.		15. SECURITY CLASS. (of this report) Unclassified
17. DISTRIBUTION STATEMENT (of the abstract entered in Block 20, if different from Report)		
18. SUPPLEMENTARY NOTES		
19. KEY WORDS (Continue on reverse side if necessary and identify by block number) Hot Flow Model Multiple Nozzle Exhaust Eductor Systems		
20. ABSTRACT (Continue on reverse side if necessary and identify by block number) Hot flow model tests of multiple nozzle exhaust eductor systems were conducted to evaluate effects of exhaust temperature on eductor performance. A one-dimensional analysis of a simple eductor system based on conservation of momentum for an incompressible gas was used in determining the non-dimensional parameters governing the flow phenomenon. Eductor performance is defined in terms of these parameters.		

UNCL^{ASSIFIED}

SECURITY CLASSIFICATION OF THIS PAGE/When Data Entered

(20. ABSTRACT Continued)

An experimental correlation of these parameters which was previously developed and used to correlate cold flow data was found to be effective in correlating both cold and hot flow data for eductor systems. Temperature data was obtained for the mixing stack wall and the exhaust flow at the mixing stack exit plane.

ACCESSION for	
NTIS	White Section <input checked="" type="checkbox"/>
DDC	Blue Section <input type="checkbox"/>
UNAMINDED <input type="checkbox"/>	
JUSTIFICATION	

BY	
DISTRIBUTION/AVAILABILITY CODES	
Dist.	AVAIL. and/or SPECIAL
A	

Approved for public release; distribution unlimited.

Hot Flow Testing of Multiple
Nozzle Exhaust Eductor Systems

by

Daniel Roy Welch
Lieutenant, United States Navy
B.S. NavArch., United States Naval Academy, 1971

Submitted in partial fulfillment of the
requirements for the degrees of

MASTER OF SCIENCE IN MECHANICAL ENGINEERING

and

MECHANICAL ENGINEER

from the

NAVAL POSTGRADUATE SCHOOL

September 1978

Author

Daniel Roy Welch

Thesis Advisor

Paul J. Succi

Second Reader

R. St. John

Chairman, Department of Mechanical Engineering

Paul J. Marto

Dean of Science and Engineering

78 3 12 11 1978

ABSTRACT

Hot flow model tests of multiple nozzle exhaust eductor systems were conducted to evaluate effects of exhaust temperature on eductor performance. A one-dimensional analysis of a simple eductor system based on conservation of momentum for an incompressible gas was used in determining the non-dimensional parameters governing the flow phenomenon.

Eductor performance is defined in terms of these parameters. An experimental correlation of these parameters which was previously developed and used to correlate cold flow data was found to be effective in correlating both cold and hot flow data for eductor systems. Temperature data was obtained for the mixing stack wall and the exhaust flow at the mixing stack exit plane.

TABLE OF CONTENTS

I.	INTRODUCTION -----	15
II.	THEORY AND ANALYSIS -----	18
	A. MODELING TECHNIQUE -----	18
	B. ONE-DIMENSIONAL ANALYSIS OF A SIMPLE EDUCTOR --	19
	C. NON-DIMENSIONAL SOLUTION OF SIMPLE EDUCTOR ANALYSIS -----	25
	D. CORRELATION OF EXPERIMENTAL DATA -----	29
III.	EXPERIMENTAL APPARATUS -----	31
	A. COMBUSTION GAS GENERATOR -----	31
	B. EDUCTOR AIR METERING BOX -----	32
	C. INSTRUMENTATION -----	33
	D. EDUCTOR SYSTEM -----	36
	1. Mixing Stack -----	36
	2. Eductor Nozzles -----	36
	3. Standoff Ratio -----	37
IV.	EXPERIMENTAL METHOD -----	38
V.	DISCUSSION OF EXPERIMENTAL RESULTS -----	40
VI.	CONCLUSIONS -----	44
VII.	RECOMMENDATIONS -----	45
VIII.	FIGURES -----	46
IX.	TABLES -----	95
	APPENDIX A: Combustion Gas Generator Operation -----	118
	APPENDIX B: Determination of the Exponent in the Non-Dimensional Pumping Coefficient -----	124
	APPENDIX C: Uncertainty Analysis -----	125

BIBLIOGRAPHY ----- 129

INITIAL DISTRIBUTION LIST ----- 130

LIST OF FIGURES

<u>Figure</u>	<u>Description</u>	<u>Page</u>
1	Schematic Diagram of Simple Exhaust Gas Eductor -----	46
2	Simple Single Nozzle Eductor System --	47
3	Schematic Diagram of Combustion Gas Generator -----	48
4	Combustion Gas Generator -----	49
5	Schematic Diagram of Gas Generator Fuel System -----	50
6	Gas Generator Fuel Supply System -----	51
7	Eductor Air Metering Box -----	52
8	Eductor Air Metering Box Arrangement -	53
9	Interior of Air Metering Box Showing Uptake Stack and Primary Nozzles -----	54
10	Interior of Air Metering Box Showing Mixing Stack and Primary Nozzles -----	55
11	Schematic Diagram of Pressure Measurement System -----	56
12	Manometer Board -----	57
13	Main Control Panel, Digital Pyrometers, Manometer Manifold Valves -----	58
14	Schematic Diagram of Temperature Measurement System -----	59
15	Entrance Nozzle Calibration Curve -----	60
16	Air Metering Box End Plate and Mixing Stack Collar -----	61
17	Dimensional Diagram of Primary Flow Nozzles -----	62

<u>Figure</u>	<u>Description</u>	<u>Page</u>
18	Dimensional Diagram of Primary Flow Nozzle Plate -----	63
19	Primary Flow Nozzle Plate (Back View) --	64
20	Primary Flow Nozzle Plate (Front View) --	65
21	Illustrative Plot of the Experimental Data Correlation in Equation 14 -----	66
22	Primary Flow Nozzle Temperature Profiles -----	67
23	Uptake Stack Temperature Profile -----	68
24	Comparison of Cold Flow Performance Plots for L/D = 3.0 -----	69
25	Comparison of Cold Flow Performance Plots for L/D = 2.5 -----	70
26	Composite Performance Plot for all Temperatures, L/D = 3.0 -----	71
27	Composite Performance Plot for all Temperatures, L/D = 2.5 -----	72
28	Performance Plot, L/D = 3.0, Cold Flow -	73
29	Performance Plot, L/D = 3.0, TUPT = 550 °F -----	74
30	Performance Plot, L/D = 3.0, TUPT = 650 °F -----	75
31	Performance Plot, L/D = 3.0, TUPT = 750 °F -----	76
32	Performance Plot, L/D = 3.0, TUPT = 850 °F -----	77
33	Performance Plot, L/D = 2.5, Cold Flow -	78
34	Performance Plot, L/D = 2.5, TUPT = 550 °F -----	79
35	Performance Plot, L/D = 2.5, TUPT = 650 °F -----	80

<u>Figure</u>	<u>Description</u>	<u>Page</u>
36	Performance Plot, L/D = 2.5, TUPT = 750 °F -----	81
37	Performance Plot, L/D = 2.5, TUPT = 850 °F -----	82
38	Mixing Stack Pressure Distribution, L/D = 3.0 -----	83
39	Mixing Stack Pressure Distribution, L/D = 2.5 -----	84
40	Mixing Stack Wall Temperature Distribution, L/D = 3.0 -----	85
41	Mixing Stack Wall Temperature Distribution, L/D = 2.5 -----	86
42	Comparison of Mixing Stack Wall Temperature Distributions -----	87
43	Mixing Stack Exit Plane Temperature Profile, L/D = 3.0 -----	88
44	Mixing Stack Exit Plane Temperature Profile, L/D = 2.5 -----	89
45	Schematic Diagram of Compressor Layout -	90
46	Cooling Tower Switches and Cooling Water Valve -----	91
47	Carrier Air Compressor, Butterfly Suction Damper and Cooling Water Valve -	92
48	Auxiliary Oil Pump and Switch -----	93
49	Main Air Supply Globe Valve -----	94

LIST OF TABLES

<u>Table</u>	<u>Description</u>	<u>Page</u>
I.	Summary of Results -----	95
II.	Entrance Transition Nozzle Calibration Data -----	96
III.	Primary Nozzle Temperature Profile Data -----	97
IV.	Uptake Stack Temperature Profile Data --	98
V.	Performance Data for L/D = 3.0 -----	99
VI.	Performance Data for L/D = 2.5 -----	104
VII.	Mixing Stack Exit Plane Temperature Profile L/D = 3.0 -----	113
VIII.	Mixing Stack Exit Plane Temperature Profile L/D = 2.5 -----	115
IX.	Uncertainties in Measured Values From Table VI -----	117

NOMENCLATURE

ENGLISH LETTER SYMBOLS

A	- Area, in ²
C	- Sonic velocity, ft/sec
D	- Diameter, in
f	- Friction factor
F	- Functional denotation
F_{fr}	- Wall skin-friction force, lbf
g_c	- Proportionality factor in Newton's Second Law, $g_c = 32.174 \text{ lbm-ft/lbf-sec}^2$
h	- Enthalpy, Btu/lbm
k	- Ratio of specific heats
L	- Length, in
P	- Pressure, in H ₂ O
P_a, B	- Atmospheric pressure, in Hg
R	- Gas constant for air, 53.34 ft-lbf/lbm-°R
S	- Standoff distance, in
T	- Temperature, °F, °R
U	- Velocity, ft/sec
W, \dot{m}	- Mass flow rate, lbm/sec
x	- Axial distance from mixing stack entrance, in

Dimensionless Groupings

A^*	- Secondary flow area to primary flow area ratio
K_e	- Kinetic energy correction factor

K_m	- Momentum correction factor at the mixing stack exit
K_p	- Momentum correction factor at the primary nozzle exit
M	- Mach number
ΔP^*	- Pressure coefficient
Re	- Reynolds number
T^*	- Secondary flow absolute temperature to primary flow absolute temperature ratio
W^*	- Secondary mass flow rate to primary mass flow rate ratio
ρ^*	- Secondary flow density to primary flow density ratio

Greek Letter Symbols

μ	- Absolute viscosity, $\text{lbf-sec}/\text{ft}^2$
ρ	- Density, lbm/ft^3
β	- $K_m + \frac{f}{2} A_w/A_m$

Subscripts

0	- Section within secondary air plenum
1	- Section at primary nozzle exit
2	- Section at mixing stack exit
B	- Burner
m	- Mixed flow or mixing stack
P	- Primary
s	- Secondary
u	- Uptake
w	- Mixing stack inside wall

Tabulated Values

DELPN, PN	- Pressure drop across entrance transition nozzle, in H_2O
FHZ	- Fuel flow meter reading, Hz
P*	- Pressure coefficient
PA, B	- Ambient pressure, in Hg
PA-PS, Δ PS	- Pressure differential across secondary flow nozzles, in H_2O
PEH	- Uptake static pressure, in H_2O
PMIX, PMS	- Mixing stack static pressure, in H_2O
PNH	- Static pressure upstream of entrance transition nozzle, in Hg
PU-PA	- Uptake static pressure, in H_2O
P*/T*	- Dimensionless pressure coefficient
T*	- Absolute temperature ratio, secondary flow to primary flow
TAMB	- Ambient temperature, °F
TMIX	- Mixing stack wall temperature, °F
TUPT	- Uptake temperature, °F
UM	- Average velocity in mixing stack, ft/sec
UP	- Primary flow velocity at nozzle exit, ft/sec
UU	- Primary flow velocity in uptake, ft/sec
WP	- Primary mass flow rate, lbm/sec
WS	- Secondary mass flow rate, lbm/sec
WPA	- Mass flow rate of primary air, lbm/sec
WPF	- Mass flow rate of fuel, lbm/sec
W*	- Secondary mass flow rate to primary flow rate ratio

ACKNOWLEDGEMENT

Sincere thanks go to the author's advisor, Professor Paul F. Pucci, whose expertise and inspiration provided the foundation and catalyst for this work. Great appreciation is also expressed to Professor T. Sarpkaya who was always available with words of wisdom and support. The assistance and ingenuity provided by the personnel of the Department of Mechanical Engineering Machine Shop, especially Mr. George Bixler, is also sincerely appreciated.

Special thanks and grateful appreciation are due to my wife, Sharon, for the never ending encouragement and understanding she provided during the long days and late nights devoted to this study.

I. INTRODUCTION

The gas turbine engine is steadily becoming more and more attractive as a prime mover for various shipboard applications. One of the unique features of the use of gas turbine engines is its relatively hot and voluminous exhaust. This presents problems such as overheating of antennae and other equipment by exhaust plume impingement and the creation of an undesirable infra-red signature of the hot exhaust plume. An effective means of reducing the exhaust gas temperature is to mix it with ambient air prior to its discharge from the stack. Exhaust gas eductor systems presently in service have demonstrated their effectiveness in facilitating such a mixing process.

The subject of this investigation is the application of multiple nozzle eductor systems for cooling the exhaust gas from gas turbine powered ships. This research is an extension of work reported by Lt. C. R. Ellin [1], Lt. C. M. Moss [2], and Lt. J. P. Harrell [3]. Whereas this previous work has been carried out with cold flow testing, this investigation is concerned with testing using hot gas as the exhaust or primary flow. The scope of the work reported here includes completion of and subsequent changes to the combustion gas generator designed and built by Lcdr. P. D. Ross [4].

For the purpose of this investigation, the exhaust gas eductor system, illustrated schematically in Figure 1, is

defined as the portion of the uptake which discharges the exhaust gas through nozzles into a mixing stack. The purpose of the eductor system is to induce a flow of cool ambient air which is mixed with the hot exhaust gas in order to lower the temperature of the exhaust stack and exhaust plume. These gas eductors must meet three major requirements. They must pump large amounts of secondary (cooling) air into the mixing stack, they must adequately mix the hot high velocity exhaust gas and the cool low velocity secondary air, and they must not adversely affect the gas turbine's performance.

A one-dimensional flow analysis of a simple single-nozzle eductor system, as a unit, facilitates determination of the non-dimensional parameters which govern the flow phenomenon. An experimental correlation of these non-dimensional parameters has been developed and is used to evaluate eductor performance.

The geometric parameters which influence the gas eductor's performance include the number and size of primary nozzles, the length of the mixing stack, the ratio of the primary nozzle flow area to the mixing stack area, and the ratio of the length of the mixing stack to its diameter. Numerous combinations of and variations in these parameters have been investigated and reported in References [1] through [3].

The intent of this investigation was to obtain data using hot flow testing of gas eductor systems to establish

the effect of uptake gas temperature on the eductor's performance. Correlation of hot flow data with previous cold flow data allows a validation of the hot gas generator and a validation of the use of cold flow models for hot flow prototypes.

Two exhaust eductor models were tested. Both geometries were tested previously using cold flow facilities. One geometry was tested by Moss [2] and by Harrell [3], each at a different scale; the other was tested by Staehli and Lemke [5]. All tests were made at the same flow parametric values.

II. THEORY AND ANALYSIS

Evaluation of the effects of eductor geometry on prototype eductor performance through experimentation with models requires the following: assurance of similitude (geometric, kinematic, and dynamic similarity) between model and prototype; the identification of the dimensionless groupings pertinent to the flow phenomenon; and a suitable means of data analysis and presentation. Dynamic similarity was maintained by using Mach number similarity to establish the model's primary flow rate. Determination of the dimensionless groupings that govern the flow was accomplished through the analysis of a simple air eductor system. Based on this analysis, an experimental correlation of the non-dimensional parameters was developed and used in presenting and evaluating experimental results.

A. MODELING TECHNIQUE

For the flow velocities considered, the primary flow through the model eductor is turbulent (Reynolds number based on diameter of approximately 10^5). Consequently, turbulent momentum exchange is a predominant mechanism over shear interaction, and the kinetic and internal energy terms are more influential on the flow than are viscous forces. Since Mach number can be shown to represent the square root of the ratio of kinetic energy of a

flow to its internal energy, it is a more significant parameter than Reynolds number in describing the primary flow through the uptake.

Similarity of Mach number was therefore used to model the primary flow. Mach number is defined as the ratio of flow velocity to sonic velocity in the medium considered. Sonic velocity, represented by c , can be calculated using the relation

$$c = (g_c kRT)^{0.5}$$

if the fluid is assumed to behave as a perfect gas.

Geometric similarity was achieved through the use of a dimensional scale factor which is influenced by test facility flow capabilities, primary flow velocities and availability of modeling materials.

B. ONE-DIMENSIONAL ANALYSIS OF A SIMPLE EDUCTOR

The theoretical analysis of an eductor may be approached in two ways. One method attempts to analyze the details of the mixing process of the primary and secondary flows which takes place inside the mixing stack and thereby determines the parameters that describe the flow. This requires an interpretation of the mixing phenomenon, which, when applied to multiple-nozzle systems, becomes extremely complex. The second method, employed in this study, analyzes the overall performance of the eductor system as a unit.

Since details of the mixing process are not considered in this method, an analysis of the simple single-nozzle eductor system shown in Figure 2 leads to a determination of the dimensionless groupings governing the flow. The one-dimensional analysis that follows is essentially that of Ellin [1].

The driving or primary fluid, flowing at a rate W_p and at a velocity U_p , discharges into the entrance of the constant area section of the mixing stack, inducing a secondary flow rate of W_s at velocity U_s . The primary and secondary flows are mixed and leave the mixing stack at a flow rate of W_m and a bulk average velocity of U_m .

The one-dimensional flow analysis of the simple eductor system described depends on the simultaneous solution of the equations of continuity, momentum, and energy with an appropriate equation of state and specified boundary conditions.

The following simplifying assumptions are made:

1. Both gas flows are treated as perfect gases with constant specific heats.
2. Steady, incompressible flow throughout the eductor and plenum exists.
3. The flow throughout the eductor is adiabatic. The flow of secondary air from the plenum (at section 0) to the entrance of the mixing stack (at section 1) is isentropic. Irreversible adiabatic mixing occurs

between the primary and secondary flows in the mixing stack (between sections 1 and 2).

4. The static pressure distributions across the entrance and exit planes of the mixing stack (at sections 1 and 2) are uniform.
5. At the mixing stack entrance (section 1), the primary flow velocity U_p and temperature T_p are uniform across the primary stream, and the secondary flow velocity U_s and temperature T_s are uniform across the secondary stream; but U_p does not equal U_s , and T_p does not equal T_s .
6. Incomplete mixing of the primary and secondary flows in the mixing stack is accounted for by the use of a non-dimensional momentum correction factor, K_m , which relates the actual momentum rate to the rate based on the bulk-average velocity and density and by the use of a non-dimensional kinetic energy correction factor, K_e , which relates the actual kinetic energy rate to the rate based on the bulk-average velocity and density.
7. Potential energy differences due to elevation are negligible.
8. Pressure changes P_o to P_1 and P_1 to P_a are small relative to the static pressure so that the gas density is essentially dependent upon temperature (and atmospheric pressure).

9. Wall friction in the mixing stack is accounted for with the conventional pipe friction factor term based on the bulk-average flow velocity U_m and the mixing stack wall area A_w .

The conservation of mass principle for steady state flow yields

$$W_m = W_p + W_s \quad (1)$$

where

$$W_p = \rho_p U_p A_p$$

$$W_s = \rho_s U_s A_s \quad (1a)$$

$$W_m = \rho_m U_m A_m$$

Substituting for W_m , the bulk-average velocity becomes

$$U_m = \frac{W_s + W_p}{\rho_m A_m} \quad (1b)$$

Now, from assumption 1

$$\rho_m = \frac{P_a}{R T_m} \quad (2)$$

where T_m is calculated as the bulk-average temperature for the mixed flow. Applying assumptions 4 and 6, the momentum

equation for the flow in the mixing stack may be written

$$K_p \left[\frac{W_p U_p}{g_c} \right]_1 + \left[\frac{W_s U_s}{g_c} \right]_1 + P_1 A_1 = K_m \left[\frac{W_m U_m}{g_c} \right]_2 + P_2 A_2 + F_{fr} \quad (3)$$

with $A_1 = A_2$. The momentum correction factor K_p is introduced to account for a possible non-uniform velocity profile across the primary nozzle exit. It is defined in a manner similar to that of K_m and by assumption 5 is equal to unity but is included here for completeness. The momentum correction factor for the mixing stack exit is defined by the relation

$$K_m = \frac{1}{W_m U_m} \int_0^{A_m} U_2^2 \rho_2 dA \quad (4)$$

The actual variable velocity and a weighted average density at section 2 are used in the integrand. The wall skin-friction force F_{fr} can be related to the mean velocity by

$$F_{fr} = f A_w \left[\frac{U_m^2 \rho_m}{2 g_c} \right] \quad (5)$$

For turbulent flow, the friction factor may be calculated from the Reynolds number as

$$f = 0.046 (Re_m)^{-0.2} , \quad \text{where} \quad Re_m = \frac{\rho_m U_m D_m}{\mu_m} \quad (6)$$

Applying the conservation of energy principle to the steady flow in the mixing stack with assumption 7

$$w_p [h_p + \frac{u_p^2}{2g_c}]_1 + w_s [h_s + \frac{u_s^2}{2g_c}]_1 = w_m [h_m + K_e \frac{u_m^2}{2g_c}]_2 \quad (7)$$

where K_e is the kinetic energy correction factor defined by the relation

$$K_e = \frac{1}{w_m u_m^2} \int_0^{A_m} u_2^3 \rho_2 dA \quad (8)$$

It may be demonstrated that for the purpose of evaluating the mixed mean flow temperature T_m , the kinetic energy terms may be neglected to yield

$$h_m = \frac{w_p}{w_m} h_p + \frac{w_s}{w_m} h_s \quad (9)$$

where $T_m = F(h_m)$ only from assumption 1.

Similarly, the energy equation applied to the flow of secondary air between the plenum entrance and the mixing stack entrance may be reduced to

$$\frac{p_0 - p_1}{\rho_s} = \frac{u_s^2}{2g_c} \quad (10)$$

The foregoing equations may be combined to yield the vacuum produced by the eductor in the plenum chamber

$$P_a - P_o = \frac{1}{g_c A_m} \left\{ K_p \frac{W_p^2}{A_p \rho_p} + \frac{W_s^2}{A_s \rho_s} \left[1 - \frac{A_m}{2 A_s} \right] - \frac{W_m^2}{A_m \rho_m} \left[K_m + \frac{f}{2} \frac{A_w}{A_m} \right] \right\} \quad (11)$$

where it is understood that A_p and ρ_p apply to the primary flow at the entrance to the mixing stack (section 1), A_s and ρ_s apply to the secondary flow at this same section, and A_m and ρ_m apply to the mixed flow at the exit of the mixing stack (section 2). P_a is atmospheric pressure and is equal to the pressure at the exit of the mixing stack P_2 . This equation also incorporates the assumption that $(\rho_s)_1 = (\rho_s)_0$ so that ρ_s may be taken as the density of the secondary flow in the plenum.

C. NON-DIMENSIONAL SOLUTION OF SIMPLE EDUCTOR ANALYSIS

In order to provide the criteria of similarity of flows with geometric similarity, the non-dimensional parameters which govern the flow must be determined. One means of determining these parameters is by normalizing equation (11) which leads to the following terms:

$$\Delta P^* = \frac{\frac{P_a - P_0}{\rho_s}}{\frac{U_p^2}{2 g_c}}$$

a pressure coefficient which compares the "pumped head" $\frac{P_a - P_0}{\rho_s}$ for the secondary flow to the "driving head" $\frac{U_p^2}{2 g_c}$ of the primary flow.

$$W^* = \frac{W_s}{W_p}$$

a flow rate ratio, secondary-to-primary mass flow rate.

$$T^* = \frac{T_s}{T_p}$$

an absolute temperature ratio, secondary-to-primary.

$$\rho^* = \frac{\rho_s}{\rho_p}$$

a flow density ratio. Note that since $P_s = P_p$ and the fluids are perfect gases, $\rho^* = \frac{T_p}{T_s} = \frac{1}{T^*}$.

$$A^* = \frac{A_s}{A_p}$$

area ratio of secondary flow area to primary flow area

$$\frac{A_p}{A_m}$$

area ratio of primary flow area to mixing stack cross sectional area

$\frac{A_w}{A_m}$

area ratio of wall friction area to
mixing stack cross sectional area

 K_p

momentum correction factor for
primary flow

 K_m

momentum correction factor for mixed
flow

 f

wall friction factor

With these non-dimensional groupings, equation (11) may be
written as

$$\frac{\Delta P^*}{T^*} = 2 \frac{A_p}{A_m} \left\{ \left[K_p - \frac{A_p}{A_m} \beta \right] - W^* (1 + T^*) \frac{A_p}{A_m} \beta \right. \\ \left. + W^{*2} T^* \left[\frac{1}{A^*} \left(1 - \frac{A_m}{2A^* A_p} \right) \beta - \frac{A_p}{A_m} \beta \right] \right\} \quad (11a)$$

where

$$\beta = K_m + \frac{f}{2} \frac{A_w}{A_m} .$$

For a given eductor geometry, equation (11a) may be expressed in the form

$$\frac{\Delta P^*}{T^*} = C_1' + C_2 W^* (T^* + 1) + C_3 W^{*2} T^* \quad (11b)$$

where

$$\begin{aligned} C_1 &= 2 \frac{A_p}{A_m} (K_p - \frac{A_p}{A_m} \beta) \\ C_2 &= -2 \left(\frac{A_p}{A_m} \right)^2 \beta \quad (11c) \\ C_3 &= 2 \frac{A_p}{A_m} \left\{ \frac{1}{A^*} \left(1 - \frac{A_m}{2 A^* A_p} \right) \beta - \frac{A_p}{A_m} \beta \right\} \end{aligned}$$

Equation (11b) may be expressed as a simple functional relationship

$$\Delta P^* = F(W^*, T^*) \quad (12)$$

A second means of determining the governing dimensionless parameters is through a dimensional analysis of the mixing process within the mixing stack. A presentation of this method by Ellin [1] yields the same simple functional relationship found in equation (12).

Two geometric dimensionless quantities were added to this investigation. The distance, S , from the primary flow nozzle exit to the mixing stack entrance and the distance,

x , from the entrance to the mixing stack, normalized with respect to the mixing stack diameter, D , were also defined as non-dimensional quantities. The two additional quantities are listed below:

$\frac{x}{D}$ ratio of the axial distance from the mixing stack entrance to the diameter of the mixing stack.

$\frac{s}{D}$ standoff; the ratio of the axial distance between the primary nozzle exit plane and the mixing stack entrance to the diameter of the mixing stack.

D. CORRELATION OF EXPERIMENTAL DATA

The previous experiments by Ellin [1], Moss [2], and Harrell [3] were done in facilities which did not have the capability for varying the primary flow temperature. Thus T^* , the ratio of the absolute secondary to primary flow temperatures was determined by the rise in temperature of the primary air in the blower supply and was near unity (approximately .85). A means of presenting the experimental data for a given geometric configuration in a form which results in a pseudo-independence of the dimensionless groupings P^* and W^* upon T^* was developed. From reference [1] a satisfactory correlation of P^* , T^* and W^* for all

temperatures and flow rates is

$$\Delta P^*/T^* = F(W^*T^*^{0.44}) \quad (13)$$

The details of the determination of 0.44 as the correlating exponent are presented in Appendix [B]. A plot of $\Delta P^*/T^*$ as a function of $W^*T^*^{0.44}$ from the experimental data yields the eductor's pumping characteristic curve. Variations in geometry will change the appearance of the pumping characteristic curve and facilitate a direct one to one comparison of pumping ability between various models and prototypes. For ease of discussion, $W^*T^*^{0.44}$ will henceforth be referred to as the pumping coefficient.

III. EXPERIMENTAL APPARATUS

Hot primary gas is supplied to the nozzle and mixing stack system by the combustion gas generator and associated ducting illustrated in Figures 3 and 4. The eductor system being tested is mounted in a secondary air plenum which facilitates the accurate measurement of the secondary air flow through the use of ASME long radius flow nozzles mounted on the secondary air plenum.

A. COMBUSTION GAS GENERATOR

The input air to the combustion gas generator is supplied by a Carrier Model 18P350 centrifugal air compressor. The compressor is located in an adjacent building and the input air is piped underground to an eight-inch inside diameter (ID) horizontal pipe with a butterfly-type shutoff valve and a globe-type bypass valve. All air demands for this testing can be met with the butterfly valve closed and the globe valve open as necessary.

The input air travels through an entrance transition piece that mates the eight inch ID compressor discharge piping with the four inch ID system piping. This nozzle is used to measure the primary air flow.

A portion of the input air travels straight through the piping to the exhaust stack while the remainder passes through the U-bend section to the combustion section. The

combustion section includes the burner can and igniter assembly from a Boeing model 502-6A gas turbine engine. Certain fuel system components from this engine were also utilized. The fuel system is shown schematically in Figure 5 and pictured in Figure 6.

After the air is heated in the combustion section, it is mixed with the cooler air after both pass through the turbine nozzle box containing the bypass air mixer. By controlling the relative amount of air passing through the burner and the amount of fuel to the burner, the exhaust stack temperature can be controlled. The procedure for system light-off and operation is included in Appendix A.

The hot gas then passes up the exhaust stack to the primary nozzles and the eductor system. A flow straightening section was added to the uptake stack to de-swirl the hot gas after it leaves the turbine nozzle box.

B. EDUCTOR AIR METERING BOX

Secondary air flow is measured with a large metering box designed to enclose the entire eductor assembly and act as an air plenum. A set of standard ASME long radius flow nozzles of varying cross-sectional areas were chosen to be mounted in the metering box away from the eductor.

The metering box was designed with interchangeable stack seal plates to enable variation of both exhaust and mixing stack sizes up to 1 foot in diameter. The seal plates also have a limited range of vertical movement to facilitate

exhaust and mixing stack alignment. The entire box was designed to be movable along an angle iron track parallel to the gas generator stack longitudinal centerline. This enables variation of the mixing stack to nozzle separation distance without adjustment and realignment of the mixing stack. The mixing stack end plate was also designed to be movable to allow centering for various mixing stack lengths. An access door was added for eductor adjustment. The metering box general arrangement is pictured in Figure 7 and a dimensional layout is given in Figure 8.

Appendix D of Reference [1] outlines the design and construction of the ASME long radius secondary air flow nozzles. Flexibility is provided this secondary air flow measuring system by utilizing three different flow nozzle sizes: four of four inch throat diameter, three of two inch throat diameter and three of one and a half inch throat diameter, various combinations of which produce a wide variety of secondary cross sectional flow areas.

Mounted inside the air metering box are supports for the uptake stack and mixing stack. The interior of the air metering box is pictured in Figures 9 and 10.

C. INSTRUMENTATION

The performance of an eductor is calculated from pressure and temperature data taken at various points in the system. Necessary measurements include the primary mass flow rate (air and fuel), the secondary mass flow rate, the uptake

stack Mach number, and the mixing stack temperature and pressure profiles.

Pressure measurements are made with one of several manometers. Available are a 20 inch mercury upright manometer, a 20 inch water upright manometer and a two inch inclined water manometer. A manifold system allows selection of the instrument of proper range. Atmospheric pressure (PA) is measured with a mercury barometer. A schematic of the pressure measurement system is shown in Figure 11. The manometer board and manifold system are pictured in Figures 12 and 13.

Temperature measurements are made with either copper-constantan or chromel-alumel thermocouples wired to Newport model 267A digital pyrometers. The pyrometers are capable of monitoring 18 inputs each through barrel-type selector switches. Secondary air or ambient air temperature (TAMB) was measured with a mercury-glass thermometer. A schematic of the temperature measurement system is shown in Figure 14.

Fuel flow measurement is made with a Cox Instrument model V40-A vortex flowmeter coupled to an Anadex Instruments model CPM-603 frequency counter.

The calculation of the primary air mass flow rate requires the measurement of the inlet absolute pressure to the transition nozzle (PNH), the pressure drop across this nozzle (DELPN), and the inlet air temperature. The calibration of this nozzle for the measurement of mass flow rate

as a function of these two pressure readings was previously accomplished by Ross and details of this calibration can be found in Reference [4]. The calibration curve is shown in Figure 15.

The calculation of the secondary air mass flow rate requires the measurement of the ambient pressure and temperature, and the pressure drop across the secondary air nozzles (PA-PS). The secondary air plenum is equipped with pressure taps mounted both in the rear section containing the air metering nozzles and in the front section containing the eductor under test. No measurable difference was detected between the two taps so the pressure tap nearest the eductor was used in the data runs.

The uptake stack Mach number calculation necessitates the measurement of the uptake temperature and pressure as well as the primary mass flow rate. The uptake temperature (TUPT) is measured with a chromel-alumel thermocouple inserted through the primary nozzle plate at the centerline and protruding approximately two inches into the stack. Uptake pressure (PEH) is measured through a four-point averaging pressure tap located approximately seven and one half inches (one diameter) upstream of the eductor nozzle entrance.

The mixing stack was constructed with pressure taps every one-half diameter down the length of the stack. The mixing stack pressure distribution (PMIX) is easily measured. Chromel-alumel thermocouples were welded every one-half

diameter to the outside of the mixing stack to facilitate measurement of the temperature distribution.

Temperature profiles at the exit plane of the primary nozzles and the mixing stack are obtained using a chromel-alumel thermocouple mounted on an adjustable traversing mechanism shown in Figure 16.

D. EDUCTOR SYSTEM

The eductor system includes the eductor nozzles and the mixing stack. Figure 1 shows the general eductor system arrangement.

1. The Mixing Stack

The mixing stack was constructed of 7.5 inch OD, 0.188 inch wall thickness stell pipe. Two lengths were tested. First a 3 diameter long (21.366 inch) stack was tested then a 2.5 diameter long (17.805 inch) stack was machined from the long stack and tested.

The mixing stack is supported inside the secondary air plenum by means of an adjustable saddle and held in place by an adjustable metal band. The stack is also supported by the adjustable collar at the plenum wall. This collar can be seen in Figure 16. The adjustable saddle and collar allows alignment of the mixing stack with the primary nozzles.

2. Eductor Nozzles

The eductor nozzles investigated consisted of two different four-nozzle geometries previously tested. The

first geometry was a mixing stack to total nozzle area ratio of 3:1 and the second was a mixing stack to total nozzle area ratio of 2.5:1. The nozzle elements were machined from steel tubing and welded to a circular nozzle plate which was bolted onto the exhaust stack. The nozzles are shown schematically in Figures 17 and 18 and are pictured in Figures 19 and 20.

3. Standoff Ratio (S/D)

Both geometries investigated were tested at an S/D value of 0.5. Previous testing [2] has shown this to be approximately the optimum standoff ratio.

IV. EXPERIMENTAL METHOD

The pumping coefficient, $W*T^{*0.44}$, provides the basis for the analysis of parameter variation effects on eductor pumping. Figure 21 graphically illustrates the eductor pumping characteristic curve defined by the experimental data correlation of equation (13). Design of the experimental apparatus facilitates determination of the dimensionless parameters in the experimental correlation with the exception of the secondary flow rate at the operating point. For the operational eductor system, little or no restriction of the secondary flow is present. Modeling of this operating point precludes the use of restrictive flow measuring devices, such as ASME flow nozzles used in model tests. The technique of determining the pumping coefficient at the operating point, then, is first to establish the pumping characteristics of the eductor system. This is accomplished by varying the secondary air flow rate from zero to its maximum measurable value, using the ASME flow nozzles mounted in the secondary air plenum and recording the temperatures and pressures required to calculate the corresponding dimensionless parameters. The "open to the environment" condition is then simulated by removal of the end plates on the secondary air plenum. Extrapolation of the characteristic curve to its intersection with the $W*T^{*0.44}$ axis locates the pumping coefficient for the operating point of the eductor system.

The mixing stack pressure and temperature distributions were obtained from a series of pressure taps and thermocouples at half diameter distances along the mixing stack. These pressures and temperatures were recorded at the "open to the environment" condition and then plotted versus the ratio of tap location (X) to mixing stack diameter (D) for each geometry tested.

A measure of the degree of mixing of the primary and secondary flows was obtained by plotting the mixing stack exit plane temperature profile at the "open to the environment" condition. Two temperature profile traverses were made. A greater degree of mixing of the flows will result in a flatter temperature profile.

V. DISCUSSION OF EXPERIMENTAL RESULTS

The intent of this investigation, as discussed earlier, was to conduct hot flow tests of exhaust eductor systems in an attempt to meet three primary objectives. The first objective was to test and verify the proper operation of the hot gas generator. The second was to validate the use of the correlating parameter ($W*T^{*44}$). The third objective was to obtain temperature data on the mixing stack wall and of the exhaust gas at the mixing stack exit plane.

Initial testing of the hot gas generator was concerned with ensuring that a sufficient range in uptake temperatures could be obtained while maintaining the desired Mach number. Uptake temperatures from 550°F to about 900°F were easily obtained. The lower limit exists due to the requirement for a minimum fuel pressure to the fuel nozzle. An attempt to lower the uptake temperature below 550°F necessitates too low a fuel flow rate to achieve proper fuel atomization and smoking or loss of ignition occurs. The upper limit exists because an attempt to go to higher uptake temperatures requires burner temperatures above the 1500°F maximum. Lower uptake temperatures are obtainable at higher Mach numbers, as are higher uptake temperatures at lower Mach numbers.

Primary nozzle exit plane temperature profiles taken by Ross [4] indicated that the exhaust was swirling up the exhaust stack. A flow straightener consisting of two wire

screens placed two inches apart was installed in the uptake stack one foot from the nozzle box. The temperature profiles shown in Figure 22 are basically consistent from one nozzle to another and are considerably flatter, indicating that the flow straightener is effective in taking the swirl out of the exhaust flow.

A temperature profile across the uptake stack at the mid-length point was taken and is presented in Figure 23. The temperatures taken at this point are normalized with a reference temperature taken on the stack centerline $1\frac{1}{2}$ inches upstream of the primary nozzles. The temperature profile is essentially flat, with the maximum temperature deviation less than 2%. The average value of this curve is approximately one. The reference position was therefore used to measure the uptake temperature, since it is essentially equal to the average mid-length temperature.

Verification of the experimental setup was made by duplicating previous cold flow results using the hot rig under cold flow conditions. Figure 24 shows the results of the cold flow test done by Moss [2] and the results obtained with this setup for an identical geometry but different scale. The pumping coefficients at the open to the environment condition ($P^*/T^* = 0$) differ by only 1.5%. Figure 25 gives a similar comparison for data taken by Staehli and Lemke [5] for a different identical geometry and different scale. Again the difference at $P^*/T^* = 0$ is about 1.5%.

Pumping performance data was taken at a range of uptake temperatures from 150°F (cold flow) to 850°F. Figures 26 and 27 show that although the performance data are contained within a narrow band, a temperature related trend is present. The cold flow data is at the upper edge of the band with data at increased temperature fanning out below it. This result is not predicted by the one-dimensional theory discussed earlier and is an area of possible future study. Possible causes include temperature effects on either primary or secondary air flow measurement. For example, a leak in the air metering box that is accentuated with temperature would lead to an underestimation of W_s which would lower W^* and in turn lower W^*T^{*44} , shifting the performance plot. Figures 28 through 37 give the pumping performance plots at each condition individually. The pumping coefficients at the open to the environment condition are all within 8% of one another. The pumping coefficients of the $A_m/A_p = 2.5$, $L/D = 2.5$ geometry (to be called the "2.5" geometry) are about 30% lower than those of the $A_m/A_p = 3.0$, $L/D = 3.0$ geometry (to be called the "3.0" geometry). This agrees with data obtained by Moss [2] and Staehli and Lemke [5].

Temperature and pressure data was acquired every half diameter down the length of the mixing stack. The pressure distributions presented in Figures 38 and 39 show a rise in pressure down the stack indicating that the degree of mixing of the primary and secondary flows increases down the stack. Previous cold flow data gives similar results.

The mixing stack axial temperature distributions are given in Figures 40 and 41. Figure 42 shows the temperature distributions at $T_{UPT} = 850^{\circ}\text{F}$ and $A_m/A_p = 3.0$ and $L/D = 3.0$ compared to the same uptake temperature and $A_m/A_p = 2.5$, $L/D = 2.5$. The smaller nozzles ($A_m/A_p = 3.0$) cool the stack more effectively than the larger ones, as predicted by the greater pumping coefficient achieved by this geometry. The maximum stack temperature for the 3.0 geometry is 368°F compared to 428°F for the 2.5 geometry at the same uptake temperature ($T_{UPT} = 850^{\circ}\text{F}$).

Temperature profiles taken at the exit plane of the mixing stack and presented in Figures 43 and 44 show that the peak exhaust temperature for the 3.0 geometry is 11% lower than the 2.5 geometry. Again, this is as expected based on the larger pumping coefficient. These measurements indicate that the peak temperatures occur about one-half inch to the right of the stack centerline. A calculation of the misalignment angle required to produce a one-half inch offset gave an angle of about $1\frac{1}{2}$ degrees. A check of stack alignment revealed a small alignment error which would corroborate the offset. It is not felt that this offset had any noticeable effect on any other data taken.

Table 1 gives results of the findings for each geometry tested.

VI. CONCLUSIONS

The experimental results were presented in Section V and the resulting conclusions are summarized here.

- A. The hot gas generator performs as desired. It was verified that a wide range of uptake temperatures could be easily obtained. The system proved to be stable, repeatable and relatively simple to operate.
- B. The pumping coefficient ($W*T^{*44}$) is an acceptable parameter to measure a system's pumping performance. The performance plots were contained within a narrow region, which shows that the use of cold flow data presented in this way accurately correlates to hot flow tests. Cold flow pumping coefficients were corroborated with hot flow data.
- C. Mixing stack wall and exhaust temperature data follow the trends predicted by cold flow testing. The $A_m/A_p = 3.0$, $L/D = 3.0$ geometry cools the exhaust gas more effectively than the 2.5 geometry.

VII. RECOMMENDATIONS

In addition to meeting the objectives mentioned in Section V, this research has also raised questions to be solved by further research. Some recommendations for further study are listed below.

- A. A study should be done to determine the cause of the slight temperature related spread in the performance data.
- B. Previous studies have used exhaust velocities as a measure of the mixing and hence, as a measure of the exhaust temperature profiles. Previously obtained velocity profiles predict a slight temperature depression at the stack centerline that is not present in the data obtained in this study. Exit velocity profiles should be obtained, allowing a direct comparison of velocity and temperature data.
- C. The end plate of the air metering box should be redesigned to allow greater freedom of mixing stack alignment.

VIII. FIGURES

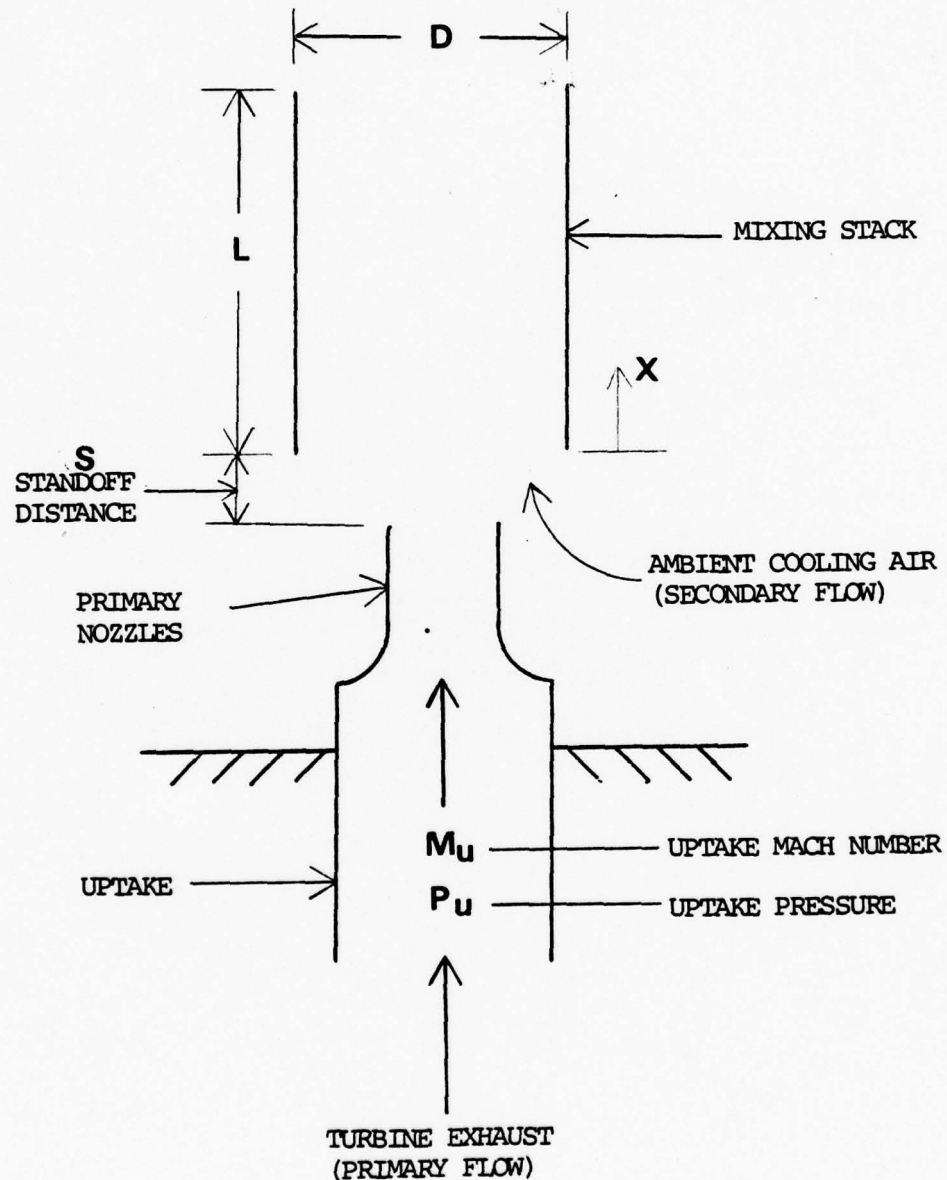


FIGURE 1. Schematic Diagram of Simple Exhaust Gas Eductor

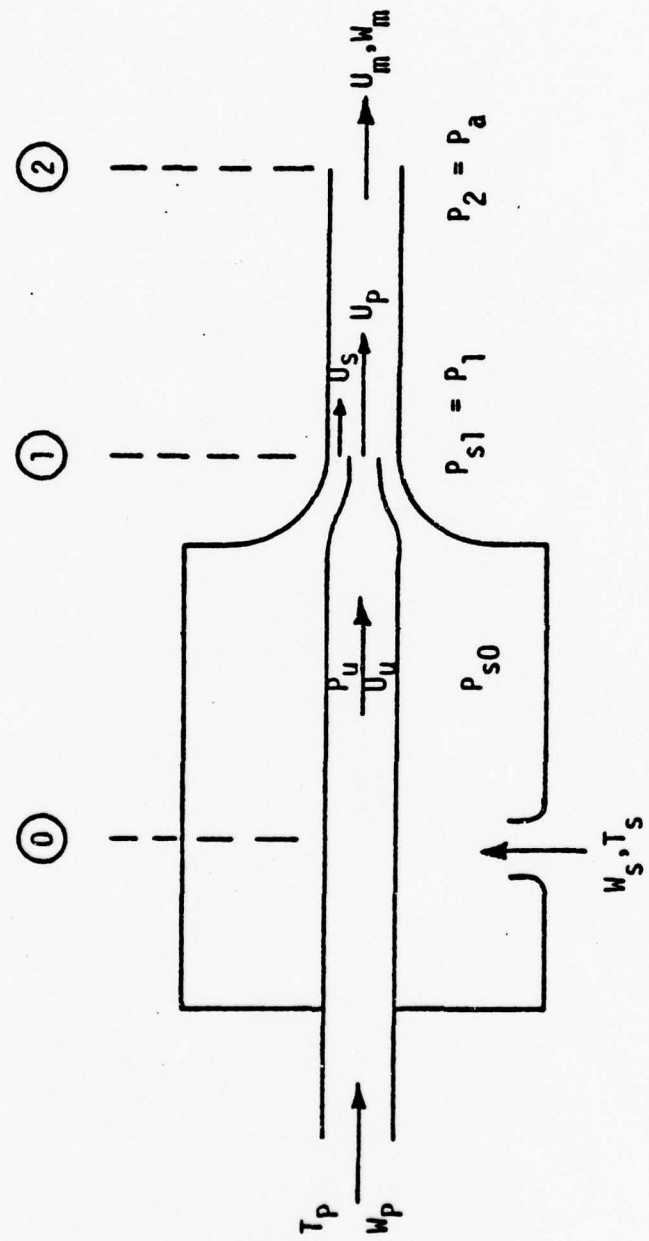


FIGURE 2. Simple Single Nozzle Eductor System.

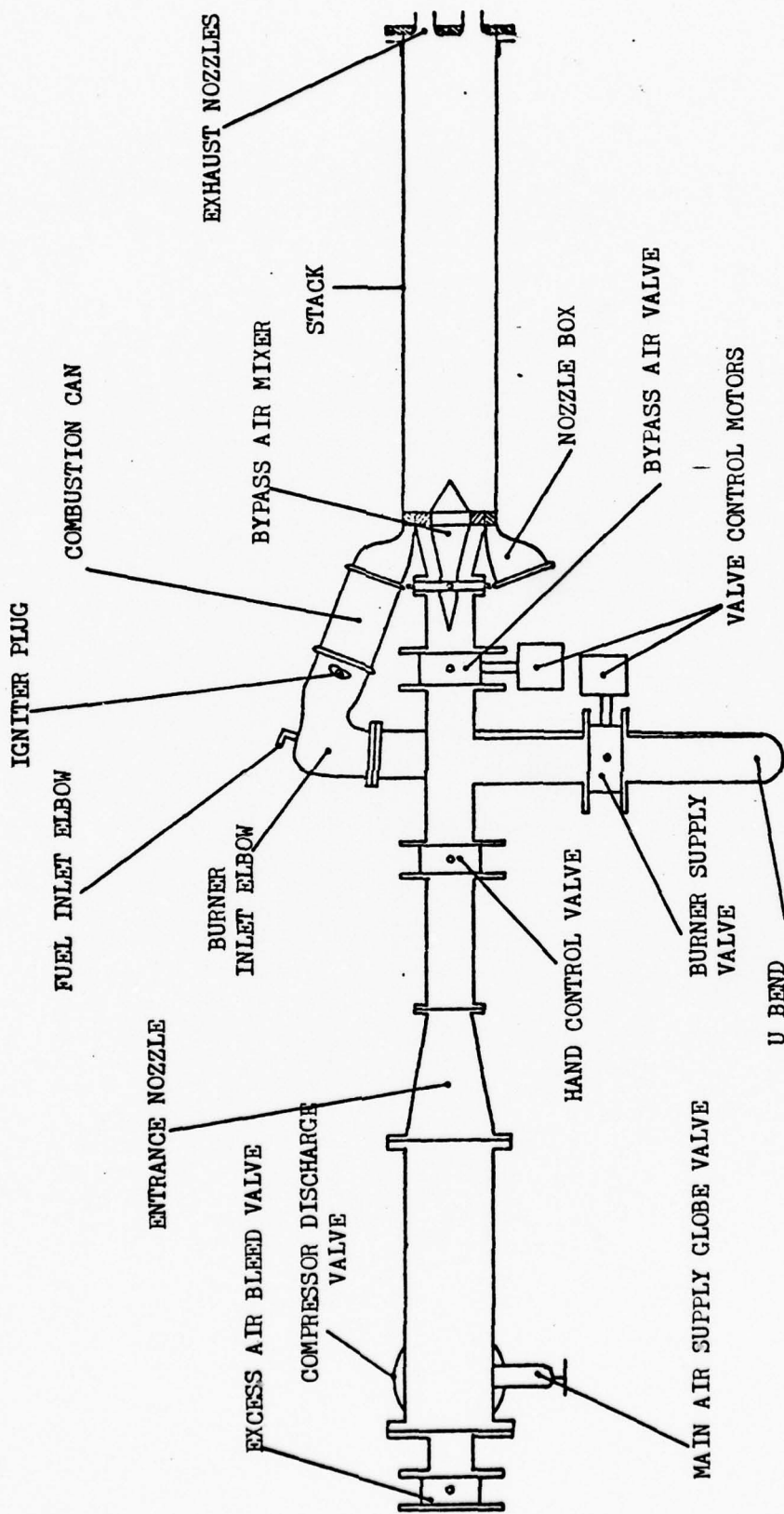


FIGURE 3. Schematic Diagram of Combustion Gas Generator

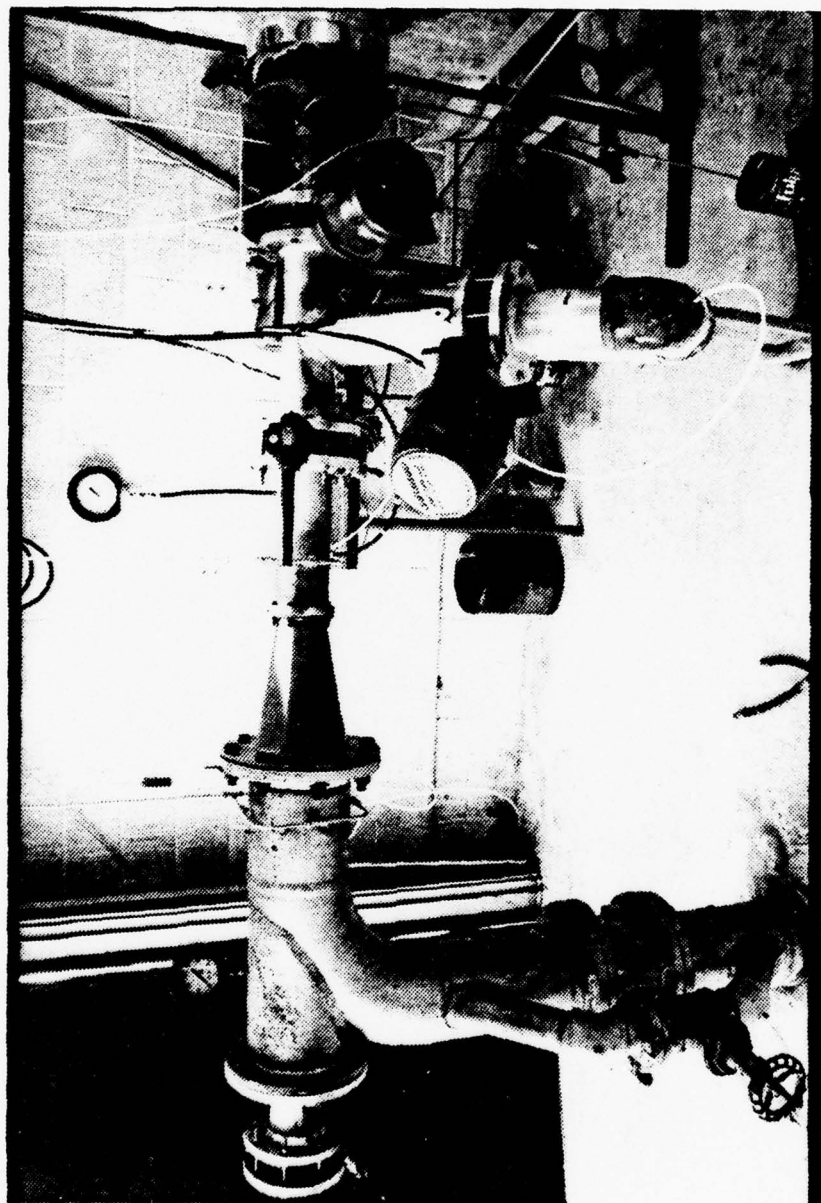


FIGURE 4. Combustion Gas Generator

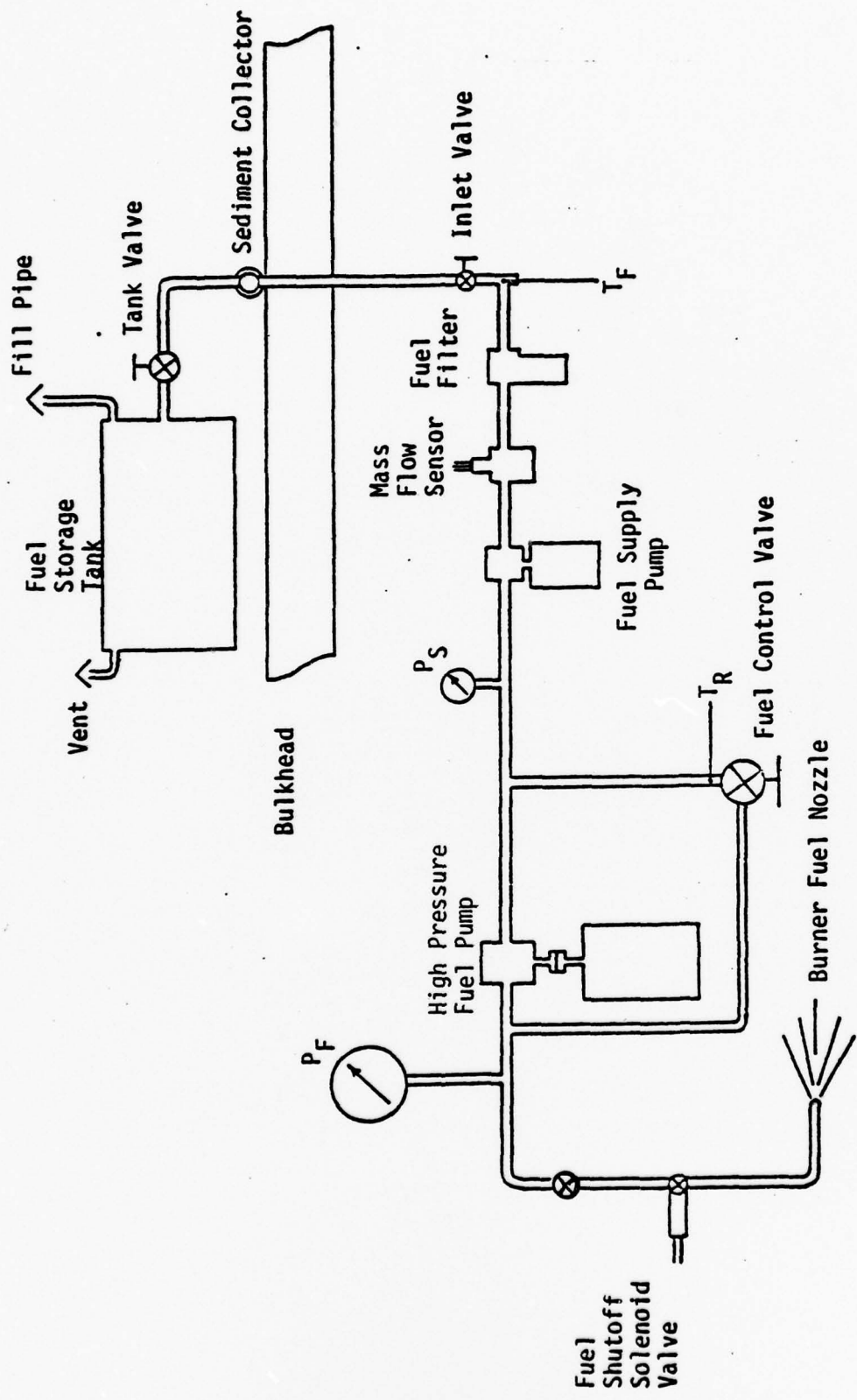


FIGURE 5. Gas Generator Fuel System

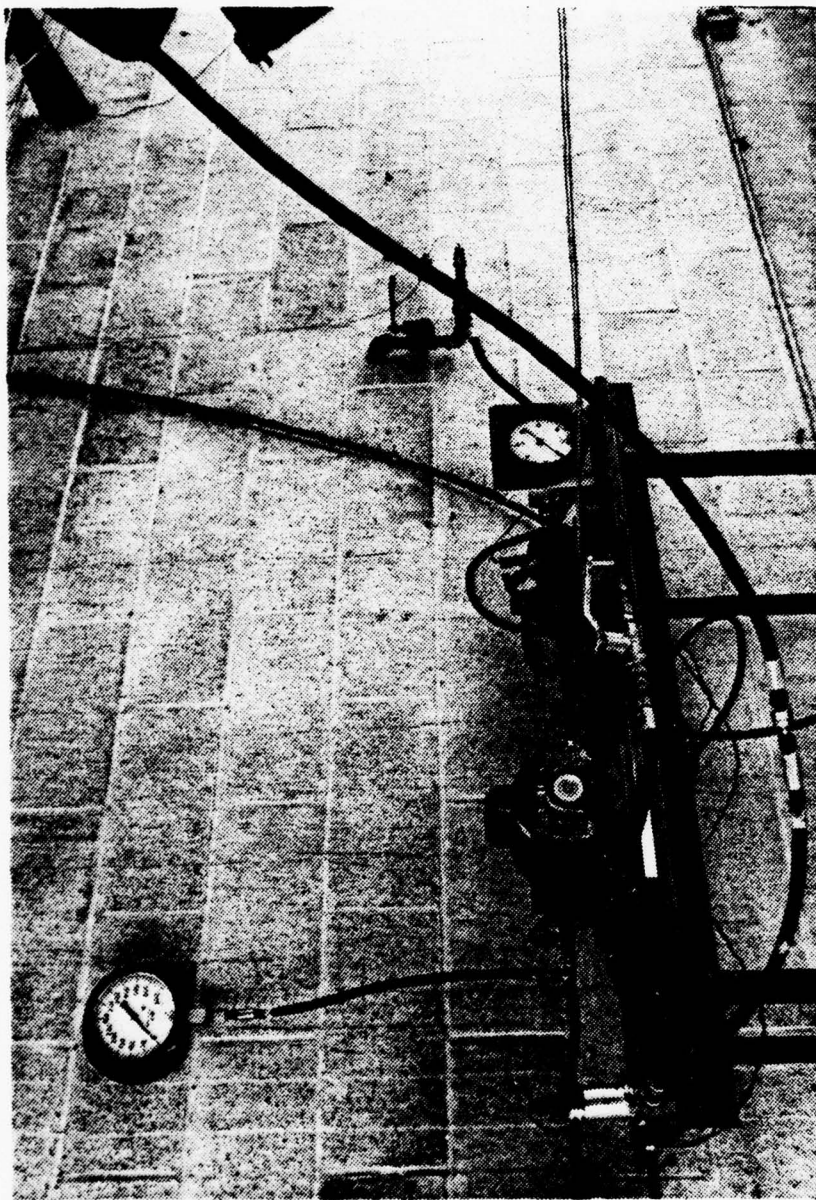


FIGURE 6. Gas Generator Fuel Supply System

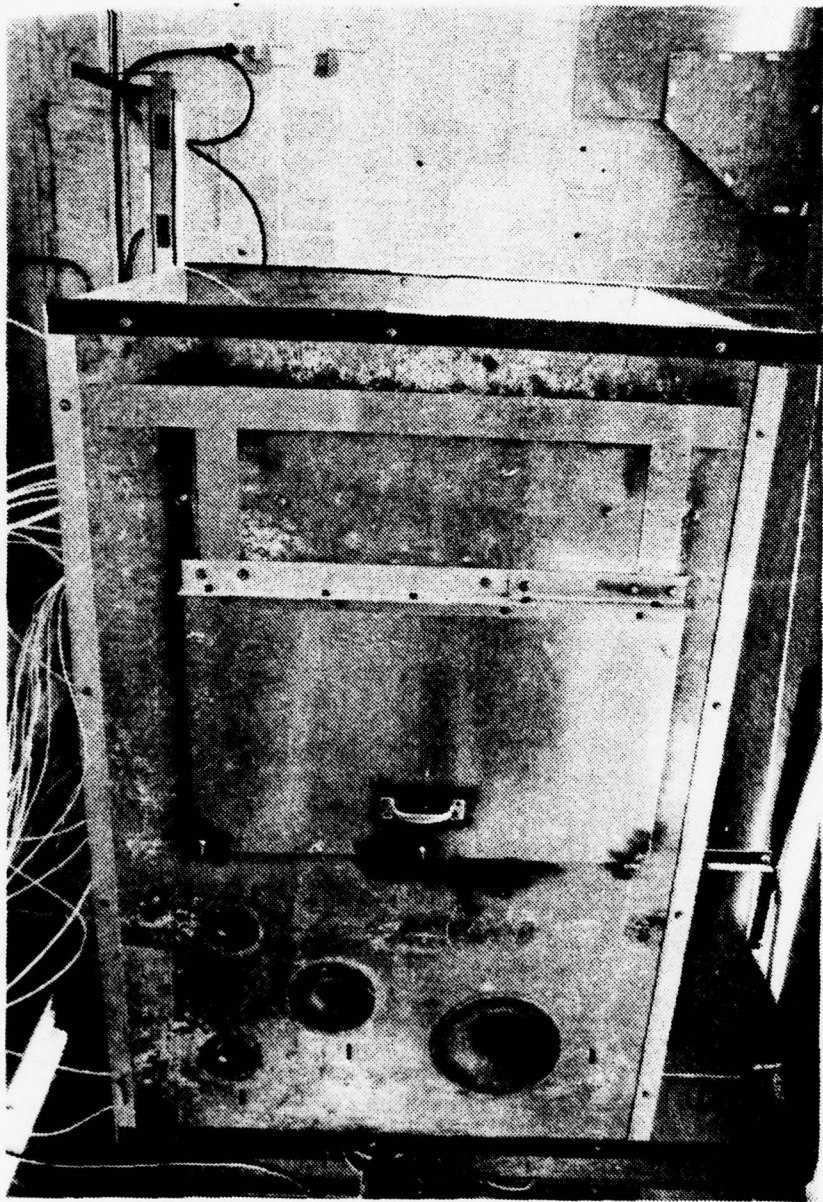
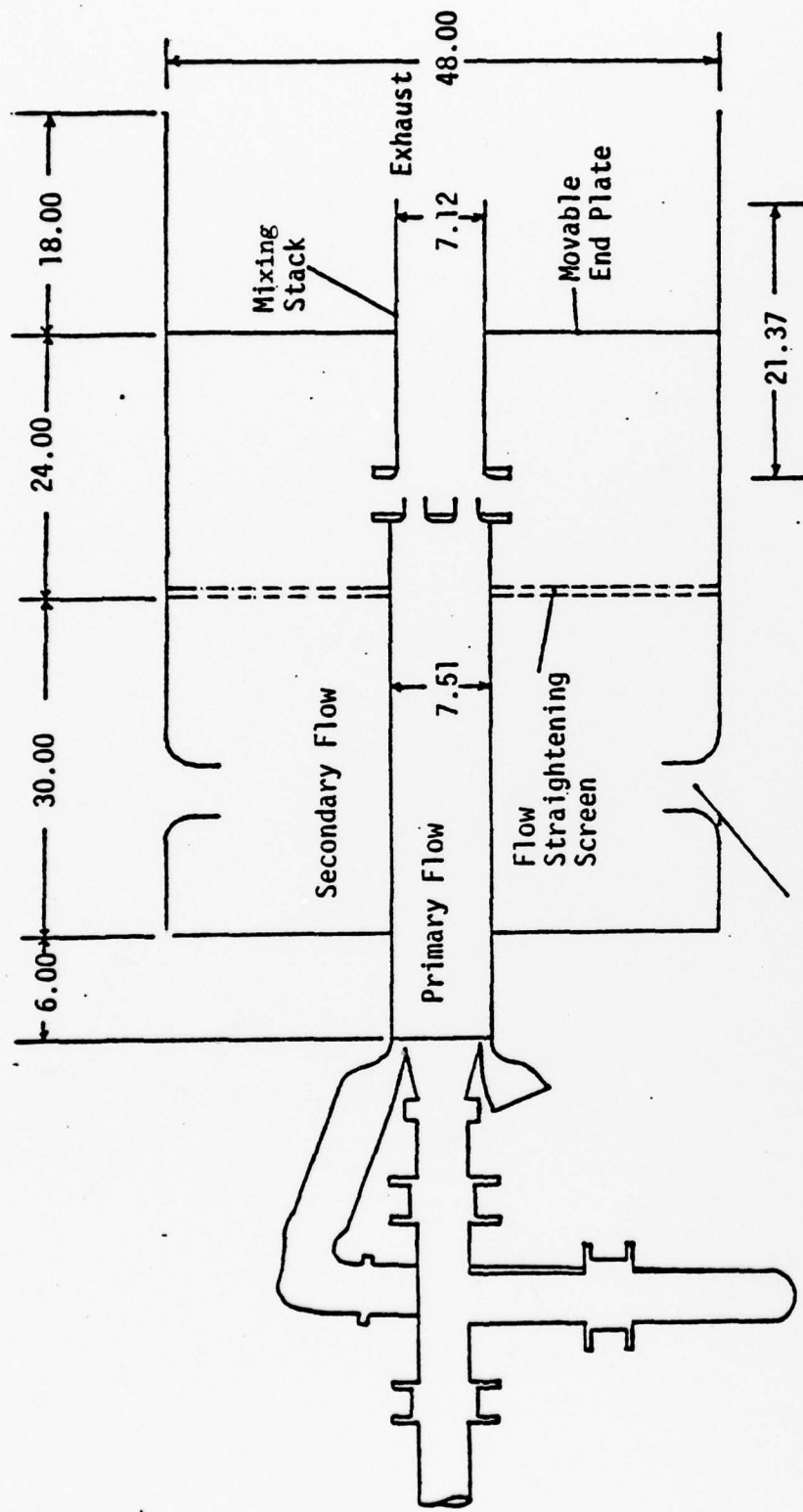


FIGURE 7. Eductor Air Metering Box



Overall box dimensions: 48x48x72
All dimensions in inches.

FIGURE 8. Eductor Air Metering Box Arrangement

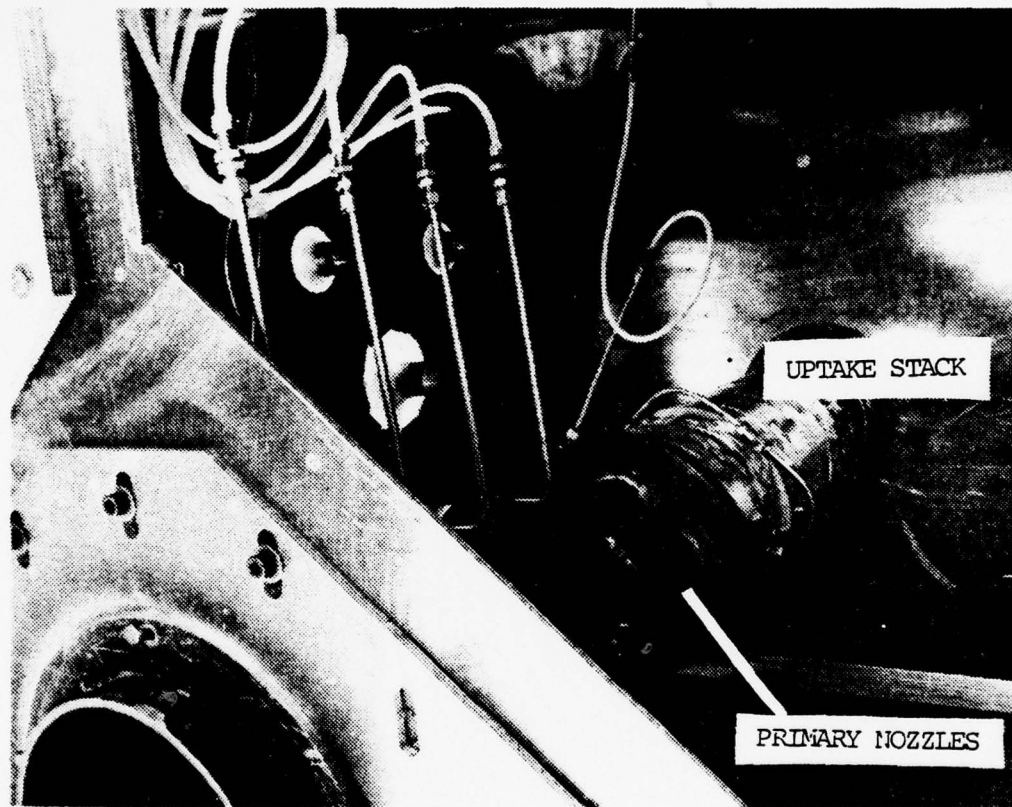


FIGURE 9. Interior of Air Metering Box Showing Uptake Stack and Primary Nozzles

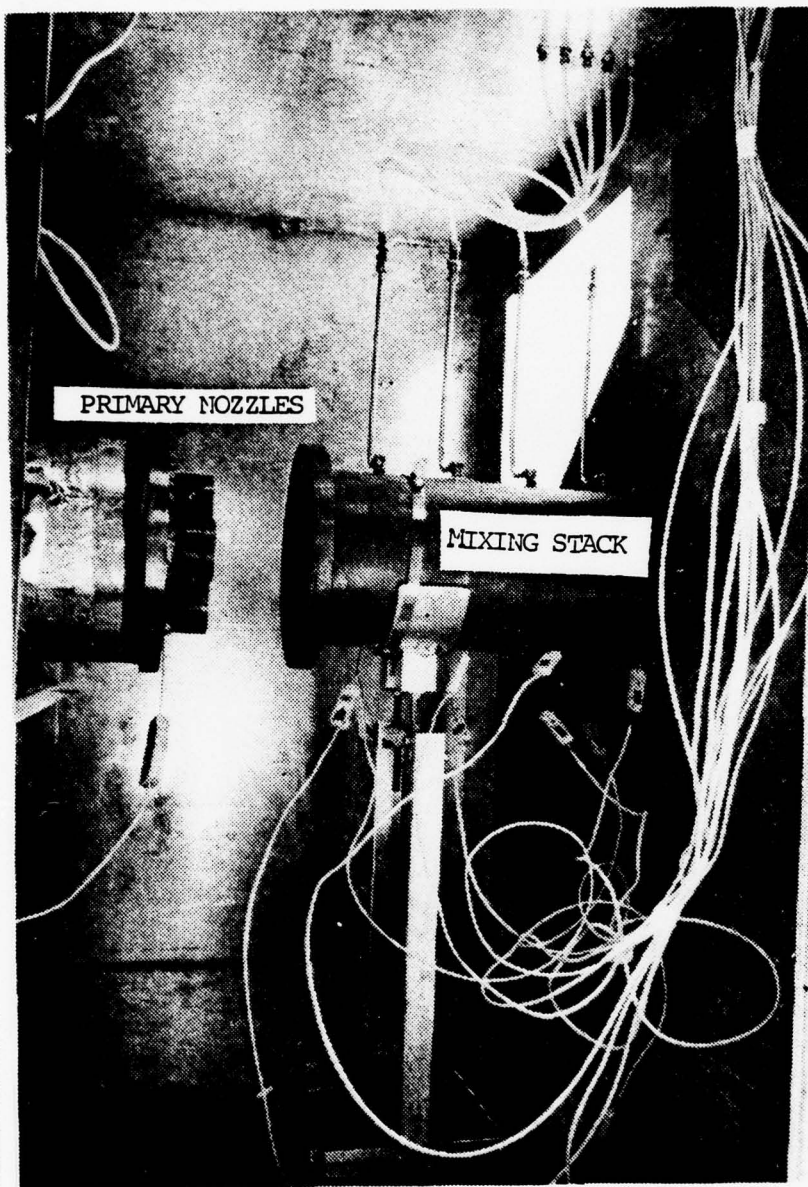


FIGURE 10. Interior of Air Metering Box Showing Mixing Stack and Primary Nozzles

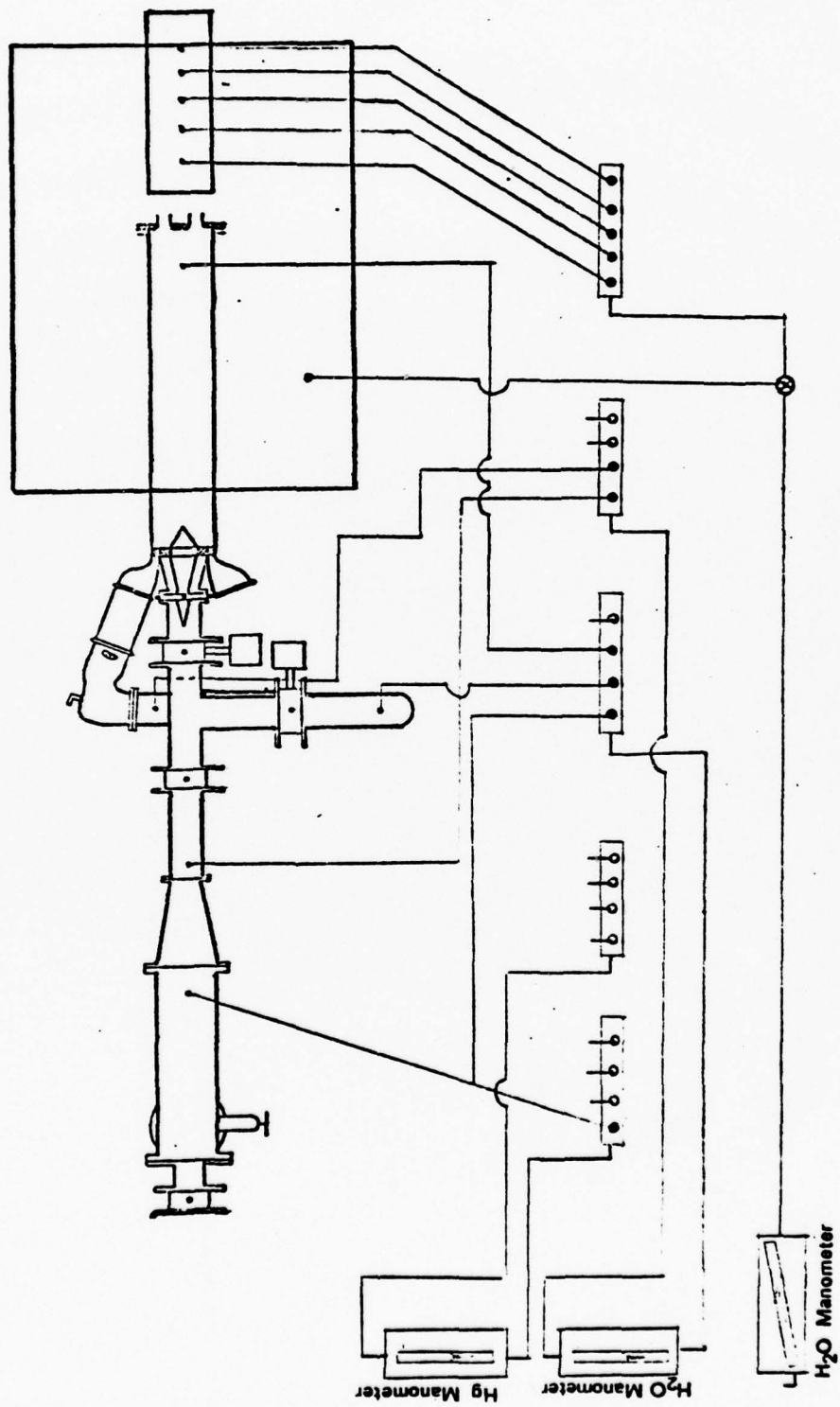


FIGURE 11. Schematic Diagram of Pressure Measurement System

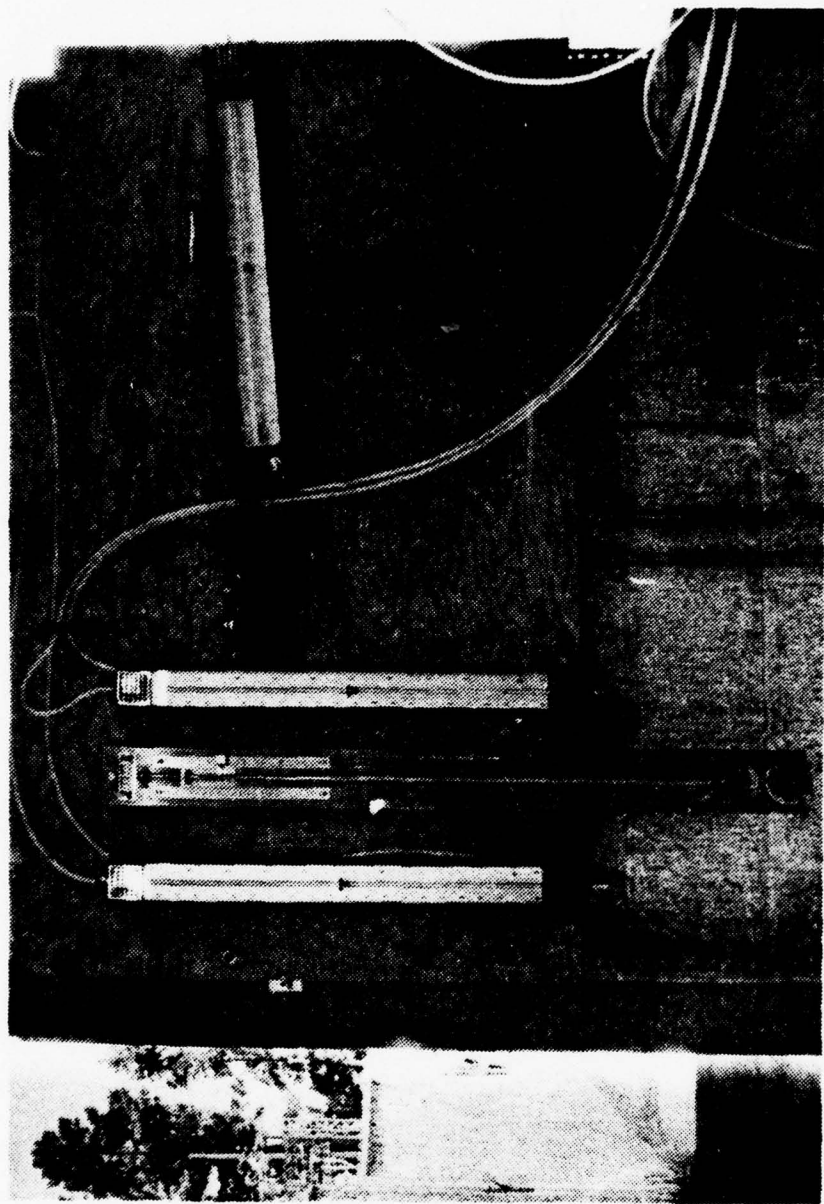


FIGURE 12. Manometer Board

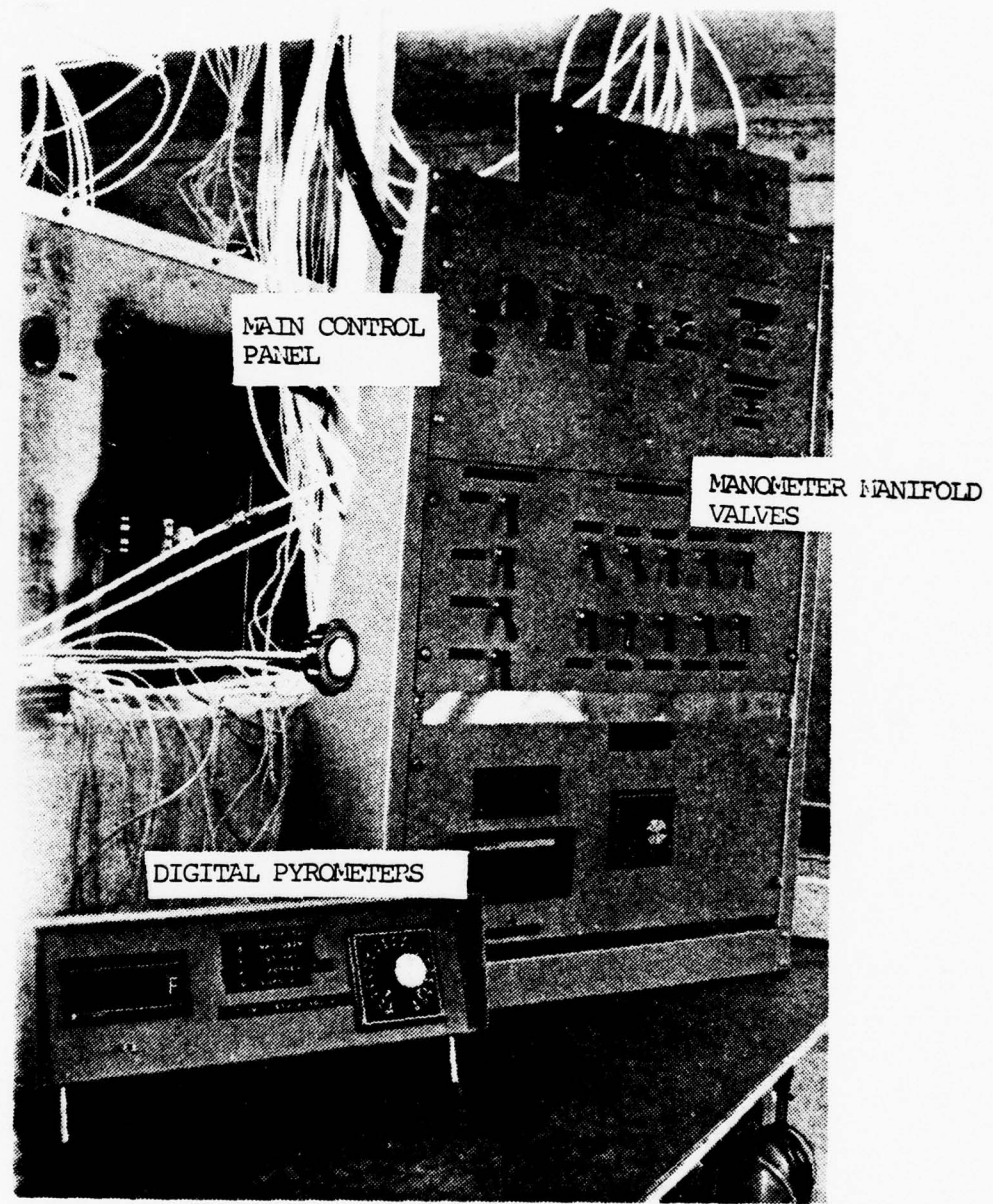


FIGURE 13. Main Control Panel, Digital Pyrometers, Manometer Manifold Valves

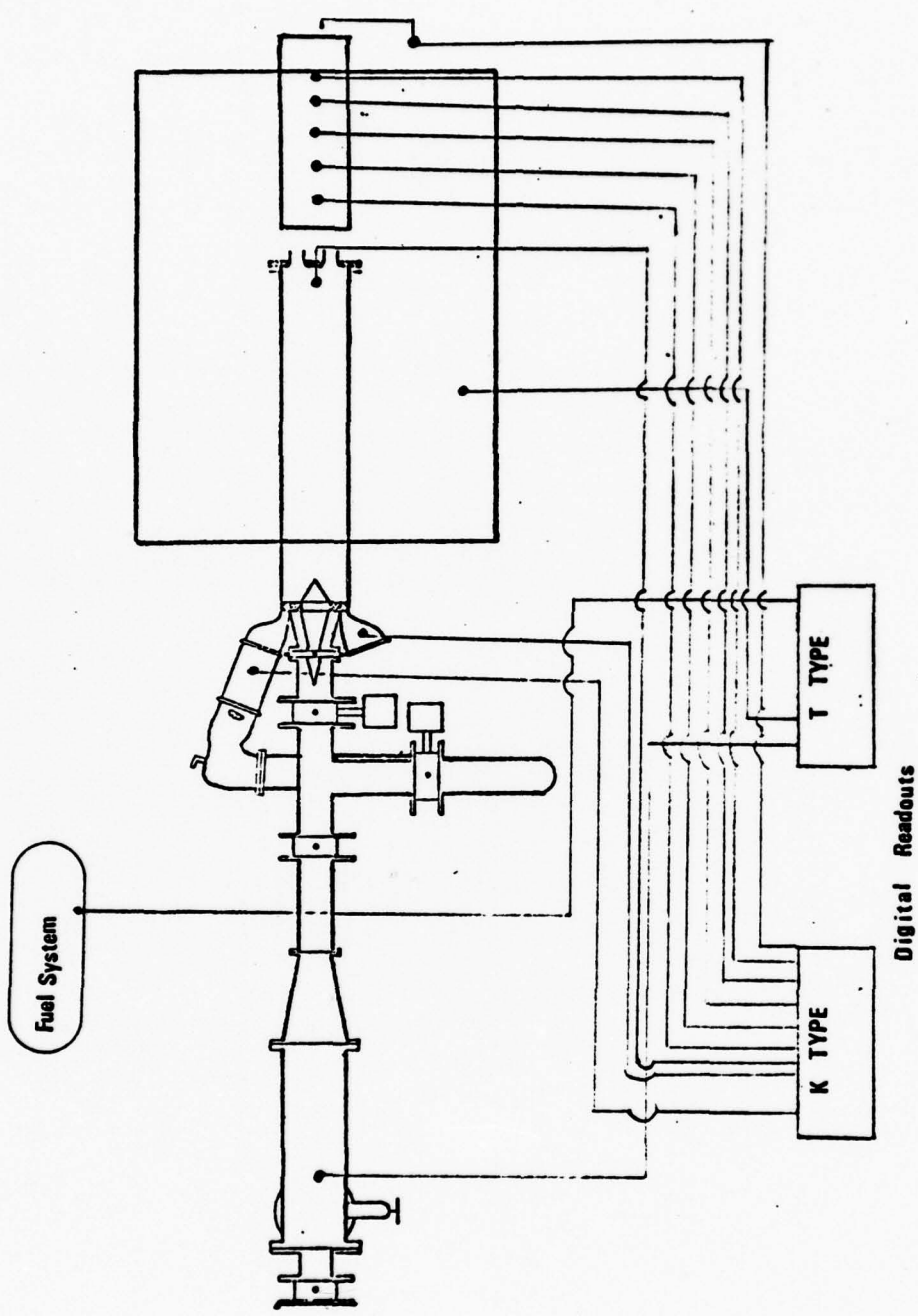


FIGURE 14. Schematic Diagram of Temperature Measurement System

Digital Readouts

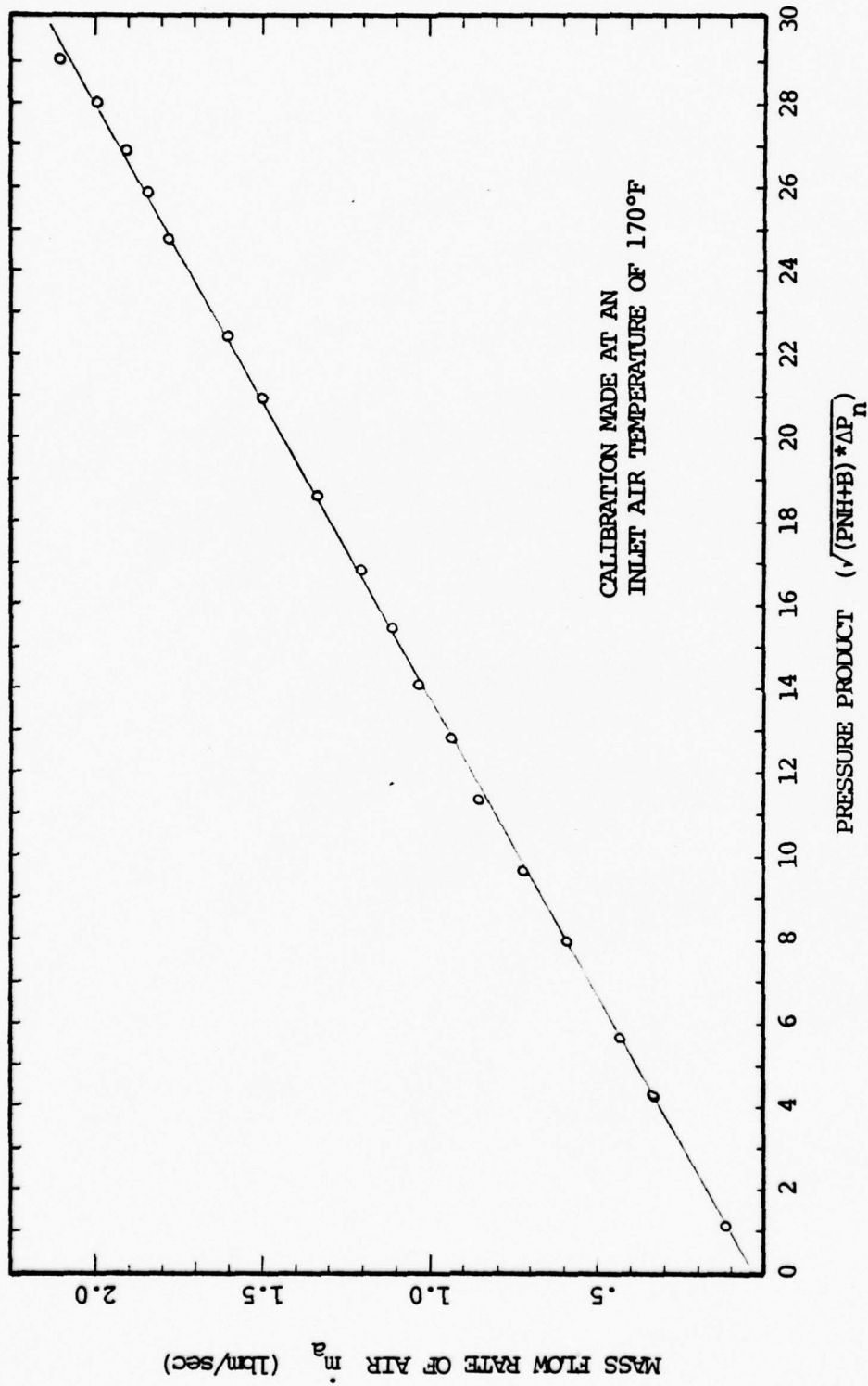


FIGURE 15. Entrance Nozzle Calibration Curve (Table III)

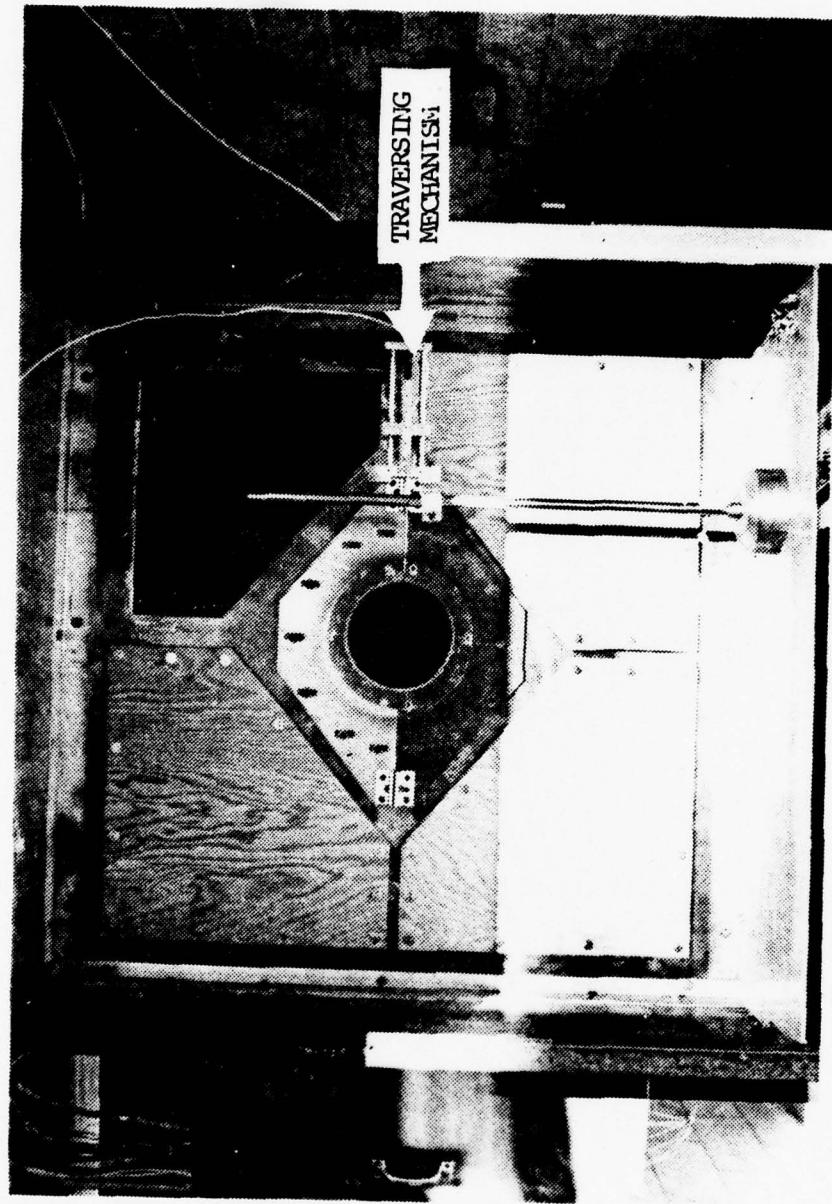


FIGURE 16. Air Metering Box End Plate and Mixing Stack Collar

$$\frac{A_m}{A_p} = 2.5 \quad \frac{A_m}{A_p} = 3.0$$

A	1.251	1.154
B	1.126	1.024
C	1.770	1.770
D	2.520	2.520
E	.250	.250
F	.125	.125
G	.500	.500

All dimensions in inches

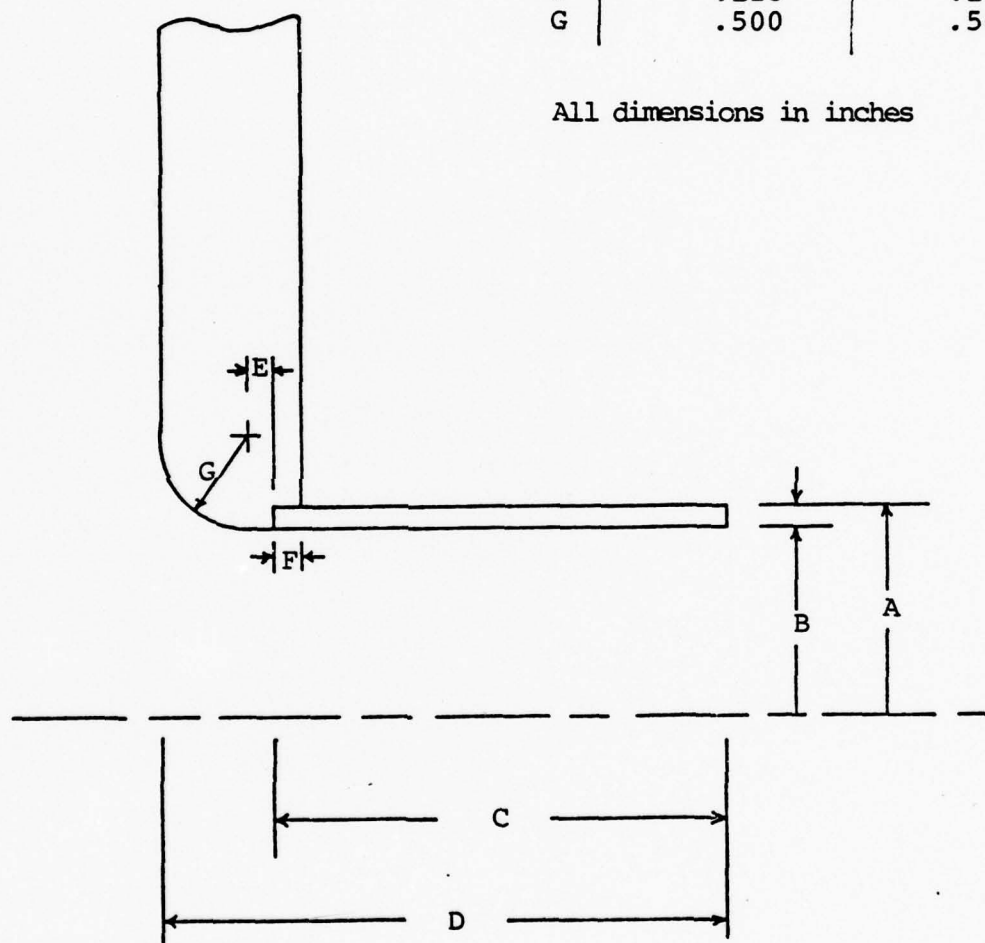


FIGURE 17. Dimensional Diagram of Primary Flow Nozzles

	$A_m/A_p = 2.5$	$A_m/A_p = 3.0$
A	10.000	10.000
B	45°	45°
R_1	1.126	1.029
R_2	1.251	1.154
R_3	2.070	2.070
R_4	4.509	4.509
R_5	3.729	3.729
R_6	4.108	4.108

All dimensions in inches

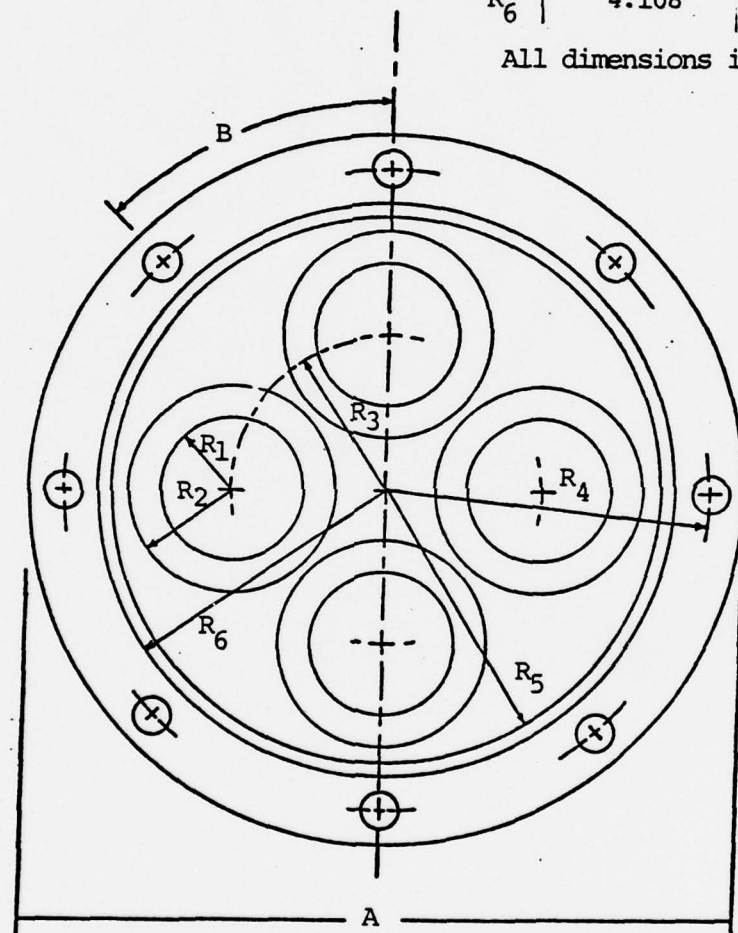


FIGURE 18. Dimension Diagram of Primary Flow Nozzle Plate



FIGURE 19. Primary Flow Nozzle Plate (Back View)

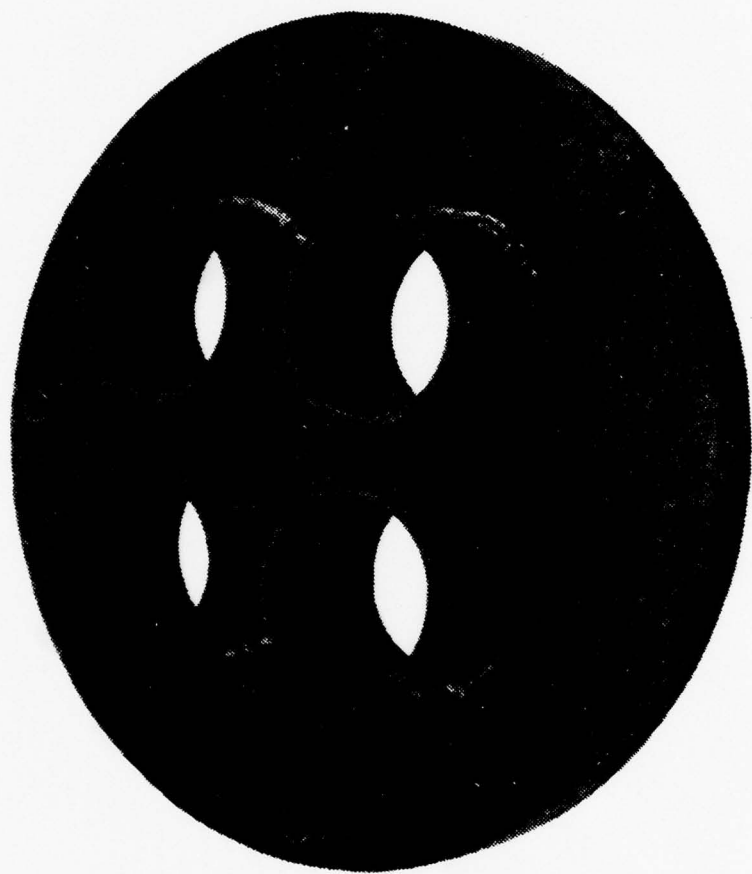


FIGURE 20. Primary Flow Nozzle Plate (Front View)

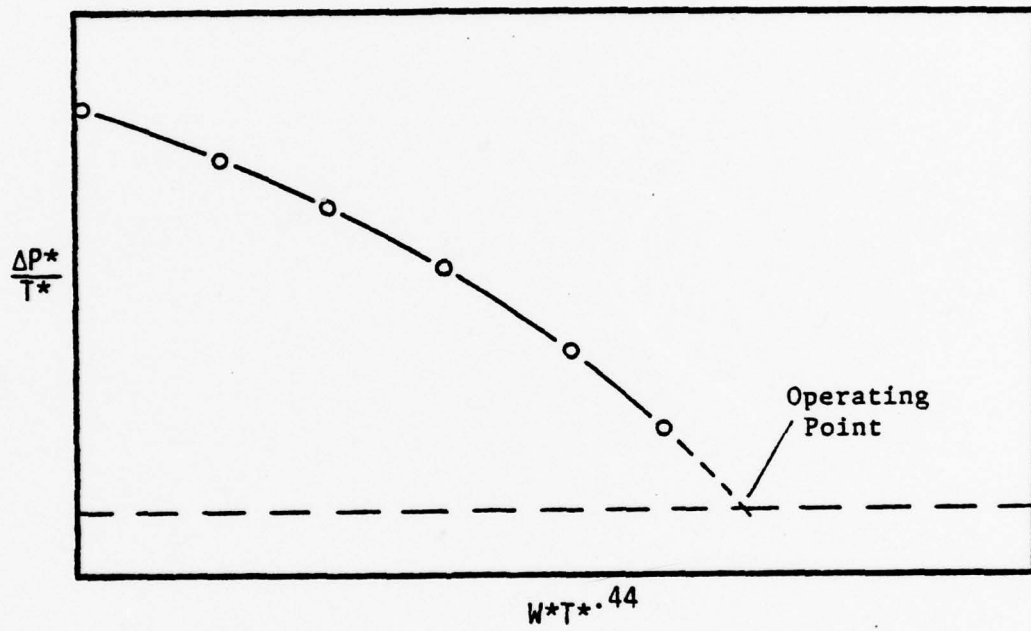


FIGURE 21. Illustrative Plot of the Experimental Data Correlation in Equation (14).

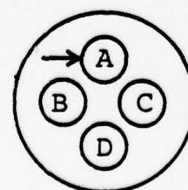
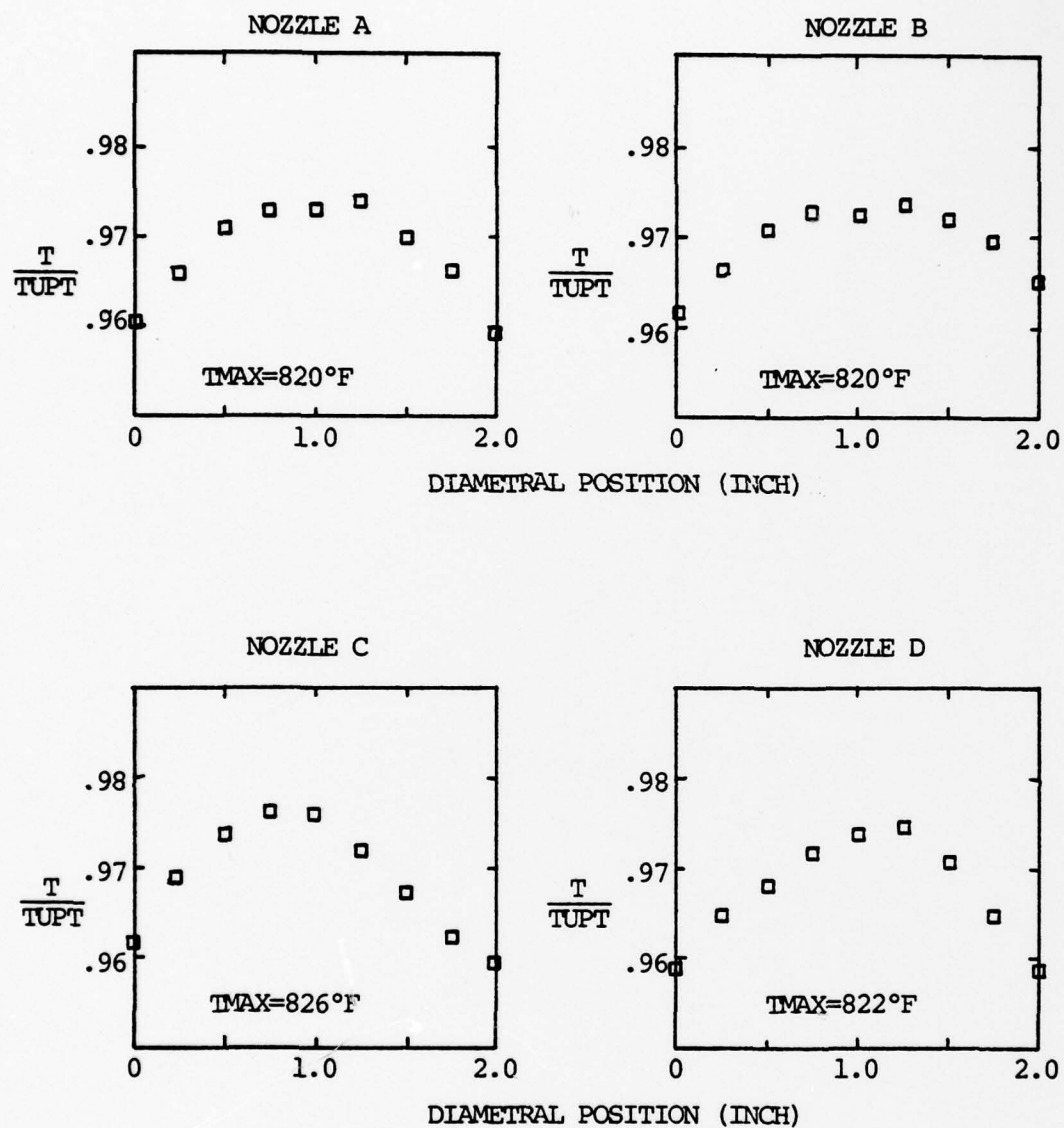


FIGURE 22. Primary Flow Nozzle Temperature Profiles
(Table III)

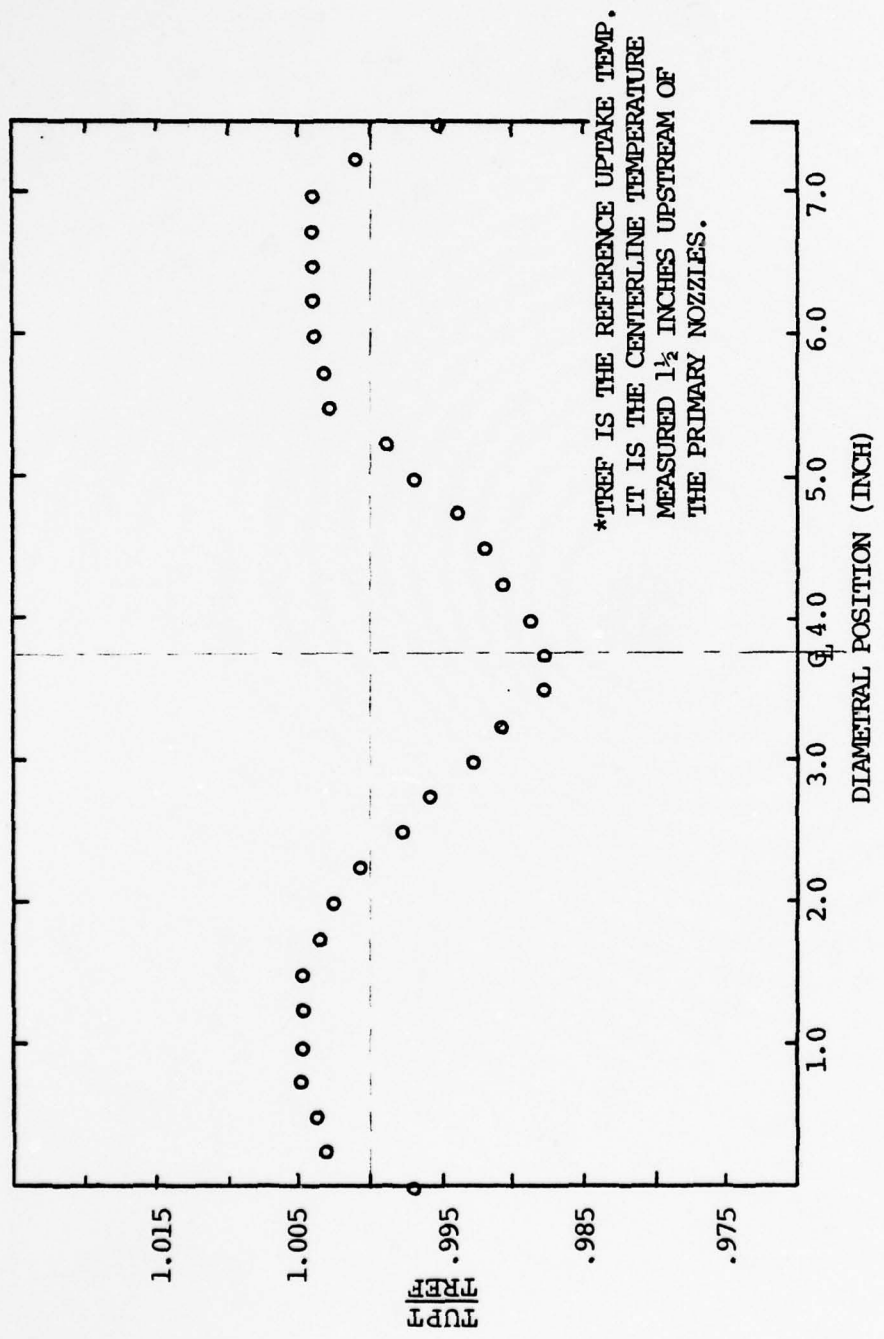


FIGURE 23. Uptake Stack Temperature Profile (Table IV)

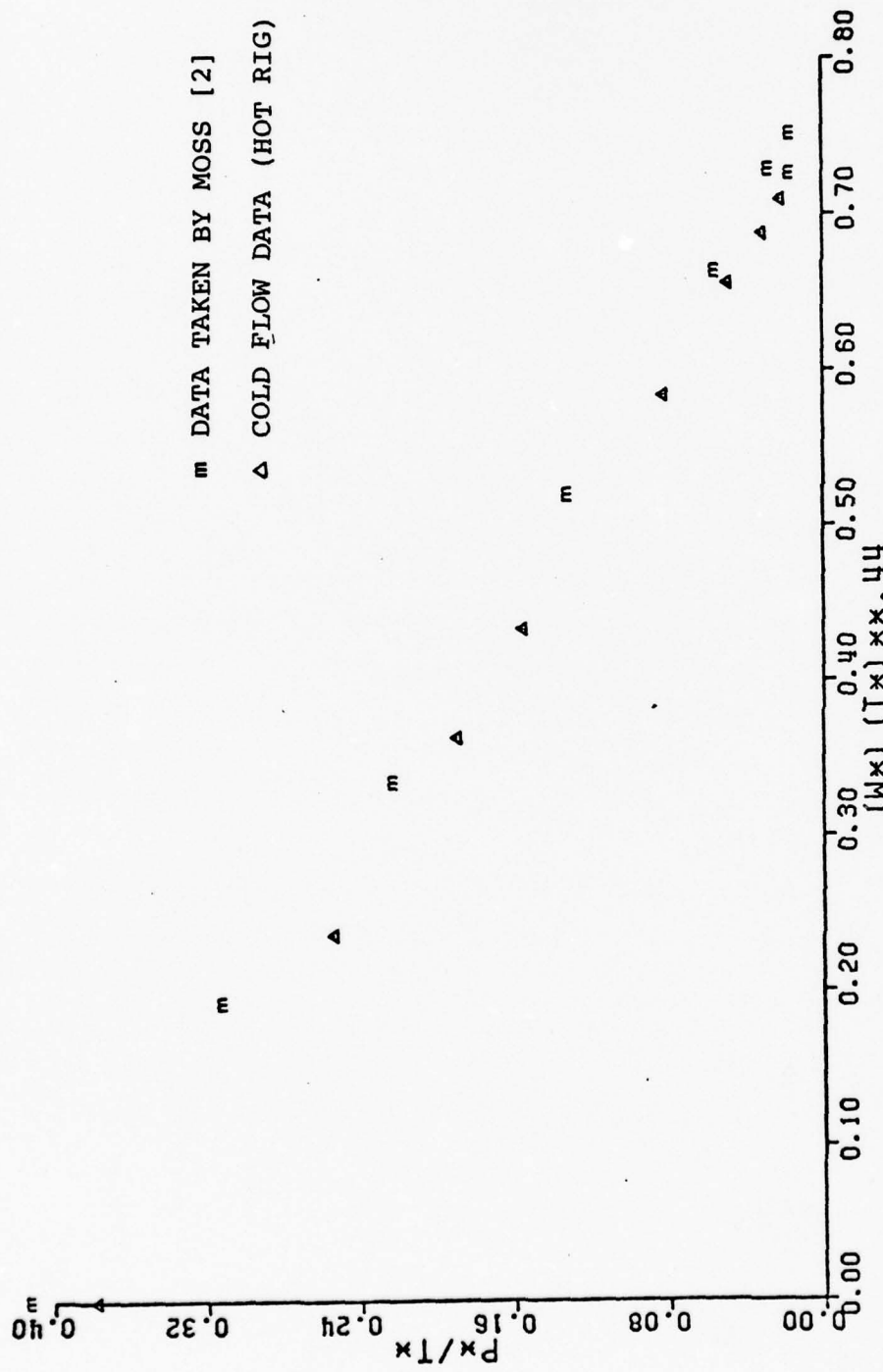


FIGURE 24. Comparison of Cold Flow Performance Plots $L/D = 3.0$
(Table V)

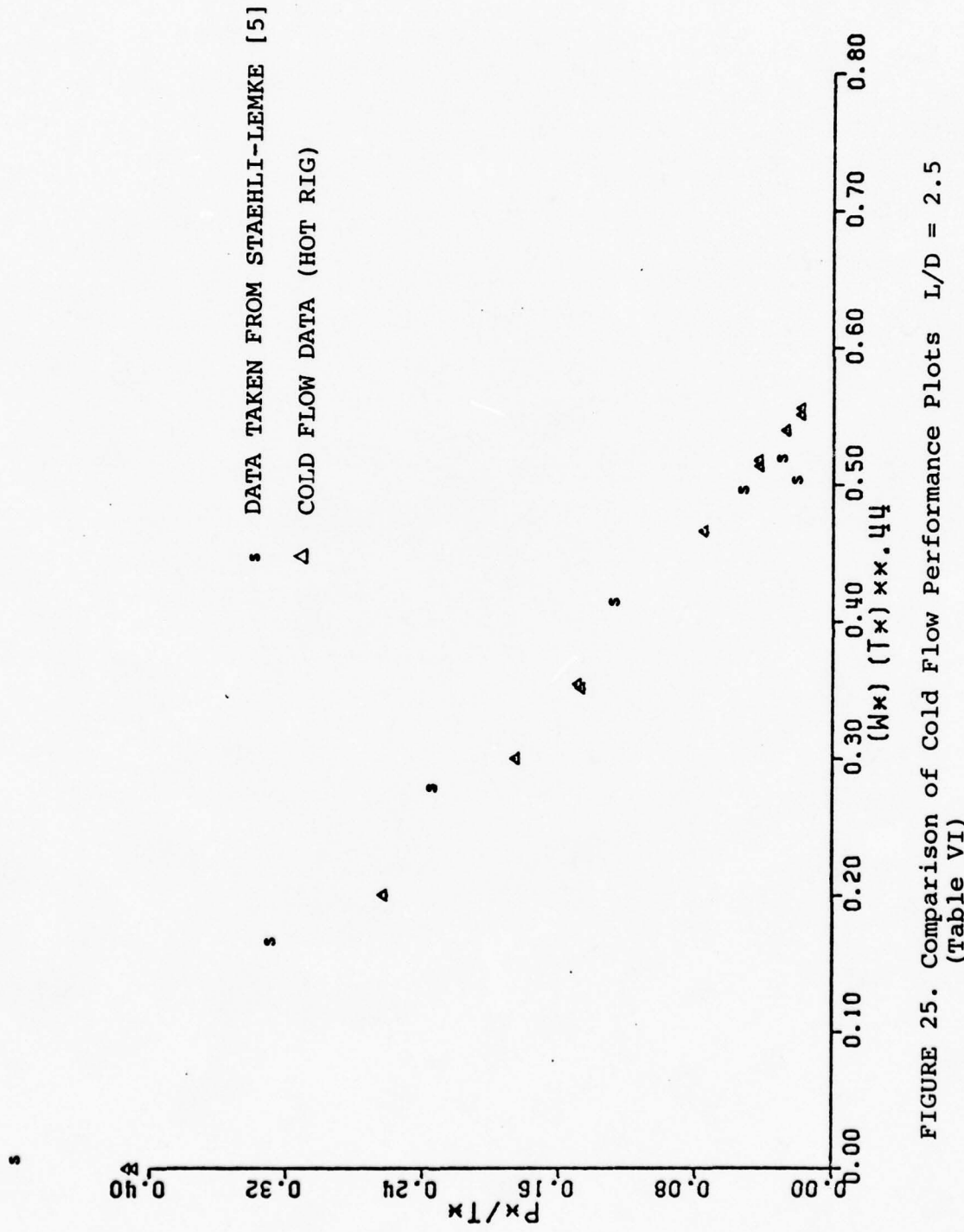


FIGURE 25. Comparison of Cold Flow Performance Plots $L/D = 2.5$
(Table VI)

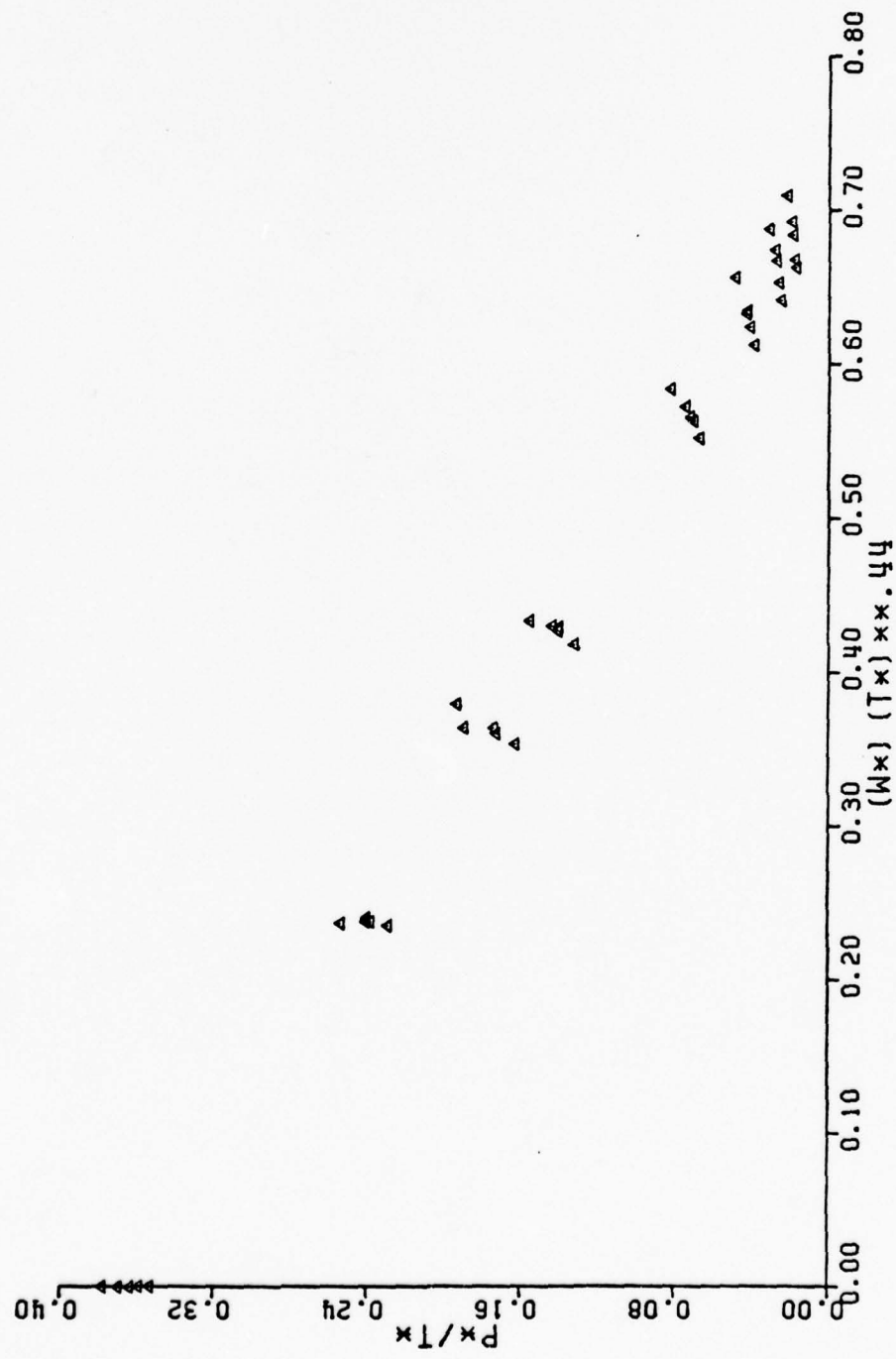


FIGURE 26. Composite Performance Plot for All Temperatures
 $L/D = 3.0$ (Table V)

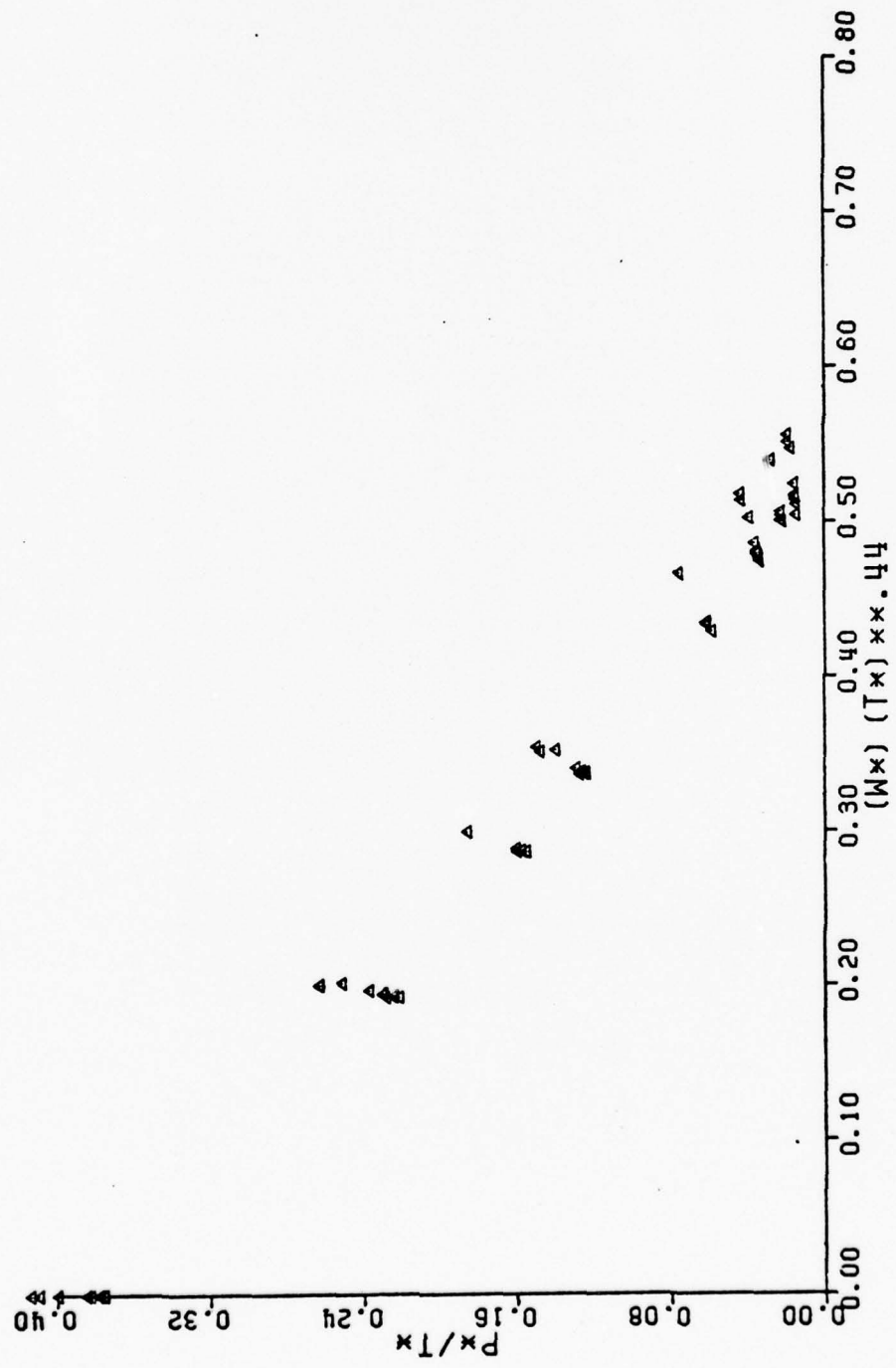


FIGURE 27. Composite Performance Plot for All Temperatures $L/D = 2.5$
(Table VI)

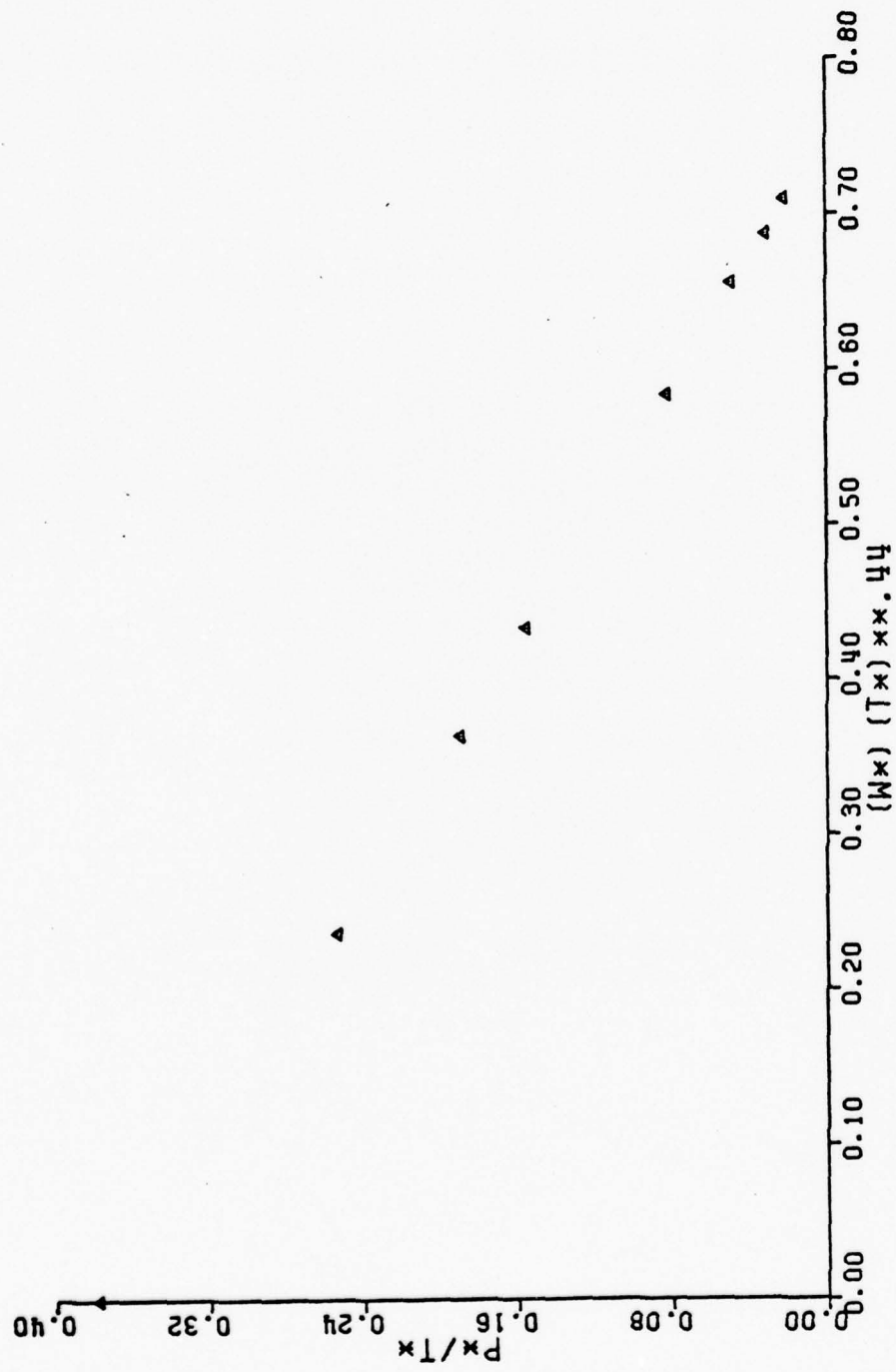


FIGURE 28. Performance Plot, $L/D = 3.0$, Cold Flow (Table V)

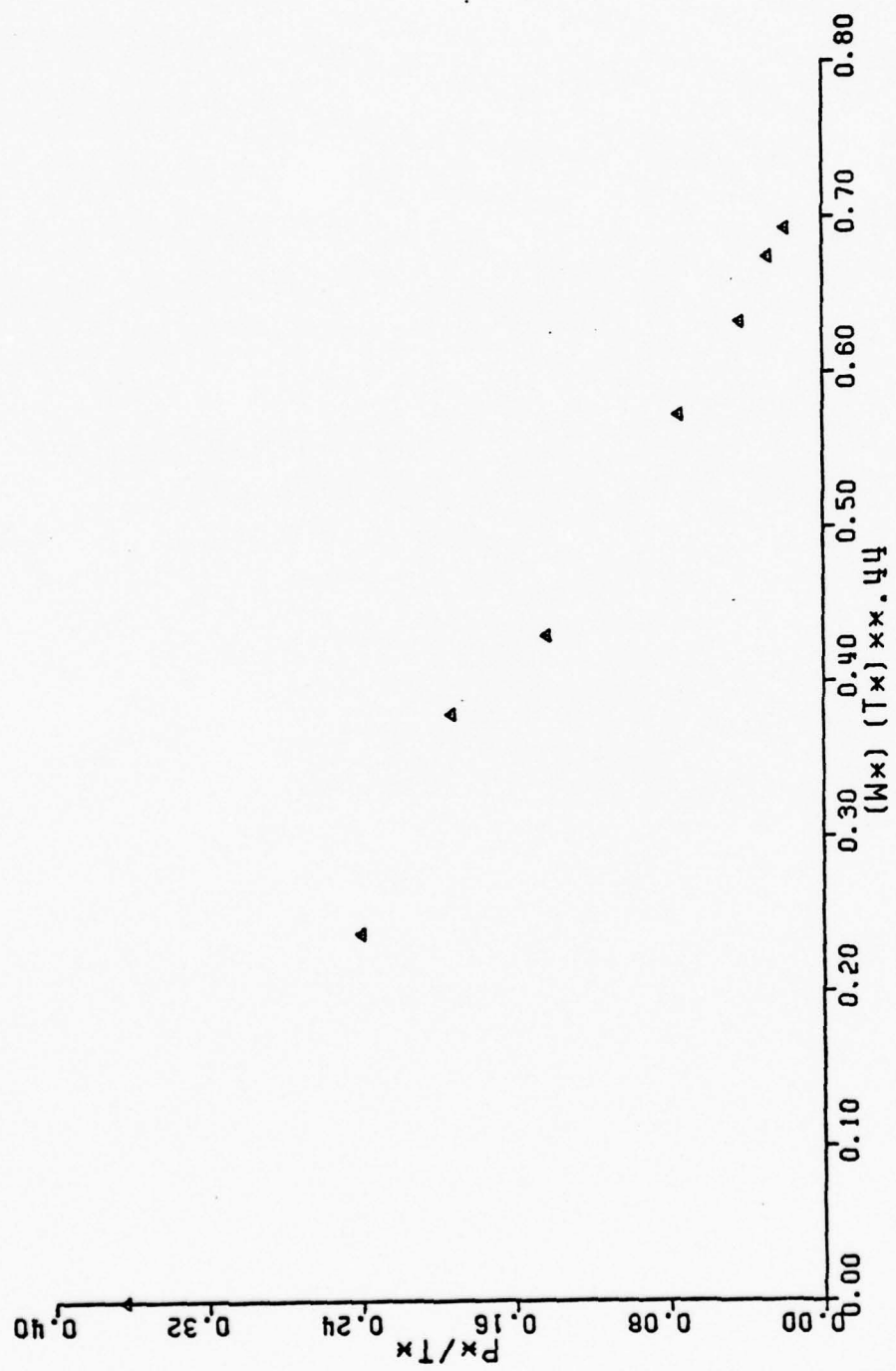


FIGURE 29. Performance Plot, $L/D = 3.0$, $T_{UPT} = 550^{\circ}\text{F}$ (Table V)

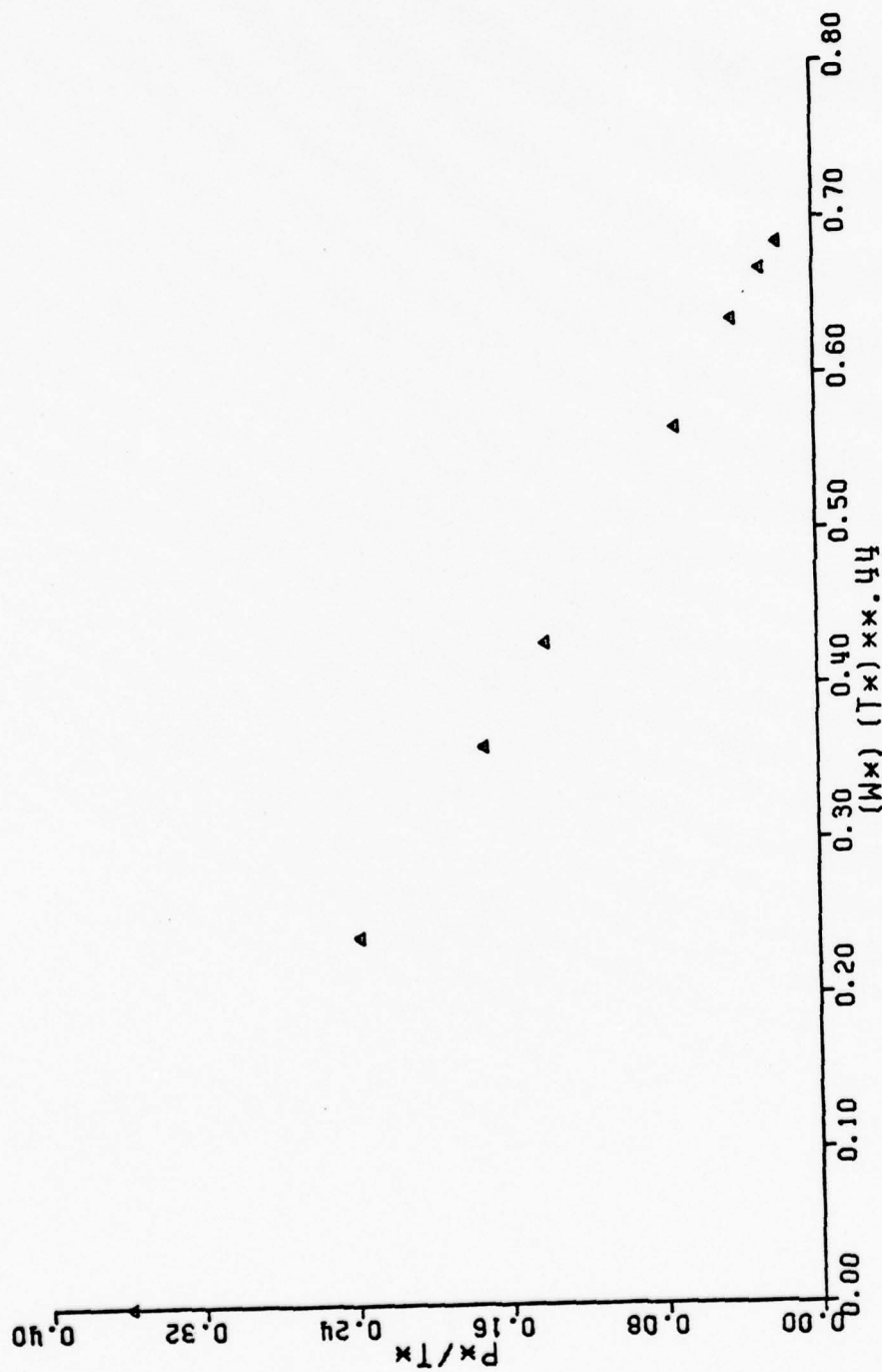


FIGURE 30. Performance Plot, $L/D = 3.0$, $T_{UPT} = 650^{\circ}\text{F}$ (Table V)

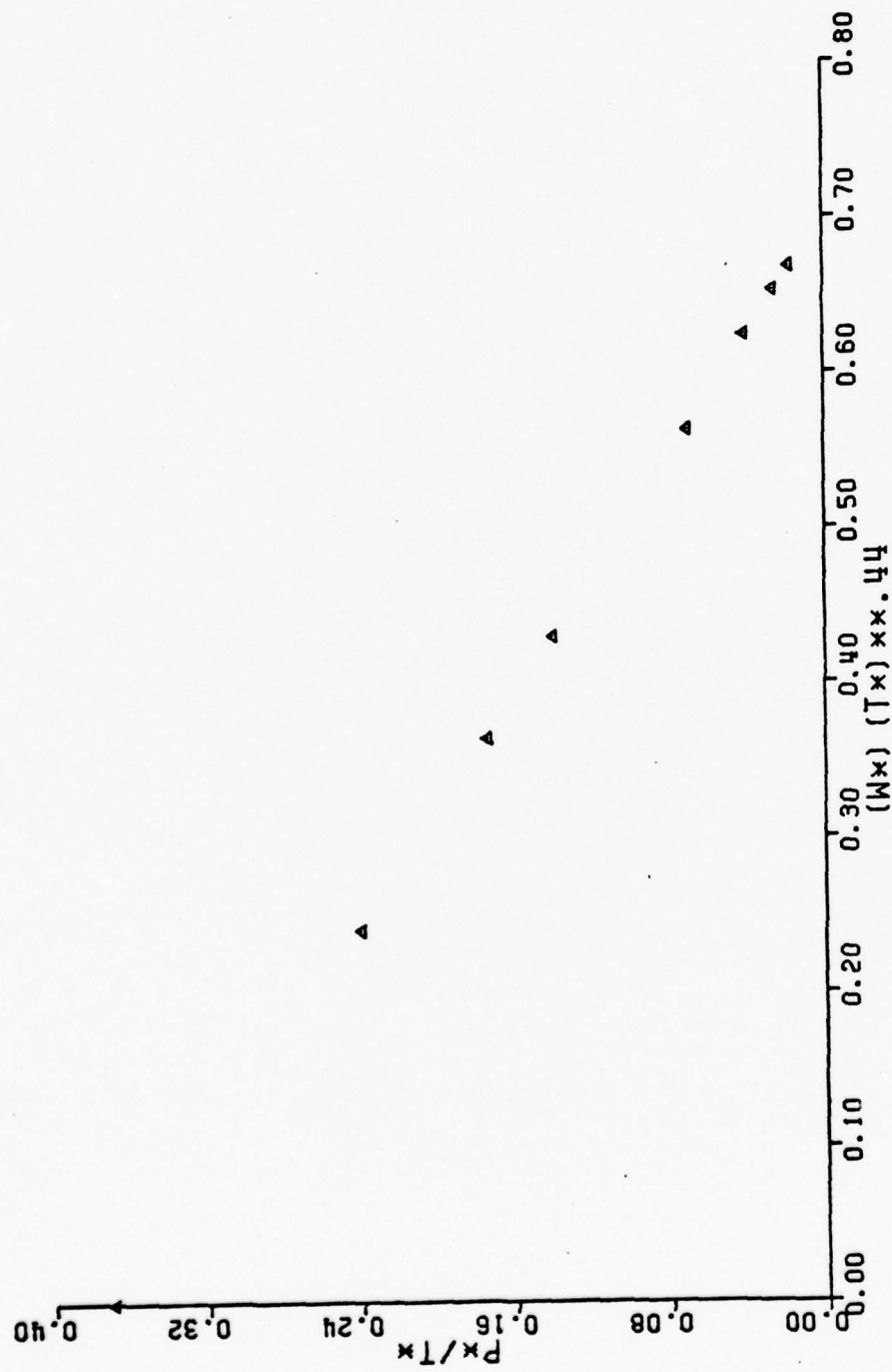


FIGURE 31. Performance Plot, $L/D = 3.0$, $T_{UPT} = 750^{\circ}\text{F}$ (Table V)

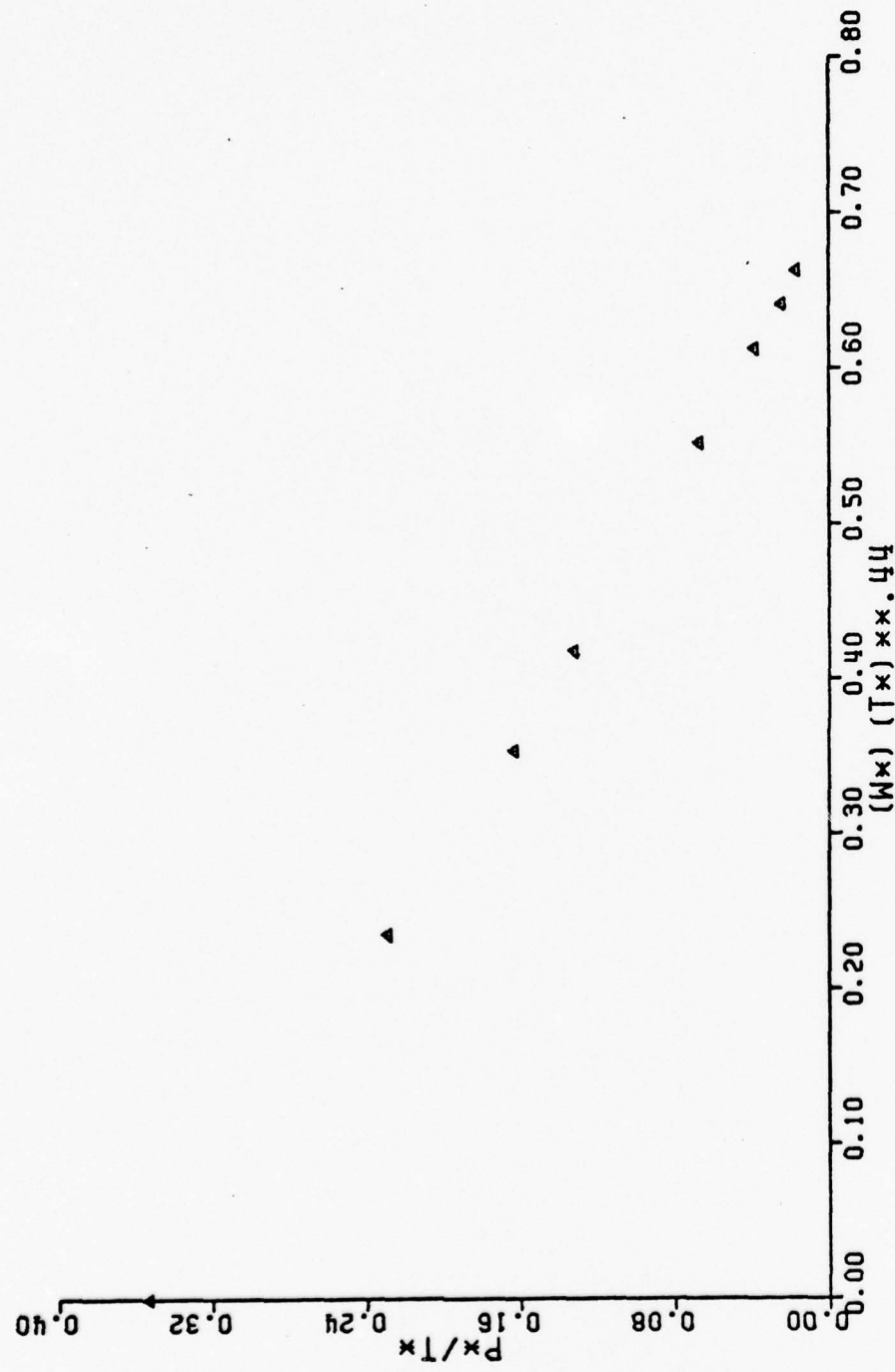


FIGURE 32. Performance Plot, L/D = 3.0, TUPT = 850°F (Table V)

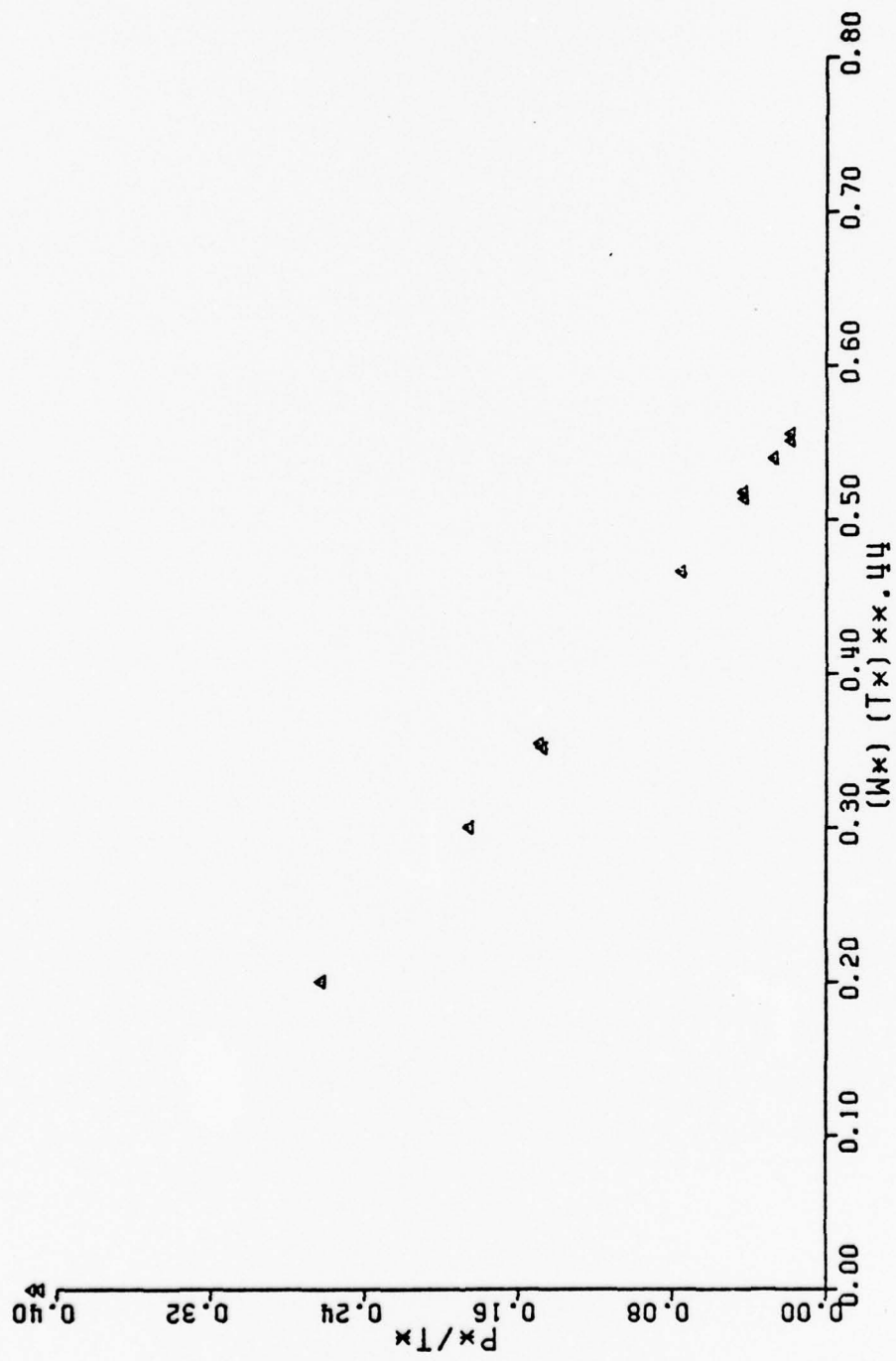


FIGURE 33. Performance Plot, $L/D = 2.5$, Cold Flow (Table VI)

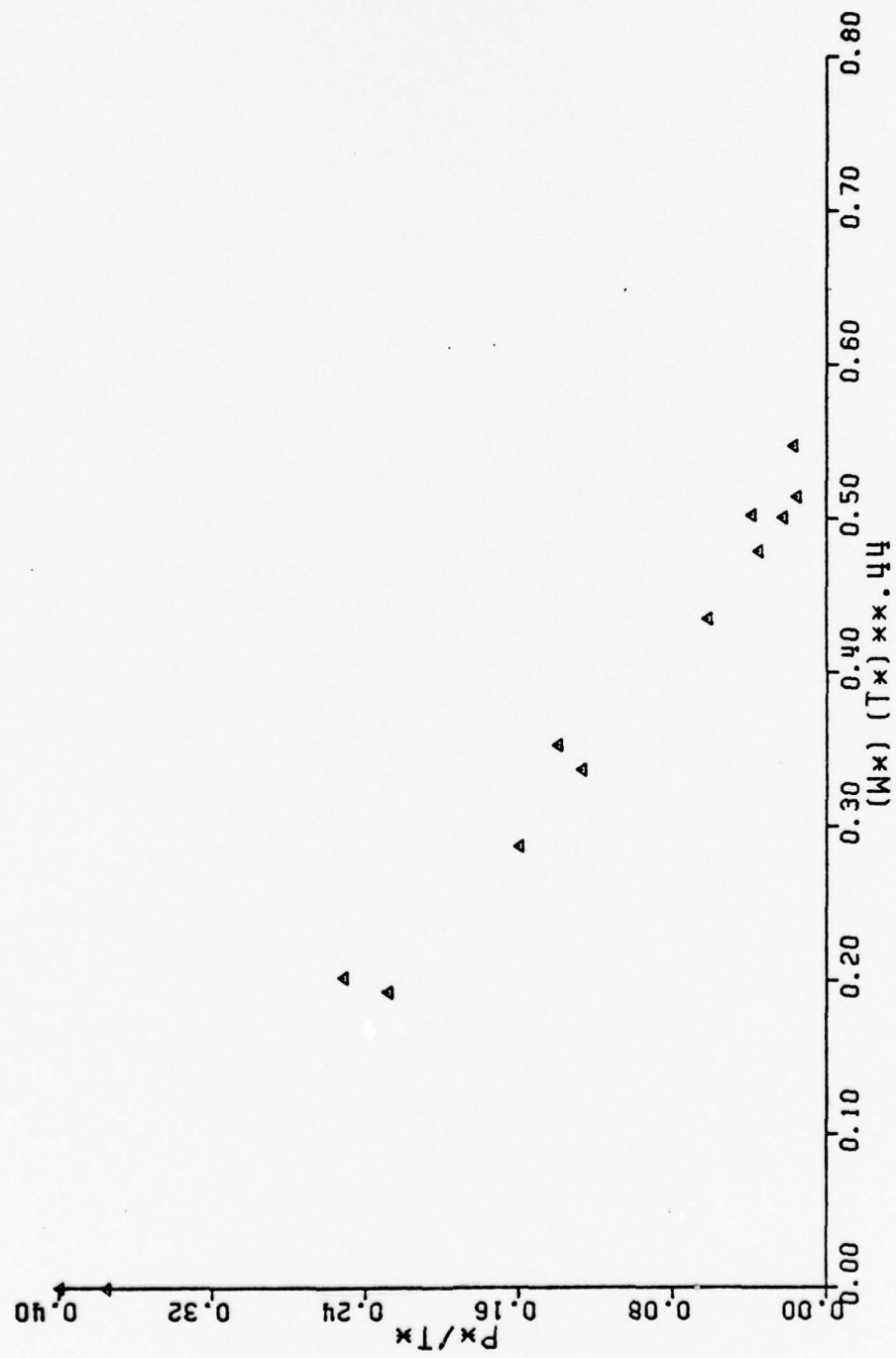


FIGURE 34. Performance Plot, $L/D = 2.5$, $T_{UPT} = 550^{\circ}\text{F}$ (Table VI)

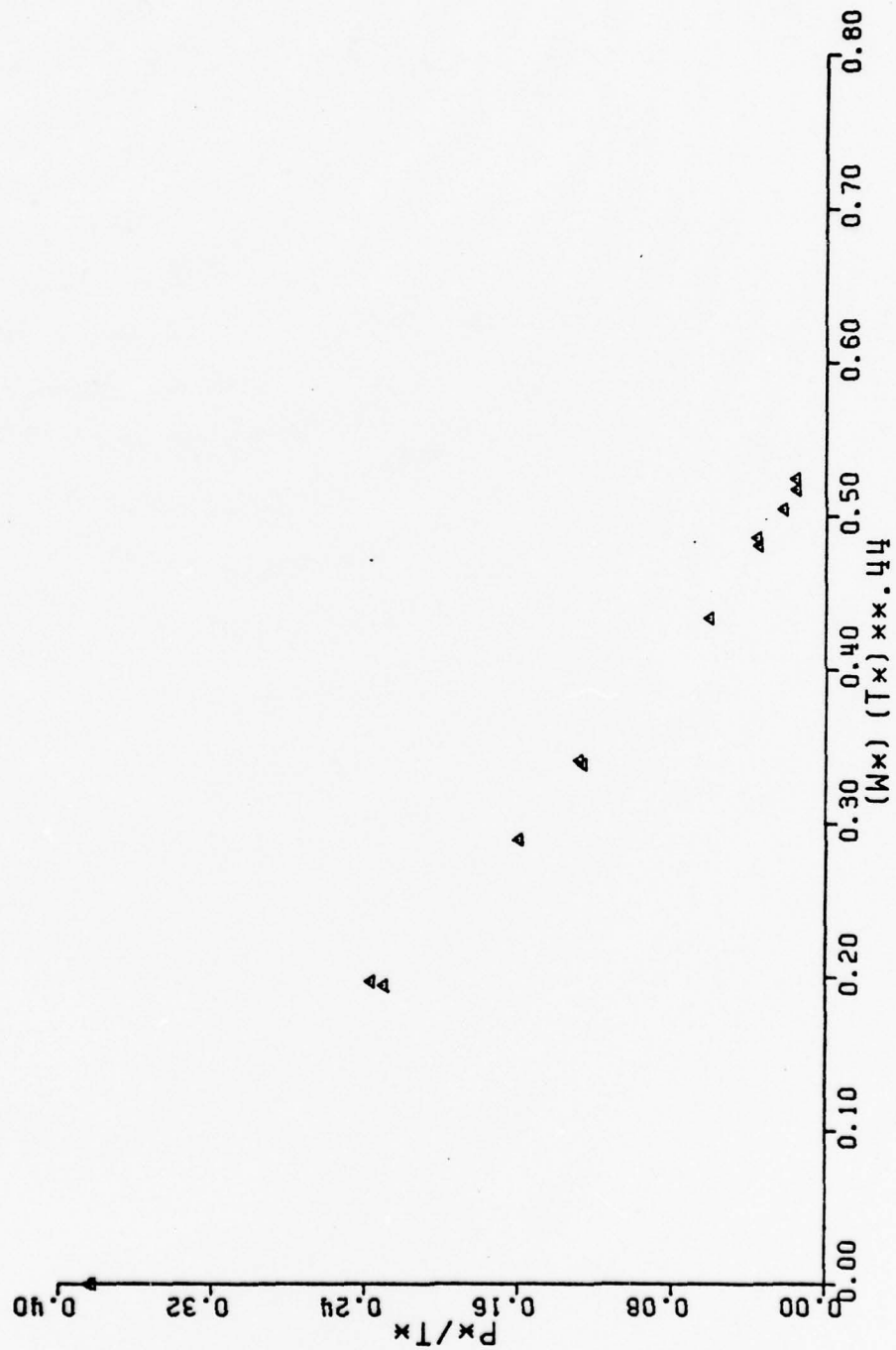


FIGURE 35. Performance Plot, $L/D = 2.5$, $T_{UPT} = 650^{\circ}\text{F}$ (Table VI)

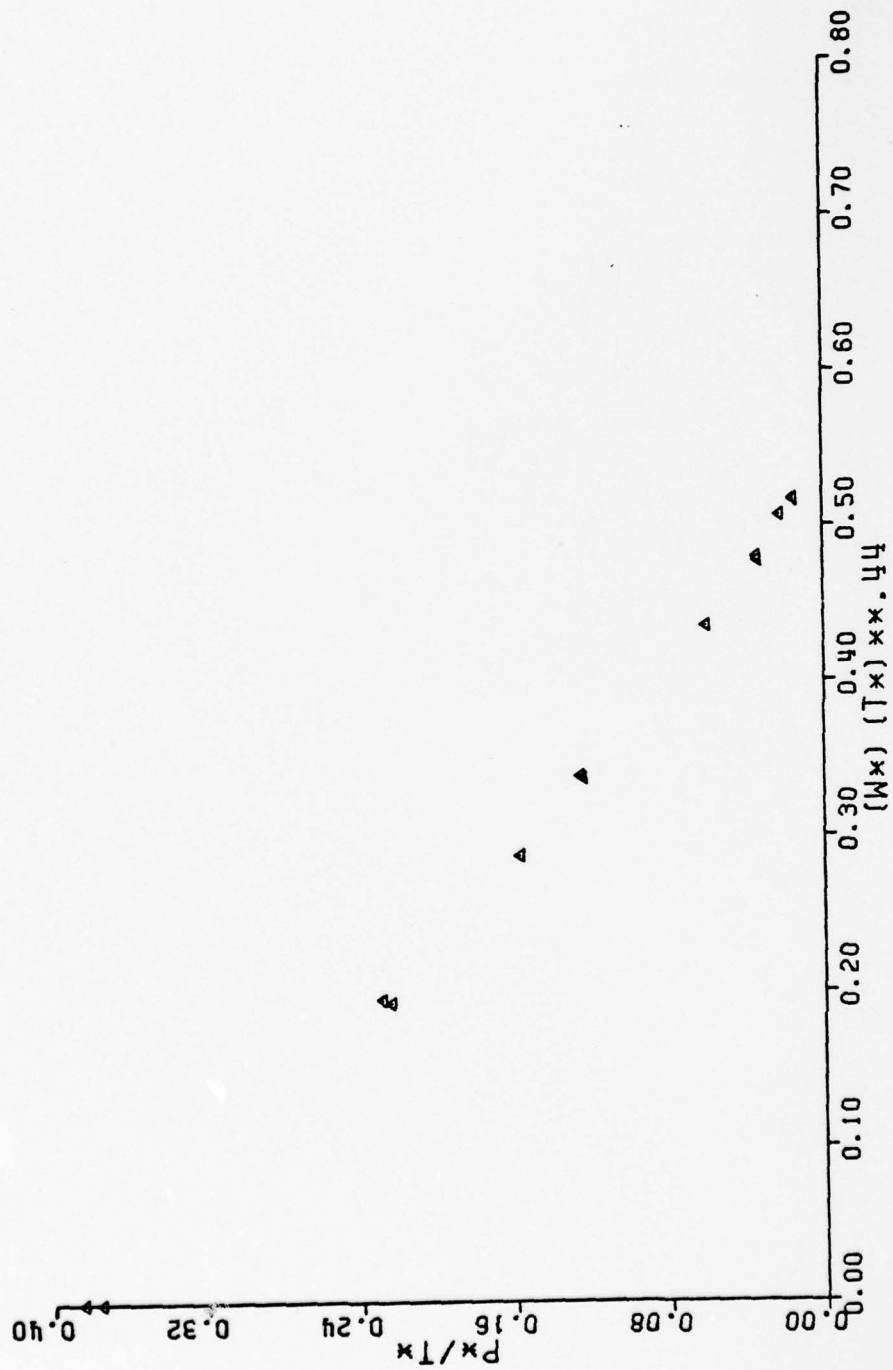


FIGURE 36. Performance Plot, $L/D = 2.5$, $T_{UPT} = 750^{\circ}\text{F}$ (Table VI)

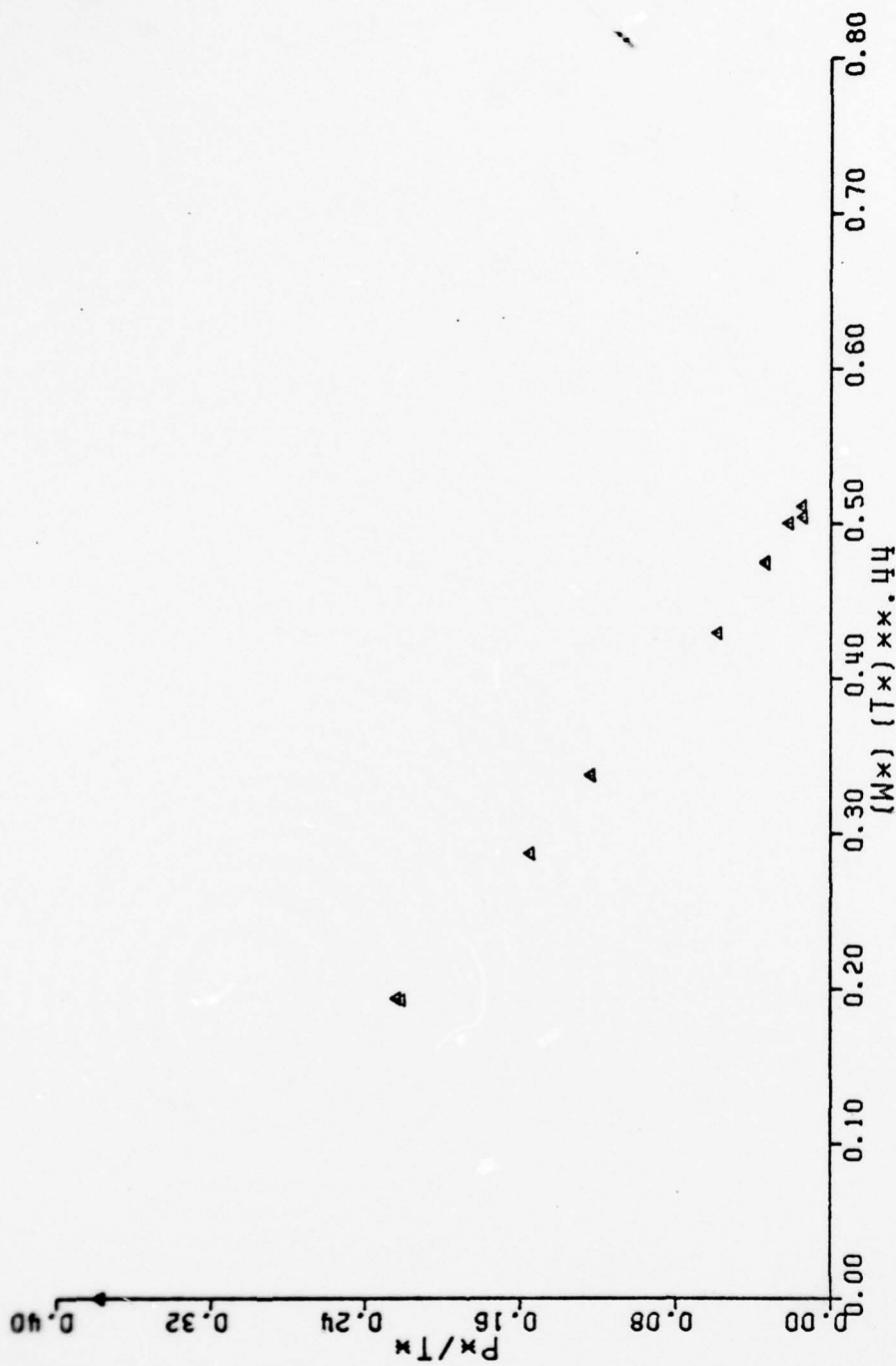


FIGURE 37. Performance Plot, L/D = 2.5, T_{UPT} = 850°F (Table VI)

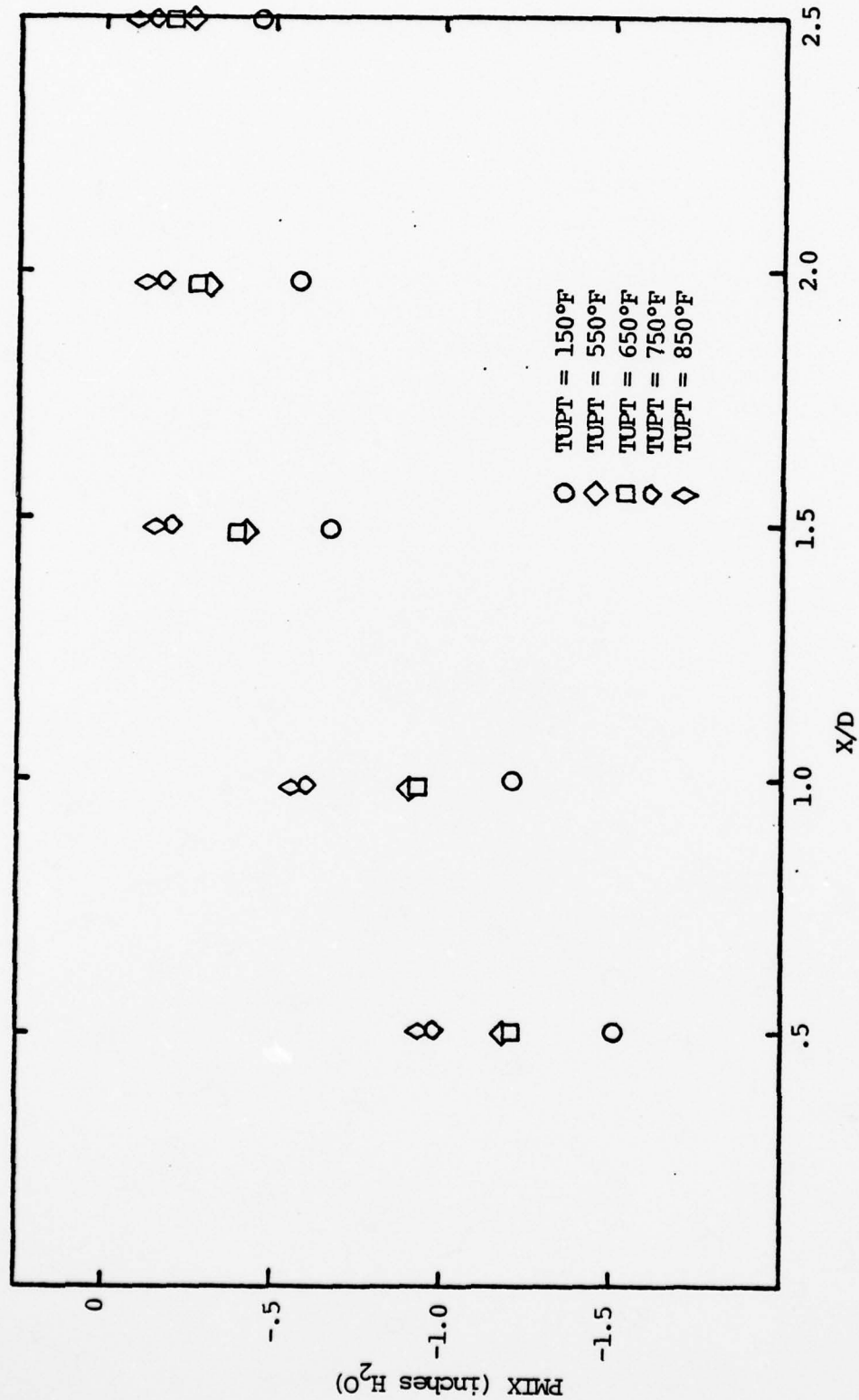


FIGURE 38. Mixing Stack Wall Pressure Distribution, L/D = 3.0 (Table V)

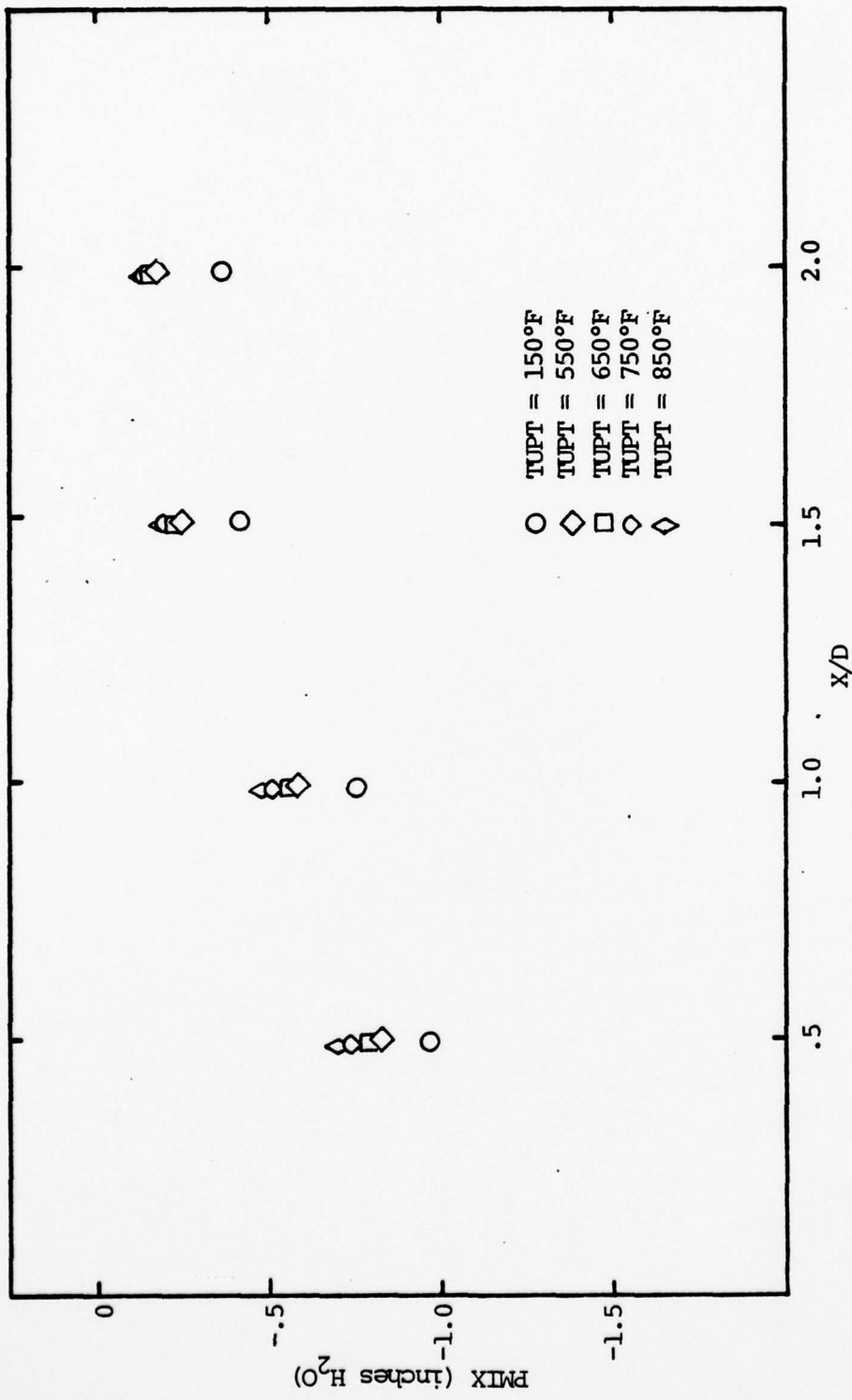


FIGURE 39. Mixing Stack Wall Pressure Distribution, $L/D = 2.5$ (Table VI)

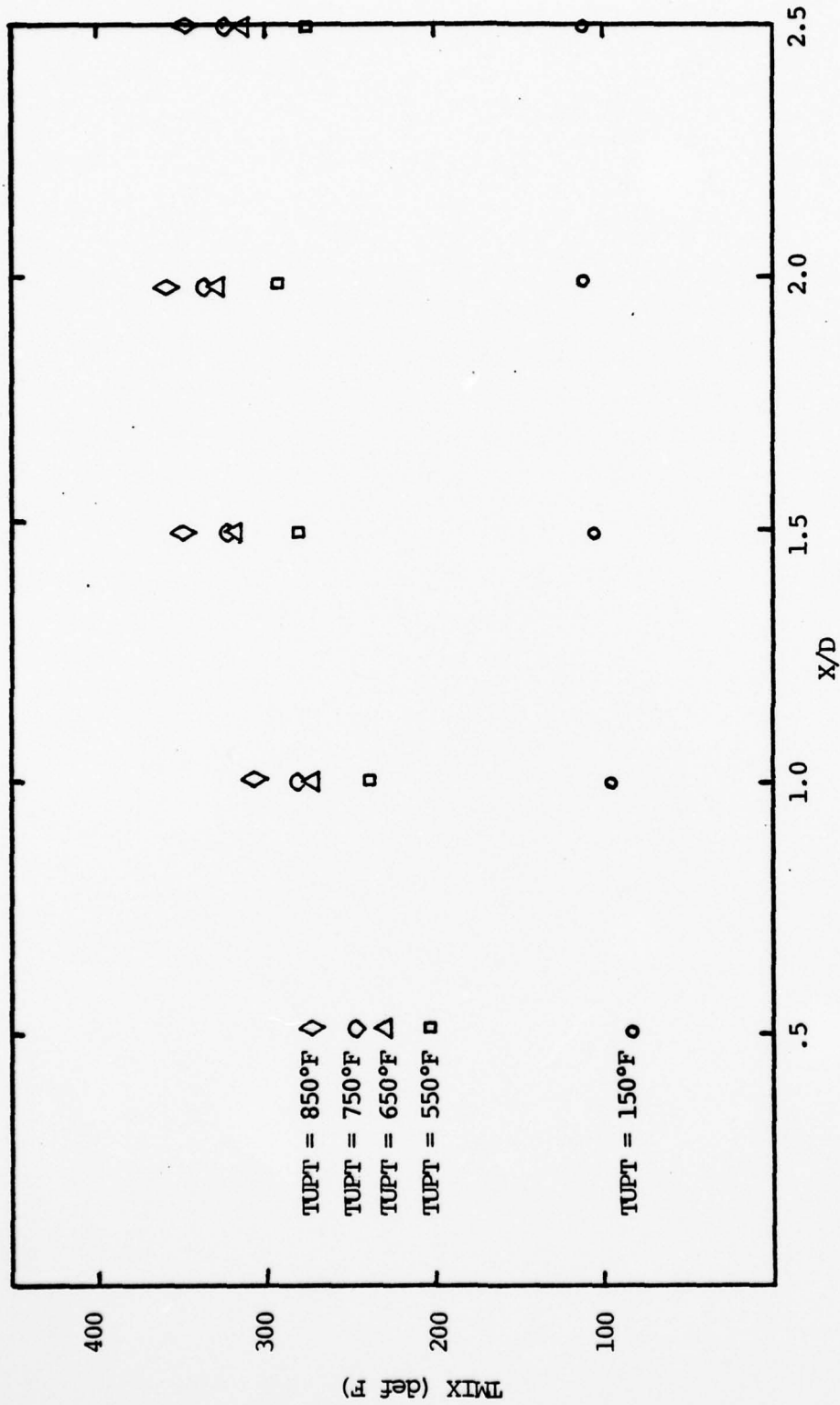


FIGURE 40. Mixing Stack Wall Temperature Distribution, $L/D = 3.0$ (Table V)

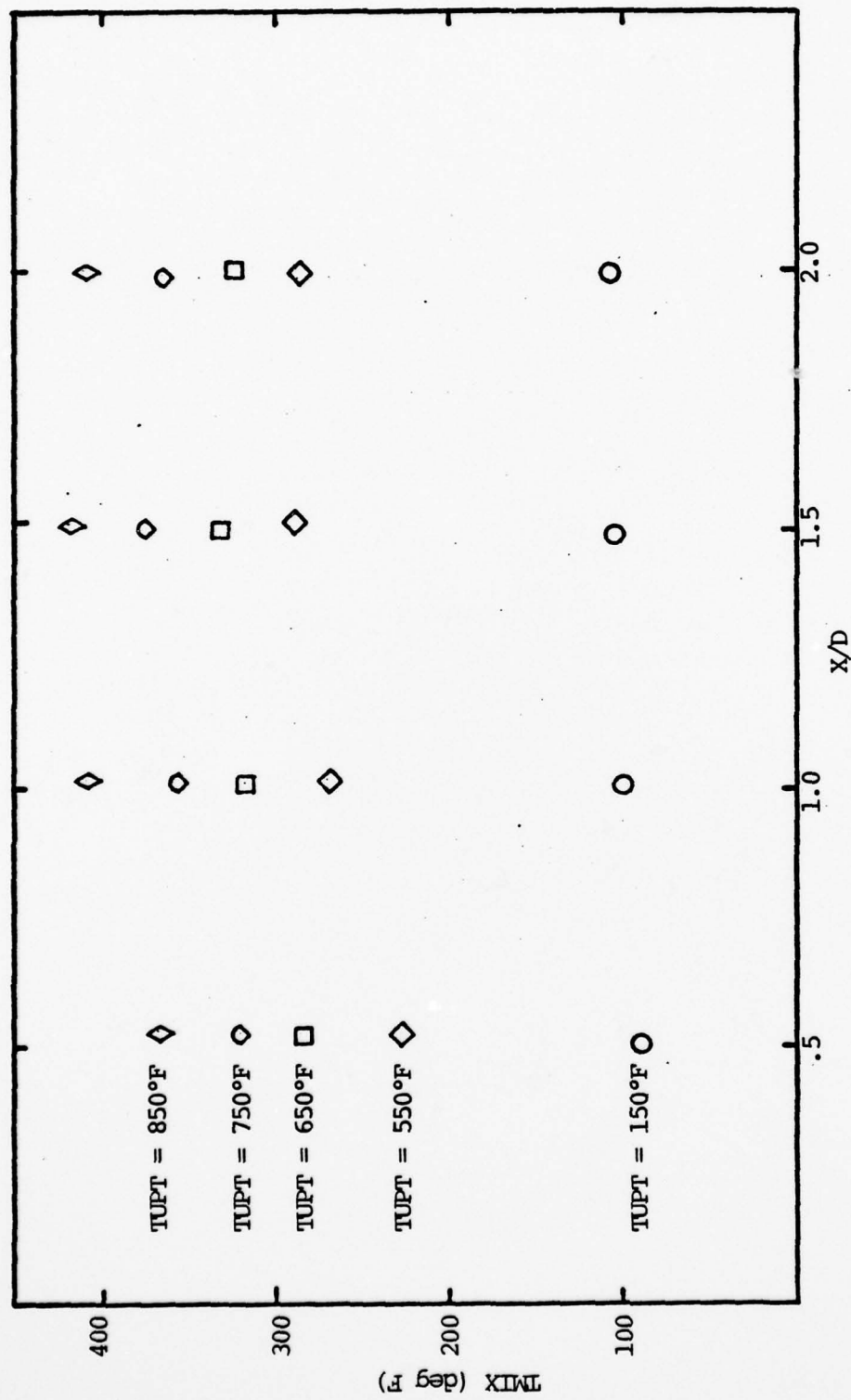


FIGURE 41. Mixing Stack Wall Temperature Distribution, $L/D = 2.5$ (Table VI)

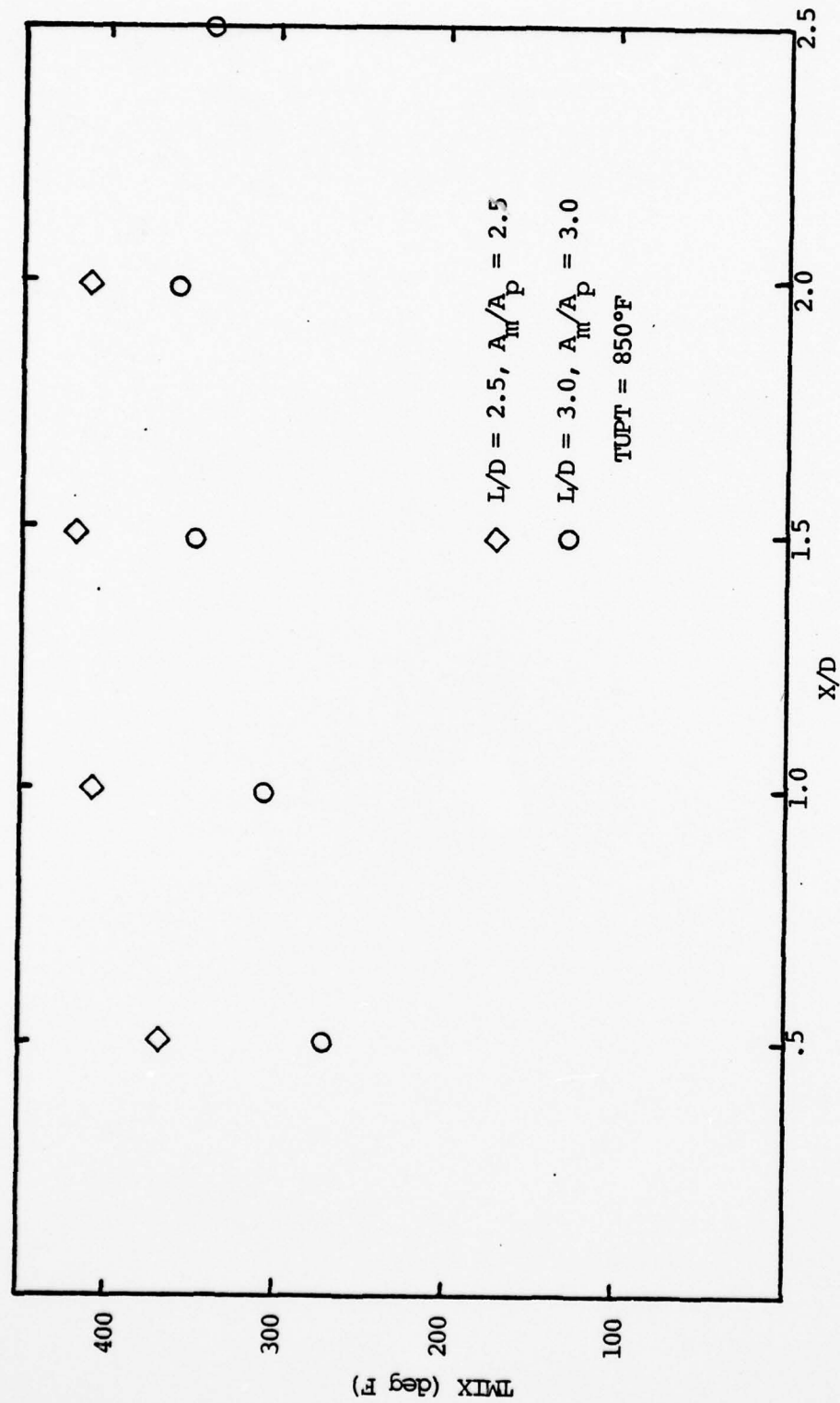


FIGURE 4.2. Comparison of Mixing Stack Wall Temperature Distributions
(Tables V and VI)

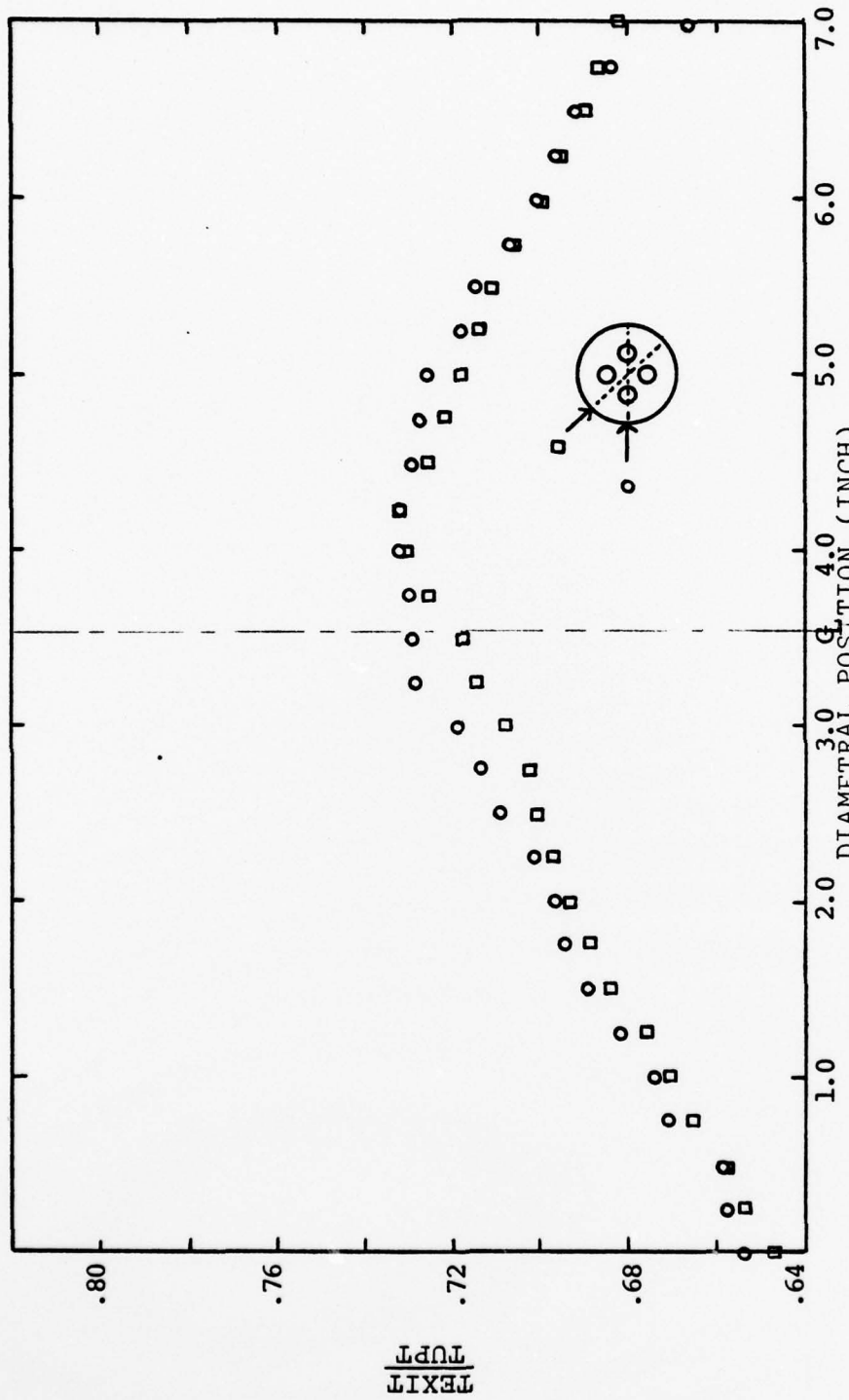


FIGURE 43. Mixing Stack Exit Plane Temperature Profile, $L/D = 3.0$
(Table VIII)

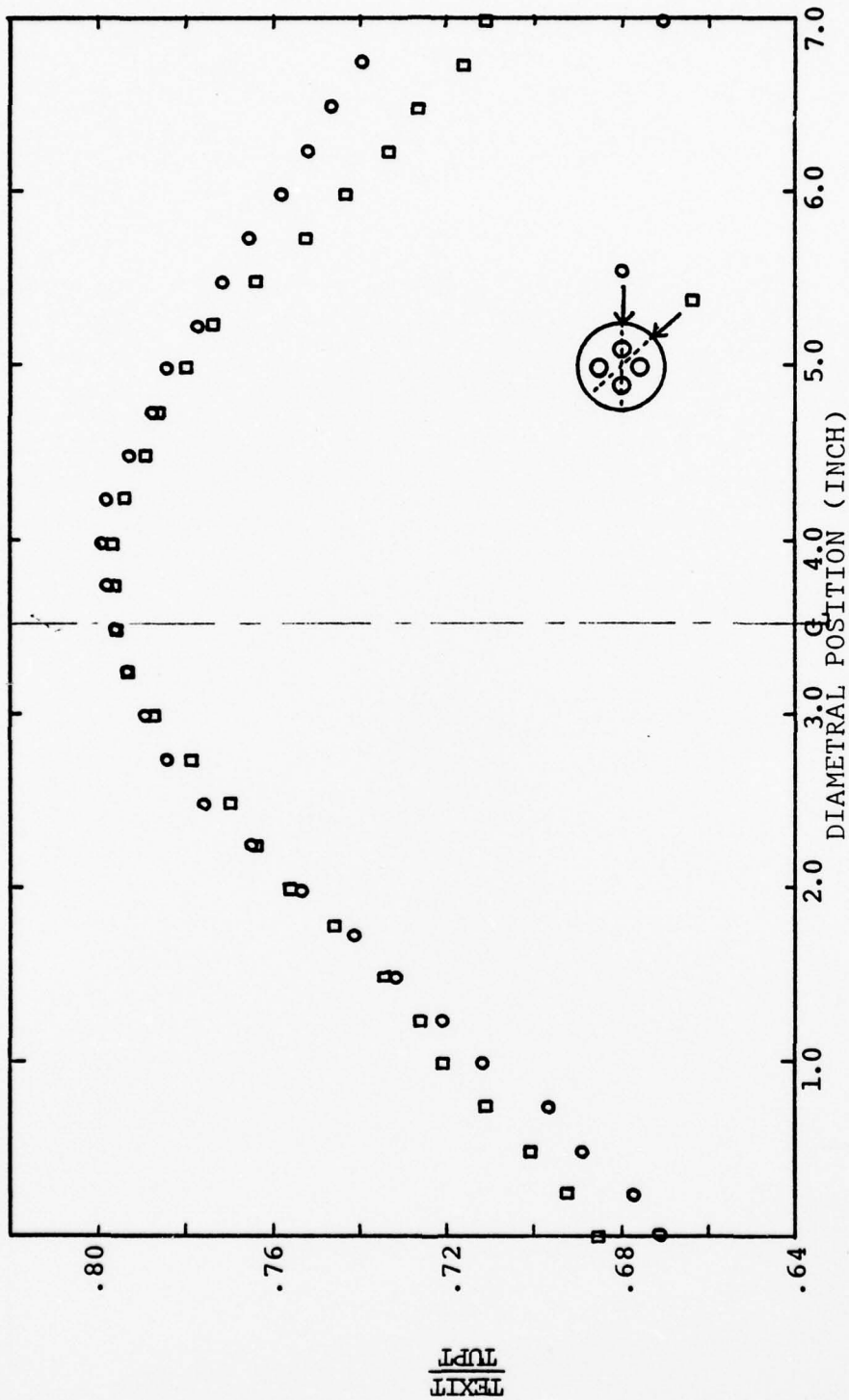


FIGURE 44. Mixing Stack Exit Plane Temperature Profile, $L/D = 2.5$
(Table VII)

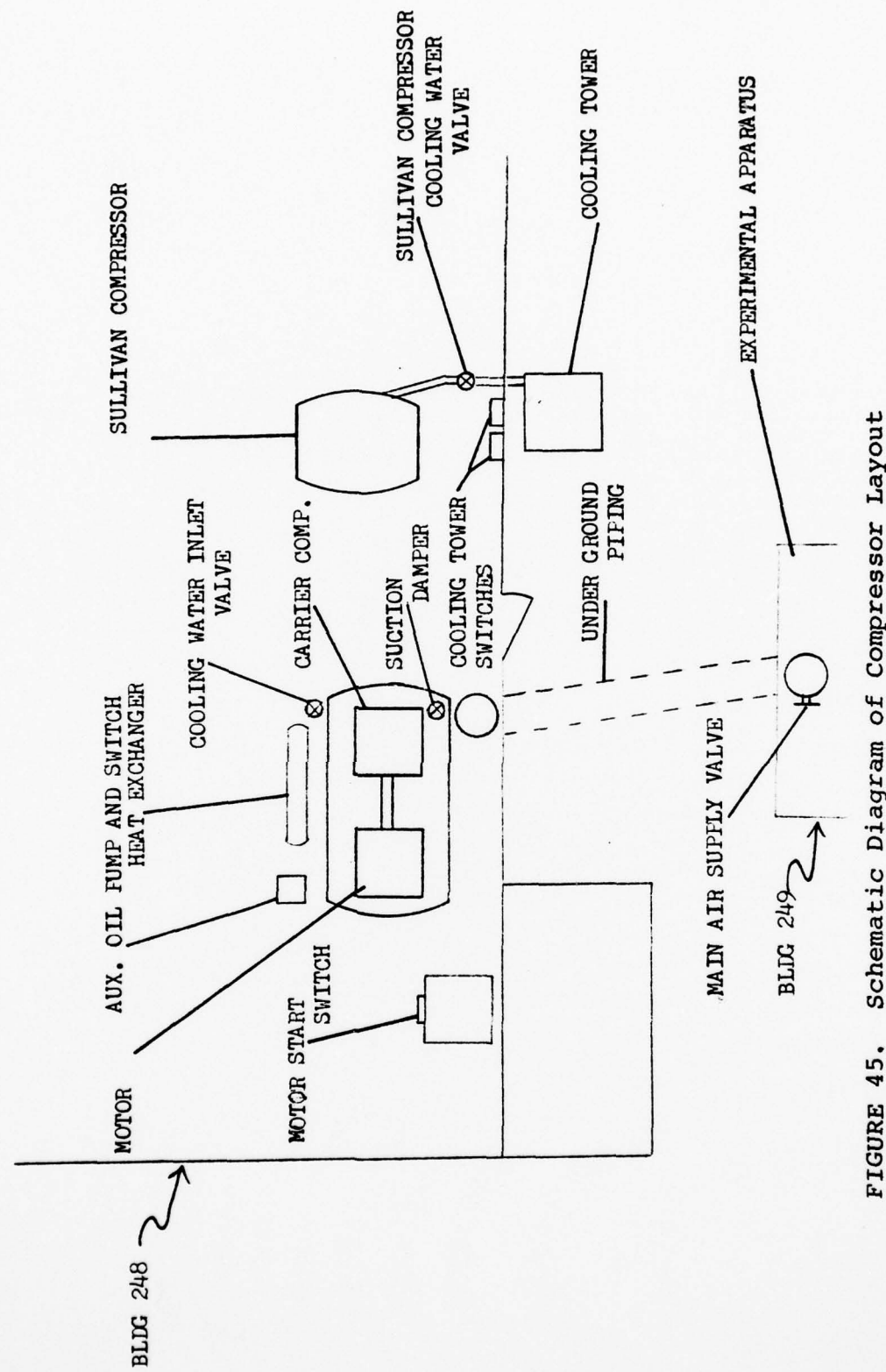


FIGURE 45. Schematic Diagram of Compressor Layout

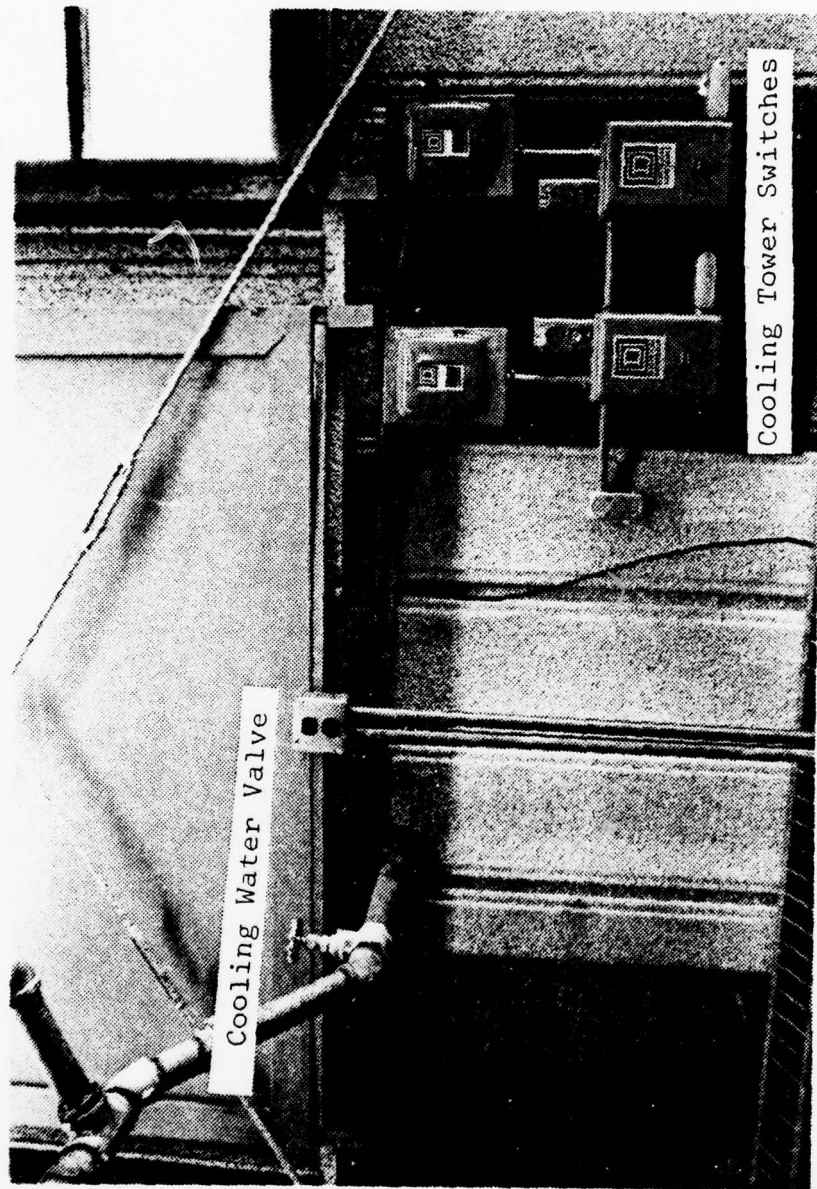


FIGURE 46. Cooling Tower Switches and Cooling Water Valve

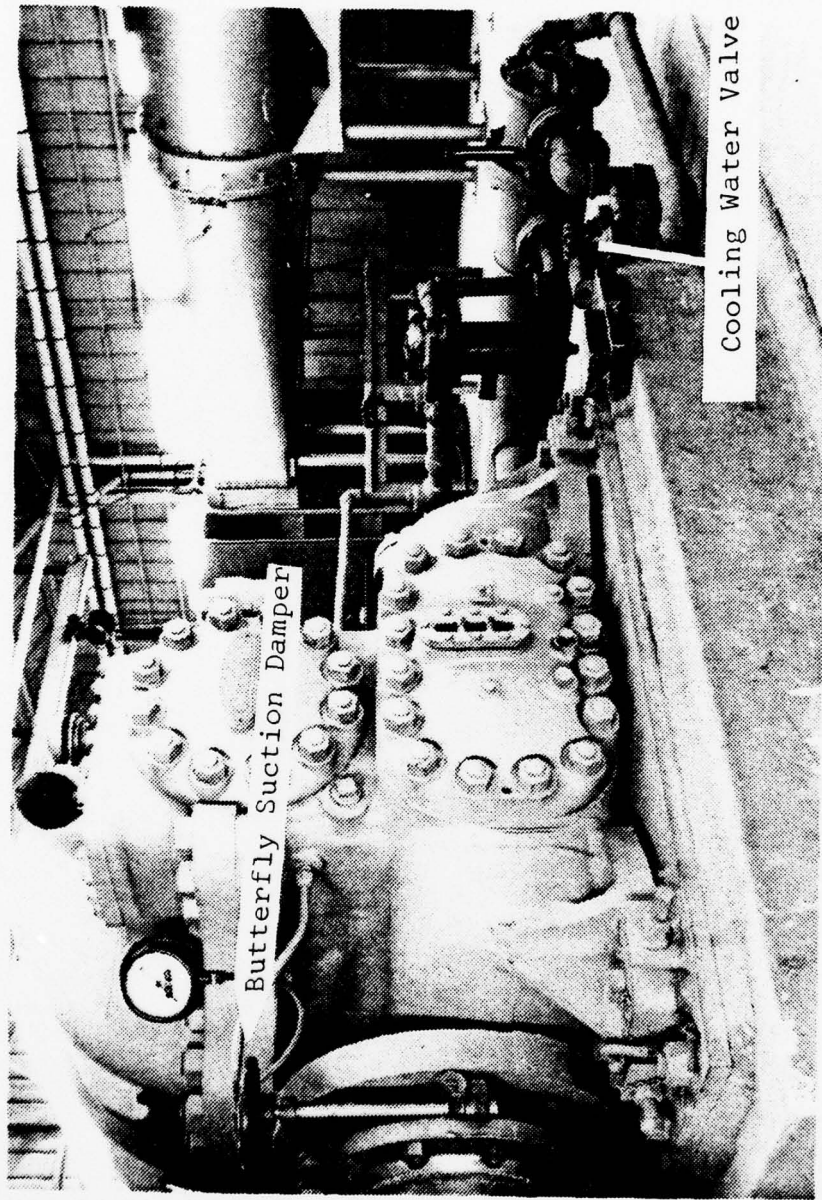


FIGURE 47. Carrier Air Compressor, Butterfly Suction Damper, and Cooling Water Valve

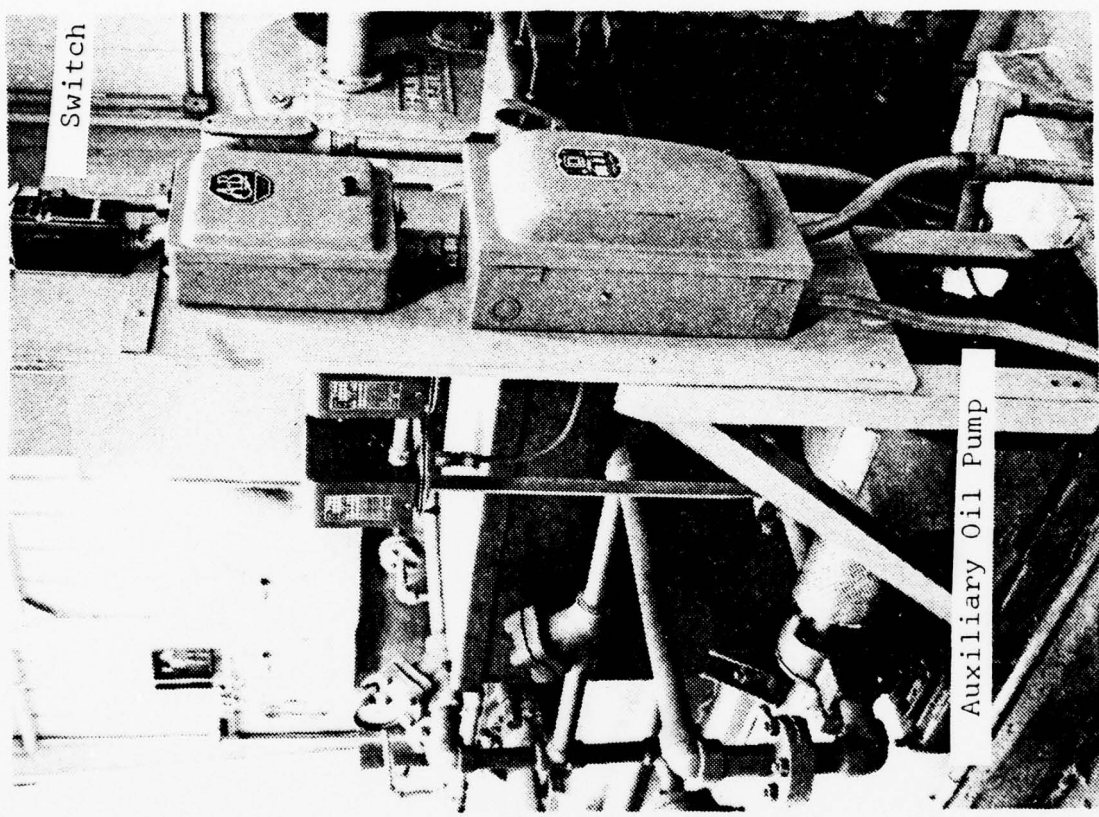


FIGURE 48. Auxiliary Oil Pump and Switch

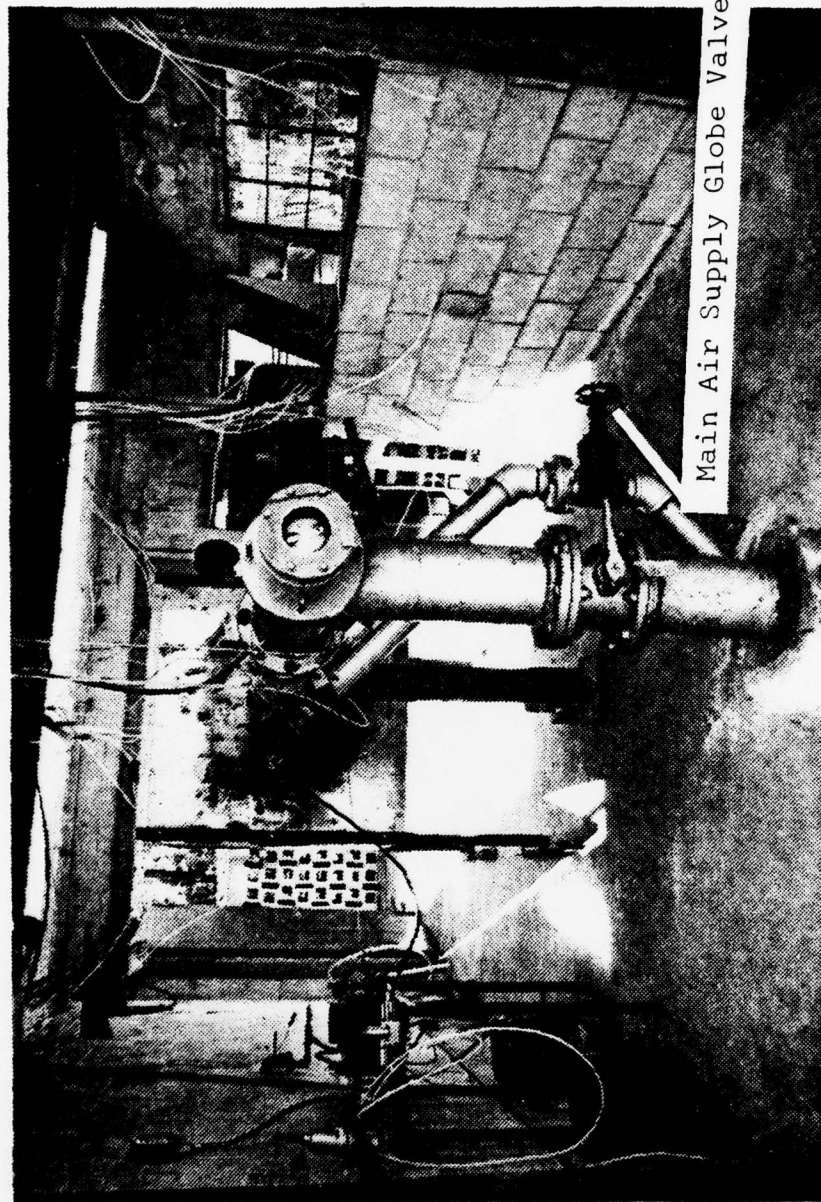


FIGURE 49. Main Air Supply Globe Valve

IX. TABLES

GEOMETRIC PARAMETERS	PUMPING COEFFICIENT	MAXIMUM MIXING STACK WALL TEMP. (TUPT = 850°F)	MAXIMUM MIXING STACK EXIT PLANE TEMP. (TUPT = 850°F)
L/D = 3.0 $A_m/A_p = 3.0$ S/D = .5	.72	368°F	501°F
L/D = 2.5 $A_m/A_p = 2.5$ S/D = .5	.56	428°F	596°F

TABLE I. Summary of Results

AD-A062 205

NAVAL POSTGRADUATE SCHOOL MONTEREY CALIF
HOT FLOW TESTING OF MULTIPLE NOZZLE EXHAUST EDUCTOR SYSTEMS. (U)
SEP 78 D R WELCH

F/G 20/4

UNCLASSIFIED

NL

2 OF 2
AD
A062205



END
DATE
FILED
3-79
DDC

PNH + B (in. Hg)	ΔPN (in. H_2O)	$\sqrt{(PNH+8) \cdot \Delta PN}$ ((in. Hg) · in. H_2O)	\dot{m}_a (lmb/sec)
55.46	13.05	26.902	1.915
56.30	13.05	27.105	1.933
55.40	12.85	26.681	1.899
54.35	12.60	26.168	1.862
53.26	12.55	25.853	1.850
53.55	12.45	25.820	1.835
52.25	12.15	25.195	1.789
51.11	12.00	24.765	1.786
51.05	11.90	24.647	1.740
50.05	11.65	24.147	1.703
48.15	11.15	23.170	1.636
46.76	11.00	22.679	1.632
46.05	10.65	22.145	1.566
44.90	10.40	21.609	1.524
43.66	9.80	20.684	1.496
43.26	10.20	21.005	1.511
40.16	9.45	19.481	1.394
38.51	9.50	19.127	1.342
36.91	8.60	17.816	1.288
35.71	8.00	16.902	1.218
35.01	7.58	16.290	1.179
34.26	7.00	15.486	1.112
34.01	6.60	14.982	1.115
33.26	6.00	14.126	1.030
32.51	5.05	12.813	0.933
31.96	4.05	11.377	0.834
31.56	3.30	10.205	0.753
31.41	3.00	9.707	0.725
30.91	2.05	7.707	0.584
30.46	1.05	5.655	0.424
30.29	0.60	4.263	0.330

TABLE II. Entrance Transition Nozzle
Calibration Data

Diametral Position (inch)	T (°F)	TUPT (°F)	
0	800	852	Nozzle A
.25	808	852	
.50	816	854	
.75	818	853	
1.00	820	855	
1.25	820	853	
1.50	814	853	
1.75	810	854	
2.00	802	855	
0	804	854	Nozzle B
.25	810	854	
.50	817	854	
.75	820	855	
1.00	818	855	
1.25	820	854	
1.50	818	855	
1.75	816	856	
2.00	809	855	
0	806	856	Nozzle C
.25	815	856	
.50	823	856	
.75	826	857	
1.00	826	858	
1.25	818	860	
1.50	810	858	
1.75	806	858	
2.00	792	858	
0	801	855	Nozzle D
.25	810	855	
.50	815	856	
.75	820	856	
1.00	822	856	
1.25	822	855	
1.50	812	854	
1.75	808	854	
2.00	798	855	

TABLE III. Primary Nozzle Temperature Profile Data

Diametral Position (inch)	TUPT (°F)	TREF (°F)
0	773	851
.25	816	851
.50	826	853
1.00	840	855
1.50	849	857
2.00	852	856
2.50	856	856
3.00	860	863
3.50	848	852
4.00	850	850
4.50	854	854
5.00	855	858
5.50	852	858
6.00	849	859
6.50	842	857
7.00	832	848
7.25	835	852
7.50	819	848

TABLE IV. UPtake Stack Temperature Profile Data

DATA TAKEN ON 16 AUGUST BY O. R. WELCH *** HOT FLOW PERFORMANCE ***

4 NOZZLES AW/AP=2.0 L/C=3.0 S/C=5

NUMBER OF PRIMARY NOZZLES: 4

PRIMARY NOZZLE DIAMETER: 2.06 INCHES

PIXING STACK LENGTH: 21.37 INCHES

PIXING STACK DIAMETER: 7.12 INCHES

PIXING STACK L/C: 3.20

UPTAKE DIAMETER: 7.51 INCHES
AREA RATIO, AW/AP: 2.99

RUN	FN _H	DELPIN	F+Z	TUPt	TAp	PU-PA	PA-PS	SECONDARY AREA	HFA	WPF	LBM/SEC	AMBENT PRESSURE: 30.03 INCHES HG
1	2.85	14.80	0.0	138.0	66.5	8.10	5.25	0.0	1.6055	0.0	1.6055	0.0
2	2.85	14.60	0.0	146.0	66.5	5.75	3.54	6.283	1.6055	3.0	1.6055	3.0
3	2.90	14.80	0.0	149.0	66.5	10.40	2.65	11.152	1.6066	0.0	1.6066	0.0
4	2.95	14.80	0.0	152.0	66.5	11.10	2.18	14.726	1.6078	0.0	1.6078	0.0
5	4.00	14.75	0.0	155.0	66.5	12.05	1.16	27.253	1.6083	0.0	1.6083	0.0
6	4.05	14.80	0.0	158.0	66.5	12.52	0.69	35.855	1.6101	0.0	1.6101	0.0
7	4.10	14.80	0.0	160.0	66.5	12.60	0.44	52.425	1.6112	0.0	1.6112	0.0
8	4.10	14.80	0.0	161.0	68.5	12.50	0.21	64.952	1.6113	0.0	1.6113	0.0
9	4.10	14.80	0.0	164.0	66.5	12.25	C.C1	*****	1.6113	0.0	1.6113	0.0
A	H#	F#	1*	P*/T*	W*T**.44	WF	WS	UF	UU	UPT MACH	F7/SEC	F7/SEC
1	0.0	2.3339	0.6637	0.3779	0.0	1.605	C.C	264.19	88.25	75.26	0.066	0.066
2	C.2517	C.2211	0.6720	0.2536	0.2210	1.605	0.604	266.60	108.48	EC.08	3.066	3.066
3	C.3677	0.1644	0.6677	0.1894	0.3612	1.607	C.623	267.52	115.28	EC.26	0.066	0.066
4	0.4623	0.1340	0.8635	0.1532	0.4234	1.606	C.743	268.72	125.46	80.72	0.067	0.067
5	C.6243	C.0708	0.6593	0.0824	0.5840	1.606	1.003	265.11	138.04	80.64	0.067	0.067
6	C.7030	0.05418	0.6551	0.0469	0.6562	1.610	1.132	270.76	144.78	81.23	0.067	0.067
7	C.7378	2.02265	0.6523	0.0311	0.6677	1.611	1.189	271.66	147.82	81.43	0.067	0.067
8	C.7615	0.01183	0.8510	0.0215	0.7033	1.611	1.227	272.01	145.77	81.71	0.067	0.067
9	*****	2.0005	0.6469	0.0006	*****	1.611	*****	273.13	*****	82.04	0.067	0.067

PIXING STACK PRESSURE DISTRIBUTION FOR RUN: 9 POSITION A

Y/C:	0.5	1.0	1.5	2.0	2.5
FPSLIA + FFCI:	-1.520	-1.200	-0.650	-0.570	-0.430
FPSI:	-0.090	-0.071	-0.039	-0.034	-0.026
TRIX (CEC + F):	80.0	51.0	1C2.0	1CE.0	108.0
TRIX:	0.503	0.509	0.923	0.520	0.520

TABLE V. Performance Data L/D = 3.0

DATA TAKEN ON 16 AUGUST BY C.R. WELCH
AT TAP 3.0 L/C = 0.5 ***

ALPEER OF PRIMARY NOZZLES: 4

PRIMARY NOZZLE DIAMETER: 2.04 INCHES

MIXING STACK LENGTH: 21.37 INCHES

MIXING STACK DIAMETER: 7.12 INCHES

MIXING STACK L/C: 3.00

UPTAKE DIAMETER: 7.51 INCHES
AREA RATIO, AM/AP: 2.59

AMBIENT PRESSURE: 30.03 INCHES HG

N RUN	FNH IN. HG	DEFLN IN. +20	F/FZ	T/PT	T/PT	PA-FA INCHES OF WATER	PA-FA SQUARE INCHES	hFA	hPF LBM/SEC
1	3.45	7.70	58.0	61.0	76.0	8.45	4.55	0.0	1.1597 0.0099
2	3.55	7.65	59.0	63.0	70.0	9.65	3.25	6.283	1.1577 0.0099
3	3.60	7.65	58.0	662.0	70.0	10.45	2.35	11.192	1.1585 0.0098
4	3.63	7.65	58.0	655.0	76.0	10.65	1.50	14.726	1.1585 0.0098
5	3.70	7.60	59.0	662.0	70.0	11.70	0.57	27.253	1.1565 0.0099
6	3.70	7.60	59.0	657.0	76.0	12.10	0.57	36.859	1.1565 0.0099
7	3.70	7.60	59.0	659.0	70.0	12.20	0.37	52.425	1.1565 0.0095
8	3.70	7.60	59.0	660.0	76.0	12.40	0.25	64.552	1.1565 0.0099
9	3.72	7.60	56.0	661.0	70.0	12.60	0.00	*****	1.1568 0.0095

MIXING STACK PRESSURE DISTRIBUTION FCR RUN: 9 POSITION A

Y/C:

F2(LN. F2):

FPS: -0.042

TIX (CECF): 230.0

TAS: C.115

FNH: 1.0

FPS: -0.032

TIX (CECF): 273.0

TAS: 0.695

1.5

-0.011

322.0

0.708

2.0

-0.009

311.0

0.687

2.5

-0.170

355.37

1.167

1.169

355.37

101.75

TABLE V. (Continued)

DATA TAKEN ON 16 AUGUST BY C. R. WEIGH. 5 *** HOT RIG PERFORMANCE ***

4 NOZZLES L/C=3.0 ALPES OF PRIMARY NOZZLES: 4

PRIMARY NOZZLE DIAMETER: 2.04 INCHES

PIPING STACK LENGTH: 21.37 INCHES

PIPING STACK DIAMETER: 7.12 INCHES

PIPING STACK L/C: 2.00

UPTAKE DIAMETER: 7.51 INCHES
AREA RATIO, AN/AP: 2.55

AMBIENT PRESSURE: 20.04 INCHES HG

N RUN	FNH IN. RG	CELFN IN.+20	FT+2	TUPT DEGREES	TAME	PU-PA INCHES OF WATER	PA-PS INCHES OF WATER	SECUNDARY AREA SCUARE INCHES	LFA	LPN/SEC	WPF
1	4.85	6.75	118.0	759.0	65.0	5.55	5.10	0.0	1.1097	0.0116	
2	4.55	6.75	118.0	762.0	65.0	11.30	3.30	6.283	1.1113	0.0116	
3	4.55	6.75	118.0	770.0	65.0	12.10	2.40	11.192	1.1113	0.0116	
4	5.00	6.70	118.0	773.0	65.0	12.40	1.52	14.726	1.1080	0.0116	
5	5.30	6.70	113.0	166.0	65.0	13.30	0.56	27.293	1.1080	0.0112	
6	5.00	6.70	113.0	166.0	65.0	13.70	0.55	35.859	1.1080	0.0112	
7	5.20	6.70	113.0	166.0	65.0	13.65	0.25	52.425	1.1111	0.0112	
8	5.40	6.70	112.0	168.0	65.0	13.50	0.24	64.952	1.1142	0.0111	
9	5.40	6.70	110.0	164.0	65.0	14.00	0.01	*****	1.1142	0.0109	
N RUN	W#	F#	T#	P#	T#	W#T#*44	W#	L#	LP	UU	UPT MACH
PLN							LBH/SEC	LBH/SEC	F# SEC	F# SEC	F# SEC
1	6.0	0.1551	0.4305	0.3695	0.0	1.121	C.C	375.59	125.65	112.54	0.066
2	0.3487	0.1030	0.4295	0.2399	C.2464	1.123	0.352	375.75	144.23	112.87	0.066
3	C.5257	0.1743	0.4267	0.1741	0.3642	1.123	0.555	377.37	154.45	113.36	0.066
4	C.6252	0.1596	0.4256	0.1401	0.4263	1.120	0.700	376.16	159.26	113.37	0.066
5	0.8175	0.0302	0.4281	0.0735	0.5626	1.115	0.915	373.58	168.44	112.22	0.065
6	C.9061	0.1175	0.4286	0.0407	0.6242	1.119	1.014	372.60	172.83	111.52	0.065
7	C.9481	0.0111	0.4286	0.0258	0.4532	1.122	1.064	373.44	175.45	112.17	0.065
8	C.51707	0.0075	0.4274	0.0176	0.6716	1.125	1.092	375.55	177.54	112.41	0.066
9	*****	0.0003	0.4288	0.0007	*****	1.125	*****	374.06	*****	112.36	0.066

PIPING STACK PRESSURE DISTRIBUTION FOR RUN: 9 POSITION A

W/C: C.5 1.0 1.5 2.0 2.5

PPS (IN. H2O): -C.550 -C.610 -0.180 -0.200 -0.140

FPS (IN. H2O): -C.030 -C.619 -0.006 -0.006 -0.005

TWX (CEC.F): 246.0 277.0 321.0 334.0 325.0

TWS (IN. H2O): 0.579 0.603 0.635 0.644 0.640

TABLE V. (Continued)

DATA TAKEN ON 18 AUGUST 85 BY C. R. WEICH
4 NOZZLES AP-3.0 L/c=3.0 WEICH E=0.5 *** HOT RIG PERFORMANCE ***

NUMBER OF PRIMARY NOZZLES: 4
PRIMARY NOZZLE DIAMETER: 2.06 INCHES
MIXING STACK LENGTH: 21.37 INCHES
MIXING STACK DIAMETER: 7.12 INCHES

MIXING STACK L/C: 3.000

N RUN	FNH IN-FG	DELPH IN-F20	F+Z IN-F2	TLP/T DEGREES	TARE F.	PU-PA INCHES CF WATER	PA-PS INCHES CF WATER	SECONDARY AREA SQUARE INCHES	LBF SEC	MPF LEM/SEC	LBF SEC	MPF LEM/SEC
1	4.45	6.30	114.0	852.0	66.0	5.10	4.85	0.0	1.0671	0.0113		
2	4.55	6.25	114.0	852.0	66.0	10.70	3.10	6.283	1.0645	0.0113		
3	4.60	6.25	114.0	852.0	66.0	11.50	2.20	11.192	1.0652	0.0113		
4	4.65	6.25	114.0	853.0	66.0	11.50	1.78	14.726	1.0660	0.0113		
5	4.65	6.20	113.0	855.0	66.0	12.70	1.50	27.293	1.0624	0.0112		
6	4.70	6.20	115.0	857.0	66.0	13.10	0.92	39.859	1.0626	0.0113		
7	4.70	6.20	115.0	858.0	66.0	13.25	0.23	52.425	1.0626	0.0113		
8	4.75	6.20	113.0	861.0	66.0	13.25	0.23	64.952	1.0633	0.0112		
9	4.70	6.20	114.0	851.0	66.0	13.45	0.01	*****	1.0626	0.0113		
N PLA	W#	F#	Y#	P*/T#	W*T**.44	WP	WS	LBM/SEC	FT/SEC	FT/SEC	FT/SEC	UPT MACH
1	C.0	0.1416	C.4008	0.3534	0.C	1.078	0.0	388.93	129.97	116.82	0.066	
2	0.2525	0.0518	C.4008	0.2290	0.2257	1.076	0.279	386.30	147.20	116.44	0.065	
3	0.5285	1.0653	0.4008	0.1630	0.2525	1.076	0.579	385.72	156.06	115.86	0.065	
4	C.6251	0.C528	C.4005	0.1319	0.4175	1.077	0.673	385.88	161.10	115.51	0.065	
5	0.8266	3.0269	0.3998	0.0673	0.5522	1.074	0.887	384.33	170.75	115.44	0.065	
6	C.9173	3.0155	0.2992	0.0389	3.6124	1.074	0.985	384.67	175.57	115.55	0.065	
7	C.5611	0.C098	0.2989	0.0247	0.6415	1.074	1.032	384.78	177.86	115.58	0.065	
8	C.5542	3.0068	0.2980	0.0172	0.6625	1.074	1.068	385.77	179.91	115.69	0.065	
9	*****	0.C003	0.4011	C.008	*****	1.074	*****	382.41	*****	114.87	0.065	

MIXING STACK PRESSURE DISTRIBUTION FOR RUN: 9 POSITION A

Y/E:	0.5	1.0	1.5	2.0	2.5
FPS (1A, 1Z):	-0.950	-0.600	-0.180	-0.170	-0.150
FPS: -0.029	-0.018	-0.005	-0.005	-0.005	-0.005
TMIX (CEC-F): 276.0	310.0	356.0	368.0	357.0	
1PS: 0.561	0.587	0.622	0.631	0.621	

TABLE V. (Continued)

DATA TAKEN ON 21 AUGUST 1962. R. WELCH
4 NOZZLES: 2.5 L/D = 2.5 S/D = 5 *** HOT RIS PERFORMANCE ***

NUMBER OF PRIMARY NOZZLES: 4
PRIMARY NOZZLE DIAMETER: 2.25 INCHES
FIXING STACK LENGTH: 17.81 INCHES
FIXING STACK DIAMETER: 7.12 INCHES
FIXING STACK L/D: 2.50

UPTAKE DIAMETER: 7.51 INCHES
AREA RATIO, AN/AP: 2.50

N RUN	FH IN. FG	DELPH IN. FG	FH ₂ DEGREES	TLPT DEGREES	TATE F.	PU-FA INCHES CF WATER	PA-PS INCHES CF WATER	SCCNDARY AREA SQUARE INCHES	WPA LBM/SEC	WPF LBM/SEC	AMBIENT PRESSURE: 29.97 INCHES HG		
											PA-FA	SCCNDARY AREA	WPA
1	3.35	12.95	0.0	146.0	65.0	4.75	3.75	0.0	1.5469	0.0			
2	3.40	13.50	0.0	148.0	65.0	6.10	2.37	6.283	1.5453	3.0			
3	3.50	13.50	0.0	152.0	65.0	6.70	1.69	11.192	1.5475	0.0			
4	3.50	13.50	0.0	154.0	65.0	7.02	1.36	14.726	1.5475	3.0			
5	3.53	13.50	0.0	154.0	65.0	7.48	0.69	27.293	1.5482	3.0			
6	3.55	13.50	0.0	156.0	65.0	7.56	0.40	39.859	1.5487	3.0			
7	3.60	13.50	0.0	157.0	65.0	8.10	0.25	52.425	1.5458	3.0			
8	3.60	12.50	0.0	158.0	65.0	8.20	0.17	64.952	1.5498	0.0			
9	3.60	13.50	0.0	159.0	65.0	8.35	0.00	*****	1.5498	0.0			
N RUN	H*	F*	T*	P*T/T*	H*T*T* ^{1/4}	WP	WS	UP	UM	UU	UPT MACH		
						LBM/SEC	LBM/SEC	F T/SEC	F T/SEC		F T/SEC		
1	0.0	0.2583	0.8663	0.4136	0.0	1.541	0.0	215.06	86.01	77.25	0.064		
2	C.2145	0.2270	C.8634	0.2629	0.2011	1.545	0.231	214.82	101.73	77.24	0.064		
3	C.3217	3.1593	0.8578	0.1858	0.2667	1.548	0.458	216.18	110.22	77.16	0.064		
4	C.3803	0.1280	C.8550	0.1497	0.3545	1.548	0.588	216.71	114.76	77.55	0.064		
5	0.4999	0.0646	0.8550	0.0756	0.4664	1.544	0.774	216.45	123.51	77.85	0.064		
6	0.5557	3.0372	0.8522	0.2437	0.5175	1.549	0.861	217.07	127.88	78.07	0.064		
7	C.5756	3.0234	C.8508	0.0274	0.5358	1.550	0.858	217.50	125.85	76.23	0.064		
8	0.5925	3.0158	0.8494	0.0186	0.5514	1.550	C.510	217.81	130.93	78.24	0.064		
9	*****	C.0005	0.8481	0.0035	*****	1.550	*****	218.07	*****	76.44	0.064		

FIXING STACK PRESSURE DISTRIBUTION FOR RUN: 9 POSITION A

Y/D:	0.5	1.0	1.5	2.0
F _{PSL} (IN. H2O):	-C.870	-C.690	-0.320	-0.260
P _{MSL} (PSI):	-0.081	-0.064	-0.039	-0.024
TMX (CEC. F1):	85.0	101.0	158.0	110.0
TMX (PSI):	C.506	C.523	C.528	0.528

TABLE VI. Performance Data L/D = 2.5

DATA TAKEN ON 31 AUGUST BY D.C. WELCH
4 NOZZLES $\Delta p = 2.5$ $\frac{L}{D} = 2.5$ $\frac{W}{D} = 0.5$

NUMBER OF PRIMARY NOZZLES: 4

PRIMARY NOZZLE DIAMETER: 2.25 INCHES

MIXING STACK LENGTH: 17.01 INCHES

MIXING STACK DIAMETER: 7.12 INCHES

MIXING STACK L/D: 2.50

*** HCT-550 EEC F
TUFT-550 EEC F
PERFORMANCE ***

UPTAKE DIAMETER: 7.51 INCHES
AREA RATIO, A_H/A_D : 2.50

AMBIENT PRESSURE: 29.97 INCHES HG

N	FN _H	DELFN	FH ₂	TUFT	TAMB	PU-PA	PA-FS	SECONDARY AREA	WFA	WPF
RUN	IN. + G	IN. + 20	IN. + 2	DEGREES	F.	INCHES OF WATER	SQUARE INCHES	LB/H/SEC	LB/H/SEC	
1	4.50	8.20	11.0	565.0	65.0	6.45	3.58	C.0	1.2129	0.0074
2	4.58	8.15	10.0	564.0	65.0	7.40	2.15	6.283	1.2106	0.0073
2	4.62	8.15	10.0	563.0	65.0	8.00	1.26	11.742	1.2113	0.0073
4	4.65	8.15	10.0	564.0	65.0	8.30	1.20	14.726	1.2116	0.0073
5	4.68	8.15	11.0	566.0	65.0	8.85	0.88	27.253	1.2123	0.0074
6	4.70	8.15	10.0	565.0	65.0	9.10	0.33	35.059	1.2127	0.0073
7	4.70	8.15	10.0	562.0	65.0	5.20	0.21	52.425	1.2127	0.0073
8	4.70	8.10	10.0	562.0	65.0	9.25	0.14	64.952	1.2050	0.0073
9	4.71	8.15	12.0	571.0	65.0	5.45	0.00	*****	1.2128	0.0075
N	W*	F*	T*	P*T/T*	W*T**/44	WP	WS	LF	UM	UPT MACH
RUN						LB/H/SEC	LB/H/SEC	FT/SEC	FT/SEC	FT/SEC
1	0.0	0.1922	0.5120	0.3754	0.4.C	1.220	C.0	286.89	114.74	103.19
2	C.2552	0.1165	0.5125	0.2281	0.1532	1.210	0.316	285.05	129.07	102.52
3	C.3854	0.0619	0.5130	0.1597	0.2674	1.215	C.410	284.48	136.15	102.52
4	0.4525	0.0652	0.5125	0.1272	0.2312	1.219	C.552	284.66	140.17	102.39
5	0.5829	0.0216	0.5115	0.0617	0.4348	1.220	0.712	284.92	147.54	102.48
6	0.6431	0.0180	0.5120	0.0352	0.4751	1.220	C.785	284.52	151.24	102.24
7	C.6716	0.0114	0.5135	0.0223	0.5005	1.220	0.819	283.62	152.53	102.01
8	C.6855	0.0079	0.5135	0.0153	0.5146	1.216	0.839	282.73	153.12	101.45
9	*****	0.0003	0.5091	0.2005	*****	1.220	*****	286.05	*****	102.69

MIXING STACK PRESSURE DISTRIBUTION FOR RUN: 9 POSITION A

Y/L:	0.5	1.0	1.5	2.0
PPS (IN. + 2C):	-0.550	-0.350	-0.080	-0.080
PPS*:	-C.030	-0.019	-0.004	-0.004
TMX (EEC + F):	250.0	282.0	252.0	284.0
TMX*:	0.693	0.725	0.735	0.726

TABLE VI. (Continued)

DATA TAKEN ON 11 SEPT BY D.R. WELCH S/E=0.5 ***

4 NOZZLES A/P=2.5 L/t=2.5 S/E=0.5 ***

HOT TURBINE PERFORMANCE 550 DEG F ***

NUMBER OF PRIMARY NOZZLES: 4

PRIMARY NOZZLE DIAMETER: 2.25 INCHES

MIXING STACK LENGTH: 17.81 INCHES

MIXING STACK DIAMETER: 7.12 INCHES

MIXING STACK L/C: 2.50

AMBIENT PRESSURE: 29.57 INCHES HG

RUN	FNH	DEPN	FT-Z	TUPT	TANG	PU-FA	PA-FS	SECONDARY AREA	LBM/SEC	WPF	LBM/SEC	WPF
								SQUARE INCHES				
1	2.56	1A+LG	1A+L20	12	542.0	64.0	4.50	3.50	0.0	1.1741	0.0086	
2	2.52	7.85	65.0	545.0	64.0	6.20	2.18	6.263	1.1708	0.0085		
3	2.58	7.85	65.0	546.0	64.0	7.08	1.21	14.726	1.1718	0.0086		
4	2.62	7.85	64.0	548.0	64.0	7.50	0.24	35.859	1.1725	0.0085		
5	2.65	7.85	63.0	550.0	64.0	6.10	0.15	64.992	1.1730	0.0085		
6	2.65	7.85	64.0	552.0	64.0	6.28	C.00	*****	1.1737	0.0085		
N	**	P*	T*	P*T*	W*T**.44	W	W	W	W	W	W	W
RUN												
1	C.0	0.2690	0.5228	0.3598	0.0	1.163	0.0	271.77	108.65	57.15	0.063	
2	C.2658	0.1320	0.5212	0.2513	0.2026	1.175	C.318	27C.52	123.51	57.44	0.063	
3	C.4707	0.0128	0.5207	0.1358	0.3532	1.180	0.556	27C.80	134.77	57.40	0.063	
4	C.6700	0.6201	0.5197	0.0387	0.5023	1.181	C.751	27C.89	146.03	57.43	0.063	
5	C.73C7	0.099	0.5187	0.0173	0.5474	1.161	0.823	271.40	149.67	57.42	0.063	
6	*****	0.0003	0.5176	0.0006	*****	1.182	*****	272.02	*****	97.84	0.063	

MIXING STACK PRESSURE DISTRIBUTION FOR RUN: 6 POSITION A

X/L:	C.5	1.0	1.5	2.0
FMSLN. H2C1:	-0.730	-0.490	-0.130	-0.120
PHS#:	-0.044	-0.029	-0.008	-0.007
TIX (CEG, F1):	228.0	270.0	253.0	291.0
TPS#:	C.687	C.726	C.748	0.745

TABLE VI. (Continued)

DATA TAKEN ON 21 AUGUST BY C. R. WELCH
4 NOZZLES AP/2.5 L/2.5 S/2.5

*** HQT RIG PERFORMANCE ***
TUFT-650 CEG F

NUMBER OF PRIMARY NOZZLES: 4

PRIMARY NOZZLE DIAMETER: 2.25 INCHES

PIXING STACK LENGTH: 17.81 INCHES

MIXING STACK DIAMETER: 7.12 INCHES

PIXING STACK L/D: 2.50

N _u	F ₁₁	DEFLN	F ₁₂	T ₀₁	T ₀₂	T _{AMB}	T _{UP}	T _{UP}	P _{U-P}	P _{A-S}	SECONDARY AREA	WFA	WPF	
												LB/SEC	FT/SEC	
1	4.2C	7.30	61.0	664.0	65.0	5.55	2.55	0.0			1.1412	0.0083		
2	4.28	7.30	61.0	662.0	65.0	7.30	2.12	6.283			1.1425	0.0083		
3	4.30	7.30	61.0	661.0	65.0	7.85	1.47	11.152			1.1428	0.0083		
4	4.30	7.30	60.0	660.0	65.0	8.15	1.16	14.726			1.1428	0.0082		
5	4.37	7.30	63.0	670.0	65.0	8.75	0.56	27.293			1.1440	0.0085		
6	4.25	7.30	62.0	668.0	65.0	9.00	0.33	35.859			1.1443	0.0084		
7	4.49	7.30	62.0	666.0	65.0	9.10	0.21	52.425			1.1444	0.0084		
8	4.40	7.20	62.0	672.0	65.0	9.15	0.15	64.992			1.1444	0.0084		
9	4.40	7.20	60.0	664.0	65.0	9.25	0.00	*****			1.1444	0.0082		
N _u	w*	F*	T*	P*T/T*	w*T*+4.44	W _P	W _S	W _U	W _P	W _S	W _U	W _P	W _S	W _U
FLN						LB/SEC	LB/SEC	FT/SEC	FT/SEC	FT/SEC	FT/SEC	FT/SEC	FT/SEC	FT/SEC
1	C.0	0.1186	0.4669	0.3826	0.0	1.145	C.C	296.24	118.52	10t.55	0.065			
2	0.2224	0.1976	0.4678	0.2300	0.1550	1.151	0.213	295.11	132.98	10t.14	0.065			
3	C.4335	0.1745	0.4682	0.1600	0.2853	1.151	0.465	294.45	135.55	1C5.51	0.065			
4	C.4722	0.0593	0.4686	0.1266	0.3282	1.151	0.543	292.94	143.5C	105.73	0.064			
5	C.6C13	0.1282	0.4644	0.0606	0.4234	1.152	0.700	296.49	151.98	10t.64	0.065			
6	C.66C7	0.1167	0.4653	0.0358	0.4861	1.152	0.765	295.86	155.77	10t.42	0.065			
7	C.7055	0.1014	0.4661	0.0223	0.5042	1.152	0.813	255.29	156.91	10t.21	0.065			
8	C.7356	0.1173	0.4636	0.157	0.5245	1.153	0.648	256.82	159.18	10t.76	0.065			
9	*****	0.0003	0.4669	0.0035	*****	1.153	*****	254.57	105.55	0.064				
PIXING STACK PRESSURE DISTRIBUTION FOR RUN: 9 POSITION A														
	X/E:	C.5	1.0	1.5	2.0									
P ₁₁₁₁	F ₂₁₁	-0.550	-0.340	-0.080	-0.080									
F ₁₁₁₁	F ₁₁₁₁	-0.028	-0.017	-0.004	-0.004									
T ₁₁₁₁	T ₁₁₁₁	267.0	319.0	326.0	318.0									
		0.647	0.686	0.701	0.695									

TABLE VI. (Continued)

DATA TAKEN ON 11 SEPT BY D. R. WELCH S/C=5 *** TOT UPTG = 650 CEG F

NOZZLE AP/2.5 L/D=2.5 S/C=5
NOZZLE NC2ZLES: 4
PRIMARY NC2ZLE DIAMETER: 2.25 INCHES
MIXING STACK LENGTH: 17.81 INCHES
MIXING STACK DIAMETER: 7.12 INCHES
MIXING STACK L/D: 2.50

UPTAKE DIAMETER: 7.51 INCHES
AREA RATIO, AM/AP: 2.50

AMBIENT PRESSURE: 29.97 INCHES HG

N RUN	PNH	DELPN	F+Z IN+G	L2 IN+G	DEGREES	F. INCHES OF WATER	PA-PS INCHES OF WATER	PA-PS SCLARE INCHES	SECONDARY AREA SCLARE INCHES	WFA	WPF
1	2.55	7.20	55.0	648.0	64.0	5.50	3.45	0.0	1.1295	0.0095	
2	4.05	7.15	54.0	647.0	64.0	6.66	2.10	6.283	1.1273	0.0094	
3	4.10	7.15	55.0	648.0	64.0	7.40	1.14	14.726	1.1281	0.0095	
4	4.12	7.15	54.0	648.0	64.0	8.48	0.31	35.859	1.1284	0.0094	
5	4.15	7.15	54.0	648.0	64.0	8.65	0.14	64.952	1.1289	0.0094	
6	4.15	7.15	55.0	649.0	64.0	8.89	0.00	*****	1.1289	0.0095	
N	W	P*	T*	P*T*	W*T*	W	W	W	W	W	W
RLA						LBM/SEC	LBM/SEC	F1/SEC	F1/SEC	FT/SEC	FT/SEC
1	0.0	0.1817	0.4728	0.3843	0.0	1.125	0.0	289.40	115.74	104.59	0.064
2	0.2147	0.1120	0.4732	0.2367	0.1577	1.127	0.212	287.60	125.90	102.44	0.063
3	0.4740	0.0609	0.4728	0.1288	0.2405	1.126	0.539	287.40	140.62	103.27	0.063
4	0.6685	0.0167	0.4728	0.0351	0.4611	1.128	0.761	286.88	150.99	103.48	0.063
5	0.7155	0.0172	0.4728	0.0153	0.5174	1.128	0.839	286.88	153.75	103.18	0.063
6	*****	0.0303	0.4723	0.0006	*****	1.128	*****	287.07	*****	103.25	0.063
MIXING STACK PRESSURE DISTRIBUTION FOR RUN: 6 POSITION A											
P/C:	0.5	1.0	1.5	2.0							
FPS (IN. F2C):	-0.580	-0.360	-0.090	-0.090							
TRIX (CEG, F):	-0.031	-0.019	-0.005	-0.005							
TRIX (PS):	287.0	320.0	326.0	327.0							
TRIX (PS):	0.674	0.705	0.718	0.710							

TABLE VI. (Continued)

DATA TAKEN ON 31 AUGUST BY C.C.R. WELCH
4 NOZZLES AP/DP=2.5 L/C=2.5 S/C=2.5
*** HOT RIG PERFORMANCE ***

NUMBER OF PRIMARY NOZZLES: 4
PRIMARY NOZZLE DIAMETER: 2.25 INCHES
MIXING STACK LENGTH: 17.81 INCHES
MIXING STACK DIAMETER: 7.12 INCHES

MIXING STACK L/D: 2.50

N RUN	F _{AN} 1N+1G	DEFLN	F+2 1N+20	TUPT DEGREES	T _{AN} F.	PU-PA INCHES OF WATER	PA-PS INCHES	SECUNDARY AREA SQUARE INCHES	WFA	LBF/SEC	LBF/SEC	LBF
1	2.56	0.70	51.0	755.0	65.0	5.50	3.45	0.0	1.0008	0.0092	0.0092	0.0092
2	4.02	6.70	51.0	756.0	65.0	7.25	2.05	6.283	1.0517	0.0092	0.0092	0.0092
3	4.13	6.65	53.0	760.0	65.0	7.85	1.43	11.192	1.0590	0.0094	0.0094	0.0094
4	4.19	6.65	52.0	760.0	65.0	8.10	1.14	14.726	1.0550	0.0093	0.0093	0.0093
5	4.12	6.65	52.0	760.0	65.0	8.60	0.55	27.293	1.0593	0.0093	0.0093	0.0093
6	4.14	6.60	52.0	758.0	65.0	8.85	0.31	35.859	1.0556	0.0093	0.0093	0.0093
7	4.15	6.60	53.0	759.0	65.0	9.10	0.20	52.425	1.0558	0.0094	0.0094	0.0094
8	4.15	6.60	52.0	758.0	65.0	9.00	0.14	64.952	1.0558	0.0093	0.0093	0.0093
9	4.16	6.63	51.0	756.0	65.0	9.15	0.00	*****	1.0560	0.0092	0.0092	0.0092
MIXING STACK PRESSURE DISTRIBUTION FOR RUN: 9 POSITION A												
	X/C:	0.5	1.0	1.5	2.0							
	PPS (IN. H ₂ O):	-0.550	-0.340	-0.053	-0.080							
	PPS _{0.5} :	-0.027	-0.016	-0.004	-0.004							
	T _{PS} (CEG.F):	265.0	352.0	346.0	354.0							
	T _{PS0.5} :	0.630	0.668	0.677	0.667							

TABLE VI. (Continued)

DATA TAKEN ON 11 SEP 5 BY C.R.WELCH S/C 2.5 ***
4 NOZZLES $A_w/A_p = 2.5$ $L/C = 2.5$ HOT RIG PERFORMANCE

HOT RIG, $T = 750$ DEG F

NUMBER OF PRIMARY NOZZLES: 4
PRIMARY NOZZLE DIAMETER: 2.25 INCHES
MIXING STACK LENGTH: 17.81 INCHES
MIXING STACK DIAMETER: 7.12 INCHES
MIXING STACK L/G: 2.50

N RLN	FNO	SLPN	F12	TUP1	TAMP	PUP-PA	PA-PS	SECONDARY AREA	WFA	HPF	LEM/SEC
DEGREES	F.	INCHES OF WATER	SCALAR INCHES								
1	3.69	6.60	1.05.0	746.0	64.0	5.50	3.45	0.0	1.0804	0.0104	
2	3.50	6.60	1.04.0	749.0	64.0	6.85	2.05	6.283	1.0815	0.0104	
3	3.50	6.60	1.04.0	752.0	64.0	7.13	1.13	14.726	1.0815	0.0104	
4	3.55	6.60	1.05.0	754.0	64.0	8.50	0.31	35.859	1.0827	0.0104	
5	4.00	6.60	1.05.0	755.0	64.0	8.65	0.14	64.952	1.0835	0.0104	
6	6.60	6.60	1.02.0	756.0	64.0	8.80	0.00	*****	1.0835	0.0103	
N	W	F#	T#	P/T*	W/T**	W/T***.44	WF	WS	LF	WP	UPT MACH
RLN							LB/SEC	LEM/SEC	F1/SEC	FT/SEC	
1	6.0	9.1672	0.4343	0.3850	0.4	1.051	0.0	301.67	120.65	1.0850	0.064
2	0.2825	0.6553	0.4333	0.2252	0.1555	1.052	0.309	301.78	135.39	108.54	0.064
3	0.4505	0.6545	0.4322	0.1260	0.2251	1.053	0.526	301.84	146.24	1.0857	0.064
4	0.6537	0.3148	0.4315	0.0342	0.4771	1.053	0.755	301.97	156.73	108.61	0.064
5	0.7487	0.6565	0.4311	0.0151	0.5171	1.054	0.839	302.31	159.92	108.73	0.064
t	*****	0.0002	0.4308	0.0006	*****	1.054	*****	302.41	*****	108.77	0.064

MIXING STACK PRESSURE DISTRIBUTION FOR RUN: 6 POSITION A

	X/C:	0.5	1.0	1.5	2.0	
TPS(1A, 12C):		-0.575	-0.345	-0.070	-0.070	
TPS(2):		-0.028	-0.017	-0.003	-0.003	
TPS(1CEC-F1):		323.0	363.0	380.0	370.0	
TPS(2):		0.645	0.681	0.693	0.684	

TABLE VI. (Continued)

DATA TAKEN ON 31 AUGUST BY E.C. WELCH
4 NOZZLES, AR/AP=2.5 L/C=2.5 *** HOT RIG PERFORMANCE ***

NUMBER OF PRIMARY NOZZLES: 4

PRIMARY NOZZLE DIAMETER: 2.25 INCHES

MIXING STACK LENGTH: 17.81 INCHES

MIXING STACK DIAMETER: 7.12 INCHES

MIXING STACK L/C: 2.50

UP TAKE DIAMETER: 7.51 INCHES
AREA RATIO, AR/AP: 2.50

AMBIENT PRESSURE: 29.97 INCHES HG

N RUN	FNR IN. #G	DELN IN. #20	F+Z DEGREES	TUP DEGREES	TAPE F.	PU-PA INCHES OF WATER	PA-FS SQUARE INCHES	SECONDARY AREA SQUARE INCHES	WFA LB/SEC	WFF LB/SEC
1	3.70	6.05	1C+0	854.0	65.7	5.60	3.38	0.0	1.0342	0.0104
2	3.60	6.05	1C+0	856.0	65.0	7.10	1.58	6.283	1.0357	0.0104
3	3.83	6.05	1C+0	856.0	65.0	7.70	1.28	11.152	1.0361	0.0104
4	3.85	6.05	1C+0	857.0	65.0	8.00	1.10	14.726	1.0364	0.0104
5	3.50	6.05	1C+0	856.0	65.7	8.50	0.52	21.253	1.0371	0.0103
6	3.90	6.00	1C2.0	857.0	65.0	8.70	0.20	35.859	1.0330	0.0102
7	3.90	6.00	1C3.0	857.0	65.0	8.80	0.19	52.425	1.0330	0.0103
8	3.90	6.00	1C3.0	857.0	65.0	8.90	0.13	64.652	1.0330	0.0103
9	3.50	6.00	1C3.0	859.0	65.0	8.57	0.00	*****	1.0330	0.0103
N	W+	F+	1*	P*+T*/*	h*T**.44	WF	hS	UP	UU	UP TACH
RUN						LB/SEC	LB/SEC	F1/SEC	F1/SEC	
1	0.0	0.1504	0.2994	0.3771	0.0	1.045	0.0	214.68	125.85	113.19
2	0.2893	0.0892	0.2588	0.2232	0.1530	1.046	0.303	314.52	140.23	113.13
3	0.4305	0.0618	0.2988	0.1549	0.2872	1.044	0.451	314.20	147.16	113.01
4	0.5056	0.0432	0.2985	0.1235	0.2312	1.047	0.529	314.31	150.96	113.05
5	0.6425	0.0233	0.2988	0.0585	0.4257	1.047	0.674	312.82	157.69	112.67
6	0.7111	0.0133	0.2985	0.0335	0.4744	1.042	0.742	312.60	160.42	112.44
7	0.7506	0.0086	0.2985	0.0216	0.5007	1.043	0.783	312.55	162.37	112.42
8	0.7667	0.0058	0.2985	0.0146	0.5115	1.042	0.800	312.50	163.15	112.40
9	*****	0.0002	0.2979	0.0006	*****	1.043	*****	312.98	*****	112.54

MIXING STACK PRESSURE DISTRIBUTION FOR RUN: 9 POSITION A

X/C:	0.5	1.0	1.5	2.0
FPS (IN. H2O):	-0.540	-0.325	-0.050	-0.050
FPS*:	-0.024	-0.015	-0.002	-0.002
TRIX (CEC/F1):	236.0	268.0	407.0	394.0
TRIX TPS*:	0.606	0.645	0.649	0.648

TABLE VI. (Continued)

DATA TAKEN ON 21 SEP 1963 BY D. R. MELCH S/C=5 ***

4 NOZZLES L/C=2.5 HGT/R = 0.650 CEG F

NUMBER OF PRIMARY NOZZLES: 4

PRIMARY NOZZLE DIAMETER: 2.25 INCHES

MIXING STACK LENGTH: 17.81 INCHES

MIXING STACK DIAMETER: 7.12 INCHES

MIXING STACK L/C: 2.50

UPTAKE DIAMETER: 7.51 INCHES
AREA RATIO, AM/AP: 2.50

AMBIENT PRESSURE: 29.97 INCHES HG

N RUN	FH IN. RG	DELPH IN. RG	FH IN. RG	TUP DEGREES	TAMB F.	PU-PA INCHES CF WATER	PA-PS INCHES CF WATER	SECONDARY AREA SQUARE INCHES	WFA	LBM/SEC	WFA LBM/SEC
1	3.55	6.00	111.0	85.0	64.0	5.45	3.25	0.0	1.0216	0.0110	
2	3.65	6.30	111.0	85.0	64.0	6.70	1.57	6.283	1.0293	0.0110	
3	3.70	6.00	112.0	85.0	64.0	7.55	1.05	14.726	1.0300	0.0111	
4	3.72	6.00	111.0	85.0	64.0	8.36	0.20	35.859	1.0303	0.0110	
5	3.75	6.00	111.0	85.0	64.0	8.45	0.13	64.992	1.0308	0.0110	
6	3.75	6.00	111.0	85.0	64.0	8.58	0.00	*****	1.0308	0.0110	
N RUN	W#	F#	T#	P#	T#	W#	L#	W#	UU	W#	UU
RLA						LBM/SEC	LBM/SEC	LBM/SEC	FT/SEC	FT/SEC	FT/SEC
1	C.0	C.1509	0.2986	0.3705	0.0	1.035	0.0	312.93	125.15	112.55	0.063
2	0.2508	0.0891	0.2986	0.2235	0.1540	1.040	0.202	312.31	135.31	112.33	0.063
3	C.5065	C.0494	C.2986	0.1240	0.3375	1.041	0.527	311.88	149.85	112.16	0.063
4	C.7131	C.0134	0.3983	0.0336	0.4746	1.041	0.743	311.57	155.98	112.07	0.063
5	C.7565	C.0057	0.2980	0.0142	0.5014	1.042	0.788	311.81	162.25	112.15	0.063
6	*****	0.0002	0.2571	C.0006	*****	1.042	*****	312.43	*****	112.38	0.063

MIXING STACK PRESSURE DISTRIBUTION FOR RUN: 6 POSITION A

FPS (IN. H2O):	0.5	1.0	1.5	2.0
FPS: -C.250	-C.330	-0.070	-0.070	
FPS: -0.025	-C.015	-C.003	-0.003	
TPX (CEG-F): 374.0	413.0	428.0	417.0	
TPS: 0.635	0.664	0.676	0.667	

TABLE VI. (Continued)

DIAMETRAL POSITION (INCH)	TEXIT (°F)	TUPT (°F)
0	393	845
.25	397	845
.50	400	847
.75	416	846
1.00	420	846
1.25	432	847
1.50	441	847
1.75	449	849
2.00	452	850
2.25	463	850
2.50	468	849
2.75	475	849
3.00	482	851
3.25	496	852
3.50	497	853
3.75	497	851
4.00	501	851
4.25	501	851
4.50	500	853
4.75	498	853
5.00	494	850
5.25	492	852
5.50	484	854
5.75	480	855
6.00	471	856
6.25	462	855
6.50	458	856
7.00	452	856
7.25	440	856
7.50	418	858

TABLE VII. Mixing Stack Exit Plane Temperature
Profile L/D = 3.0

DIAMETRAL POSITION (INCH)	TEXIT (°F)	TUPT (°F)
0	385	848
.25	395	848
.50	403	852
.75	412	852
1.00	419	851
1.25	426	851
1.50	437	851
1.75	443	852
2.00	450	853
2.25	455	853
2.50	460	855
2.75	464	855
3.00	471	855
3.25	480	857
3.50	483	855
3.75	491	852
4.00	498	851
4.25	500	851
4.50	491	852
4.75	486	852
5.00	480	851
5.25	476	851
5.50	472	851
5.75	468	853
6.00	458	852
6.25	452	852
6.50	446	853
6.75	440	851
7.00	435	853

TABLE VII. (Continued)

DIAMETRAL POSITION (INCH)	TEXIT (°F)	TUPT (°F)
0	416	856
.25	512	856
.50	523	857
.75	530	858
1.00	540	859
1.25	548	858
1.50	555	857
1.75	564	858
2.00	572	857
2.25	579	858
2.50	585	858
2.75	594	860
3.00	594	859
3.25	596	863
3.50	594	862
3.75	590	862
4.00	582	859
4.25	571	856
4.50	560	855
4.75	546	855
5.00	532	857
5.25	516	858
5.50	502	856
5.75	490	857
6.00	480	859
6.25	460	862
6.50	452	862
6.75	436	862
7.00	429	863

TABLE VIII. Mixing Stack Exit Plane Temperature
Profile Data L/D = 2.5

DIAMETRAL POSITION (INCH)	TEXIT (°F)	TUPT (°F)
0	476	857
.25	483	857
.50	497	858
.75	506	857
1.00	519	858
1.25	532	859
1.50	548	859
1.75	561	859
2.00	569	859
2.25	577	860
2.50	581	860
2.75	588	859
3.00	592	860
3.25	593	861
3.50	593	861
3.75	588	861
4.00	580	861
4.25	570	861
4.50	558	861
4.75	551	861
5.00	537	860
5.25	523	860
5.50	509	860
5.75	500	862
6.00	494	862
6.25	480	863
6.50	468	862
6.75	456	862
7.00	446	862

TABLE VIII. (Continued)

Variable	Value	Uncertainty
T_s	525°R	± 1°R
T_p	1316°R	± 1°R
B, Pa	30.04 in Hg	± .01 in Hg
ΔPN	6.05 in H_2O	± .05 in H_2O
ΔEH	8.50 in H_2O	± .05 in H_2O
ΔPS	.52 in H_2O	± .005 in H_2O
FHZ	103 Hz	± 1 Hz
PNH	3.90 in Hg	± .02 in Hg
r	1.126 in	± .005

Values in this table are from $L/D = 2.5$,
 $A_m/A_p = 2.5$, $TUPT = 850^{\circ}F$ (Table VI)

TABLE IX. Uncertainties in Measured Values from Table VI

APPENDIX A

OPERATION OF THE COMBUSTION GAS GENERATOR

A. COMPRESSOR LIGHT OFF

The primary air flow is supplied by the Carrier Model 18P350 centrifugal air compressor located in Building 248. This compressor's cooling system is piped into the cooling tower system located behind the building. Figure 45 gives a schematic of the compressor layout.

In preparation for compressor light off ensure that the cooling water valve to the Sullivan compressor is closed, then start the cooling tower pump and fan by pushing both start buttons located on the south wall of Building 248 (see Figure 46). The compressor can then be started by completing the following steps.

- 1) Ensure that the compressor butterfly suction damper in the airstream between the filter (on the roof) and the compressor is closed (Figure 47).
- 2) Operate the let water valve to the oil cooler (Figure 47) wide enough to obtain an adequate flow of cooling water.
- 3) Start the auxiliary oil pump by positioning the on-off automatic switch (Figure 48) in the "hand" position, thereby bypassing the auxiliary oil pump out-in control.
- 4) When the oil pressure rises to at least 16 PSIG, adequate pressure exists in the bearings and the

compressor may be started by pressing the start pushbutton. The compressor will then come up to speed, at which time the auxiliary oil pump switch is turned to the "automatic" position.

- 5) Open the compressor butterfly suction damper.

Precautions:

- 1) During the period in which the compressor is coming up to speed, the operator should check for:
 - (a) oil pressure in the range 20 to 22 PSIG
 - (b) any undue noise in the motor, gear, or compressor.
- 2) During operation, check the bearing thermometers periodically to ensure the bearing temperatures do not exceed 185°F.

B. GAS GENERATOR LIGHT OFF

After the supply air compressor is in operation, the following is a recommended starting sequence.

- 1) Energize the main power panel and the thermocouple and mass flowmeter readouts.
- 2) Calculate the required mass flow rate to achieve the desired uptake Mach number, M_u . The formula for this calculation (derived in Reference [4]) follows:

$$M_u = \frac{.0502(\dot{m}_a + \dot{m}_f) T U P T^{0.5}}{(\frac{P_U}{13.57}) + B}$$

where

TUPT = uptake temperature (DEG. R)
 PU = uptake pressure (in. H₂O)
 (PU can be assumed to be 0.0 for the first iteration)
 B = atmospheric pressure (in. Hg)
 \dot{m}_a = mass flow rate of air (lbm/sec)
 \dot{m}_f = mass flow rate of fuel (lbm/sec)
 (\dot{m}_f can be assumed to be .01 lbm/sec for this calculation)

3) Figure 15 gives the primary air mass flow rate versus the pressure product. The pressure product comes from the transition nozzle calibration and is defined as:

$$((PNH + B) * \Delta PN)^{.5}$$

where:

PNH = nozzle high pressure (IN. Hg)
 B = atmospheric pressure (IN. Hg)
 ΔPN = pressure drop across nozzle (IN. H₂O)

From Figure 15 find the pressure product corresponding to the required mass flow rate found in Step 2 above.

4) With the burner air valve 100% open and the bypass air valve (see Figure 3) 50% closed, open the main air supply globe valve (Figure 49) until the desired pressure product is reached.

- 5) Adjust the bypass air valve until the U-bend pressure difference (ΔP_u) is one inch of water.
- 6) Turn on the fuel supply pump and the high pressure fuel pump.
- 7) Adjust the fuel control valve to obtain 150 PSIG on the high pressure fuel gage (see Figure 5).
(Note: It is desired to obtain about 115 Hz on the fuel flow meter, but this reading is not available until the fuel shutoff valve is opened. The fuel pressure is therefore used as an initial approximation of fuel flow rate.)
- 8) Energize the igniter plug and glow coil by depressing the igniter switch. Hold this switch down for a few seconds before opening the fuel shutoff.
- 9) Open the fuel shutoff valve by putting the emergency shutoff switch in the "on" position. Watch the fuel flowmeter; the reading should quickly come to the 110-120 Hz range. Ignition should be noted within 3-4 seconds. If ignition does not occur quickly, turn off the emergency shutoff switch.
- 10) If ignition does not occur and the fuel flowmeter indicated a flow outside the 110-120 Hz range, adjust the fuel control valve to achieve a reading in this range and repeat the procedure starting at Step 7.
- 11) If ignition does not occur and the fuel flowmeter indicated a flow in the 110-120 Hz range,

- a) Check to ensure the U-bend pressure differential (ΔP_u) is one inch of water. If not, adjust the cooling air valve to achieve this.
- b) If the U-bend pressure differential is one inch of water, check the igniter. The igniter can be checked by activating the igniter switch with no fuel flow and watching for a 3-5 degree increase in burner temperature.

12) When ignition does occur:

- a) Deactivate the igniter.
- b) Begin closing the bypass air valve immediately while monitoring burner temperature (T_B). Continue closing the bypass air valve until T_B stabilizes. (Do not allow burner temperature to exceed 1500°F.)

C. TEMPERATURE ADJUSTMENT

The temperature adjustment is an iterative process consisting of the following steps.

- 1) Adjust the fuel control valve to achieve approximately the desired uptake temperature (while monitoring the burner temperature).
- 2) Check the pressure product. Re-adjust the main air supply globe valve to obtain the correct value.
- 3) Adjust the fuel control valve and/or the bypass air valve (see Figure 3) to achieve the desired temperature. Rough temperature control can be

achieved with the bypass air valve and fine control with the fuel control valve.

- 4) Go to Step 2 and continue until the pressure product and temperatures are satisfactory.

D. SYSTEM SHUT DOWN

- 1) Close the fuel shutoff valve.
- 2) Turn off the fuel supply pump and the high pressure fuel pump.
- 3) Allow the system to cool for 5-10 minutes.
- 4) Close the compressor butterfly suction damper.
- 5) Turn off the compressor. Immediately after turning off the compressor turn the auxiliary oil pump switch to the "hand" position.
- 6) Allow the bearing temperatures to reach 80°F before turning off the oil pump and the cooling tower pump and fan.

APPENDIX B

DETERMINATION OF THE EXPONENT IN THE NONDIMENSIONAL PUMPING COEFFICIENT

The method used to determine the value of the exponent n in equation (13) is outlined below.

(1) Select a given geometry, assume reasonable values for K_p , K_m and f , and calculate C_1 , C_2 and C_3 for use in equation (11b).

(2) Set $T^* = 1.0$, $\Delta P^* = 0$, and solve for W^*_{max} .

Equation (11b) plots as indicated in Figure 20; for $\Delta P^* = 0$ and $T^* = 1.0$, the intersection of the curve with the W^*T^{*n} axis yields the value of W^*_{max} . Note that for each value of $T^* < 1.0$ ($T^* = T_s/T_p$ and $T_s < T_p$ therefore $T^* < 1.0$) a different curve will result.

(3) For the same geometric configuration and other values assumed and calculated in step (1), calculate $\Delta P^*/T^*$ using equation (11b) with W^*T^{*n} for different values of T^* in each case varying W^* from 0 to W^*_{max} in equal increments of W^*_{max} . For each new value of T^* tried, vary n until the resulting plots of $\Delta P^*/T^*$ vs W^*T^{*n} for $T^* < 1.0$ come close enough to the initial plot obtained in step (2) where $T^* = 1.0$ that, for all practical purposes, all such plots can be represented by a single curve.

(4) The value of n which most effectively collapses all performance curves onto the $T^* = 1.0$ case is $n = 0.44$.

APPENDIX C

UNCERTAINTY ANALYSIS

The experimentally determined pressure coefficient and pumping coefficient are used in determining eductor operating points which in turn provide the basis for comparison and evaluation of eductor system performance. A determination of the uncertainties in these coefficients was made using the method described by Kline and McClintock [10]. Data for the eductor configuration described in Table VI is considered a representative case and is used to calculate representative uncertainties in the pumping and pressure coefficients.

For a single sample measurement the value of a specific variable should be given in the format:

$$x = \bar{x} \pm \delta x$$

where

\bar{x} = mean value of the variable x

δx = estimated uncertainty in x .

Variations for the variables in the defining equations for the two coefficients are listed in Table IX. Having described the uncertainties in the basic variables of a

relationship, it is now necessary to determine how these uncertainties propagate into the result. Consider the relation where the result R is the product of a sequence of terms.

$$R = x_1^a x_2^b x_3^c \quad (a)$$

A reasonable prediction of the uncertainty in the result R is obtained by using the Second Order Equation suggested by Kline and McClintock [10].

$$\delta R = \left[\left(\frac{\partial R}{\partial x_1} \delta x_1 \right)^2 + \left(\frac{\partial R}{\partial x_2} \delta x_2 \right)^2 + \left(\frac{\partial R}{\partial x_3} \delta x_3 \right)^2 \right]^{1/2} \quad (b)$$

Evaluating the partial derivatives appearing in equation (b), and normalizing by dividing through by result R yields the simplified form of equation (b) which will be used in this analysis.

$$\frac{\delta R}{R} = \left[\left(\frac{a \delta x_1}{x_1} \right)^2 + \left(\frac{b \delta x_2}{x_2} \right)^2 + \left(\frac{c \delta x_3}{x_3} \right)^2 \right]^{1/2} \quad (c)$$

Determination of the uncertainty in the pressure coefficient is facilitated by writing it as the product of a series of terms,

$$\frac{\Delta P^*}{T^*} = (\rho_s)^{-1} (\Delta P) (U_p)^{-2} (T^*)^{-1} \quad (d)$$

where P represents the pressure difference $(P_a - P_0)$. Constants such as $2 g_c$ in the equation for the pressure coefficient will be cancelled out when used in equation (c) and are therefore not included in this analysis. Applying equation (c) to the pumping coefficient in equation (d) yields the following expression for its uncertainty:

$$\frac{\delta \frac{\Delta P^*}{T^*}}{\frac{\Delta P^*}{T^*}} = \left[\left(\frac{(-1) \delta \rho_s}{\rho_s} \right)^2 + \left(\frac{(1) \delta (\Delta P)}{\Delta P} \right)^2 + \left(\frac{(-2) \delta U_p}{U_p} \right)^2 + \left(\frac{(-1) \delta T^*}{T^*} \right)^2 \right]^{1/2} \quad (e)$$

Taking into account the respective equations defining the individual variables, the terms of equation (e) are expanded as follows:

$$\rho_s = \frac{P_a}{R T_s}, \quad \left[\frac{\delta \rho_s}{\rho_s} \right]^2 = \left[\frac{\delta P_a}{P_a} \right]^2 + \left[\frac{\delta T_s}{T_s} \right]^2$$

$$\rho_p = \frac{PEH}{R T_p}, \quad \left[\frac{\delta \rho_p}{\rho_p} \right]^2 = \left[\frac{\delta PEH}{PEH} \right]^2 + \left[\frac{\delta T_p}{T_p} \right]^2$$

$$U_p = \frac{W_p}{\rho_p A_p}, \quad \left[\frac{\delta U_p}{U_p} \right]^2 = \left[\left(\frac{\delta W_p}{W_p} \right)^2 + \left(\frac{\delta \rho_p}{\rho_p} \right)^2 + \left(\frac{\delta A_p}{A_p} \right)^2 \right]$$

$$A_p = 4\pi r^2, \quad \left[\frac{\sigma A_p}{A_p} \right]^2 = \left(\frac{2 \delta r}{r} \right)^2$$

$$w_p = .0310 + .0704((PNH+B) \cdot \Delta PN)^5 + .00009 \text{GHz},$$

$$\left[\frac{\delta w_p}{w_p} \right]^2 = \left[\left(\frac{C_1 \delta PNH}{w_p} \right)^2 + \left(\frac{C_2 \delta B}{w_p} \right)^2 + \left(\frac{C_2 \delta \Delta PN}{w_p} \right)^2 + \left(\frac{C_3 \delta F \text{Hz}}{w_p} \right)^2 \right]$$

$$C_1 = .0310$$

$$C_2 = .0704$$

$$C_3 = .00009$$

$$T^* = \frac{T_s}{T_p}, \quad \left[\frac{\delta T^*}{T^*} \right]^2 = \left[\frac{\delta T_s}{T_s} \right]^2 + \left[\frac{\delta T_p}{T_p} \right]^2$$

Using the values of the variable and their respective uncertainties listed in Table IX, the uncertainty in the pressure coefficient is estimated to be

$$\frac{\delta \left(\frac{\Delta P^*}{T^*} \right)}{\frac{\Delta P^*}{T^*}} = .0187 = \pm 1.9\%$$

By a similar process, the uncertainty in the pumping coefficient is estimated to be

$$\frac{\delta \left(\frac{W^* T^* \cdot 4^4}{W^* T^* \cdot 4^4} \right)}{\frac{W^* T^* \cdot 4^4}{W^* T^* \cdot 4^4}} = .0213 = \pm 2.1\%.$$

BIBLIOGRAPHY

1. Ellin, C. R., Model Tests of Multiple Nozzle Exhaust Eductor Systems For Gas Turbine Powered Ships, Engineers Thesis, Naval Postgraduate School, June 1977.
2. Moss, C. M., Effects of Several Geometric Parameters on the Performance of a Multiple Nozzle Eductor System, MS Thesis, Naval Postgraduate School, September, 1977.
3. Harrell, J. P., Experimentally Determined Effects of Eductor Geometry on the Performance of Exhaust Gas Eductors for Gas Turbine Powered Ships, Engineers Thesis, Naval Postgraduate School, September, 1977.
4. Ross, P. D., Combustion Gas Generator for Gas Turbine Exhaust Systems Modeling, MS Thesis, Naval Postgraduate School, December 1977.
5. Staehli, C. P., and Lemke R. J., Performance of Multiple Nozzle Eductor Systems with Several Geometric Configurations, MS Thesis, Naval Postgraduate School, September, 1978.
6. Keenan, J. H. and Kaye, J., Gas Tables, John Wiley and Sons, Inc., 1963.
7. Pucci, P. F., Simple Ejector Design Parameters, Ph.D. Thesis, Stanford University, September 1954.
8. Boeing Airplane Company, Boeing Model 502-2E Gas Turbine Engine, February, 1953.
9. Carrier Corporation, Operating Instructions for Carrier Model 18P352 Air Compressor, October, 1955.
10. Kline, S. J. and McClintock, F. A., "Describing Uncertainties in Single Sample Experiments," Mechanical Engineering, p. 3-8, January, 1953.

INITIAL DISTRIBUTION LIST

	No. Copies
1. Defense Documentation Center Cameron Station Alexandria, Virginia 22314	2
2. Library, Code 0142 Naval Postgraduate School Monterey, California 93940	2
3. Department Chairman, Code 69 Department of Mechanical Engineering Naval Postgraduate School Monterey, California 93940	2
4. Professor Paul F. Pucci (Code 69Pc) Department of Mechanical Engineering Naval Postgraduate School Monterey, California 93940	10
5. LT Charles R. Ellin 13512 Westwind Drive Silver Spring, Maryland 20904	1
6. Mr. Charles Miller NAVSEA Code 0331 Naval Ship Systems Command Washington, D. C. 20362	1
7. Mr. Olin M. Pearcy NSRDC Code 2833 Naval Ship Research and Development Center Annapolis, Maryland 21402	1
8. Mr. Mark Goldberg NSRDC Code 2833 Naval Ship Research and Development Center Annapolis, Maryland 21402	1
9. Mr. Eugene P. Wienert Head, Combined Power and Gas Turbine Branch Naval Ship Engineering Center Philadelphia, Pennsylvania 19112	1
10. Mr. Donald N. McCallum NAVSEC Code 6136 Naval Ship Engineering Center Washington, D. C. 20362	1

	No. Copies
11. Lt. J. P. Harrell, JR., USN 2004 Cloverleaf Place Ardmore, Oklahoma 73401	1
12. Lt. C. M. Moss 625 Midway Road Powder Springs, Georgia 30073	1
13. LCDR P. D. Ross, JR., USN 673 Chestnut St. Waynesboro, Va. 22980	1
14. Lt. D. R. Welch 1036 Brestwick Commons Virginia Beach, Virginia 23512	2
15. Lt. R. J. Lemke 2902 No. Cheyenne Tacoma, Washington 98407	1
16. Lt. Chris P. Staehli Route 2 Box 648 Burton Washington 98013	1
17. Professor R. Nunn, Code 69Nn Department of Mechanical Engineering Naval Postgraduate School Monterey, Calif. 93940	1